A Systems Biology Approach to DNA Damage Repair

David William Peter Dolan

Doctor of Philosophy

Institute for Ageing and Health

September 2012

Abstract

The presence of DNA double-stranded breaks in a mammalian cell typically activates the Non-Homologous End Joining (NHEJ) pathway to repair the damage and signal to downstream systems that govern cellular decisions such as apoptosis or senescence. The signalling system also stimulates effects such as the generation of reactive oxygen species (ROS) which in turn feed back into the damage response. Although the overall process of NHEJ is well documented, and much is known about downstream processes that together constitute the DNA damage response (DDR), we know little of the dynamics and how the system operates as a whole. To further our understanding of this we have constructed computational models which integrate current knowledge of the DNA repair process and key downstream signalling systems. The models are coded in Systems Biology Mark-up Language and BioNetGen Language and are quantified as far as possible with experimental data generated within our own laboratories or otherwise gathered from the literature. They are designed to simulate the observed stochastic dynamics of repair by DNA Protein Kinase (DNA-PK) dependent NHEJ (D-NHEJ) and back-up NHEJ mechanisms (B-NHEJ) following damage induced by gamma irradiation in human fibroblasts and the response this causes in the p53-p21 senescence signalling pathway. We have used the models to investigate a number of issues relevant to the study of ageing cells. Our work suggests that this observed heterogeneity in the repair of DNA damage foci that is influenced by levels of damage cannot be explained solely by inherent stochasticity in the NHEJ system. We find that the presence of multiple repair mechanisms and the modulation of key repair factors by oxidation along with further damage inducing feedback triggered by p53 and changes brought about by cellular processes such as senescence all play a cumulative role in causing the differences between stressed and unstressed cells. Our model highlights the importance of Ku oxidation which leads to increased Ku dissociation rates from DNA damage foci and shifts in favour of the less efficient B-NHEJ system. Furthermore we have utilised the model to investigate the role that various levels of DNA damage and repair have on the maintenance of the important p53 oscillations in a cell. We find that, contrary to the current view, p53 levels are affected by temporal dynamics of DNA damage and have used our model to inform the design of further experimental work to investigate the effect of

maintained low levels of DNA damage induced by frequent low pulses of γ irradiation on the p53 mediated DDR.

Acknowledgements

This thesis and by extension my whole PhD is the product of a lot of time and effort not only from myself but from the people around me who have aided and supported me over the last four years and I would like to take the opportunity to express my gratitude.

In particular, a big thank you has to go to my supervisors, Daryl Shanley and Tom Kirkwood. Not only did you give me the chance to undertake my PhD but you have always been there to provide help and advice whenever I needed it. I would also like to extend my warmest thanks to Anze Zupanic, Carole Proctor, Chris Redfern, Glyn Nelson, and Graham Smith for all the invaluable input you have had in guiding and shaping my work. You all took time out of your own work to teach me about the tools needed to carry out my research or just point me in the right direction and for that I am extremely grateful.

The work has been hard at times, but it was worth the effort and thanks to you I enjoyed every minute of it.

It has been an absolute pleasure to work with all of you.

Now if you would excuse me, I'm off to roll some dice and slay a dragon.

Contents

Table and Figures

Glossary

BER: Base Excision Repair

DDR: DNA Damage Response

DNA: Deoxyribonucleic acid

DSB: Double Strand Break

HR: Homologous Recombination

MMR: Mismatch Repair

NHEJ: Non-Homologous End Joining

- B-NHEJ: Backup NHEJ
- D-NHEJ: DNA-PK Dependant NHEJ

NER: Nucleotide Excision Repair

ROS: Reactive Oxygen Species

SBML: Systems Biology Mark-up Language

Chapter 1: An introduction to Ageing, DNA Damage and Systems Biology

1.1 Ageing

Ageing can be described as the irreversible decline in the function of an organism over time and applies over a wide range of time related alterations that occur in biological systems, from molecules and cells up to tissues and organs (1). Ageing is not commonly seen in wild populations as most individuals die of extrinsic causes such as predation or disease before reaching old age (2), although some old individuals are reported (3). The situation in humans is less clear. At the population level we are living longer and longer, and as yet no upper limit has firmly been established (4). It is therefore important to understand the underlying biology of ageing in order better to equip humanity to cope with an increasingly aged population. There are two complementary questions that require answering if we are to fully understand ageing: Why do we age and how do we age?

1.2 Why do we Age?

There have been many theories proposed as to why we age (5). These explanations can be divided into one of two groups, adaptive or non-adaptive. Adaptive ageing theories put forward the idea that ageing has evolved due to some advantage gained by adopting a phenotype, whereas Non-adaptive ageing theories champion the idea that ageing has not evolved and is instead simply a by-product of other fitness enhancing processes that have evolved as part of an organism's life history.

1.3 Adaptive Theories of Ageing

Until the early 20th century the predominant theory was that ageing was programmed into an organism. The reasoning was that organisms age and die to enable further evolution of the species by ensuring a turnover of generations and to avoid overcrowding. In an influential text, August Weismann wrote "Worn out individuals are not only valueless to the species, but they are even harmful, for they take the place of those which are sound." (6).

This simple and straightforward theory was widely accepted by biologists for some time and although there are circumstances where it may be applicable (7) there are too many essential flaws for it to offer a general explanation (8,9). Firstly, most wild organisms rarely survive to an age in which the effects of ageing become apparent, so there is no need for ageing to remove the older organisms (the worn-out individuals) as the environment around them presents a range of effective means such as diseases, predators and geological events such as floods. To date there is no evidence that ageing is a significant cause of mortality in the wild (2). As individuals usually die before old age there is little opportunity for ageing genes to evolve as a result of natural selection because the genes would be of little benefit to the organism within its usual lifespan. The other major flaw in Weismann's theory is that it suggests that ageing is a process designed to benefit a species rather than an individual. Now, if a mutation occurs that causes the negation of the theoretical ageing program you would get an individual that would not have to sacrifice itself for the benefit of the species. This maverick individual as a result of its mutation would be fitter than the others around it and so have a greater chance of reproducing and passing on its genes into the next generation, and so yield more maverick individuals who would also be fitter than those around them, and so would survive instead of sacrificing themselves to pass on their genes. Eventually the species would be made up of these mavericks that don't age. However this is not the case in any species, nor is there a known mutation within any species that stops the ageing process (9).

1.4 Non-adaptive Theories of Ageing

So ageing evolving as a beneficial adaptation is unlikely as a general explanation, but where does that leave us? Instead of viewing ageing as a process unto itself, it may be better to think of it as a by-product of living and all the millions of processes that go to make up life. In 1952 Peter Medawar published a theory of ageing that suggested that ageing was a result of mutations accumulating within genomes over generations (10). Mutations that only take effect in late life with respect to the start of an organism's reproduction would only be subject to weak selection. The genes would be passed on from generation to generation and accumulate in the genomes of that lineage. Then if an individual organism survives all the extrinsic causes of mortality for long enough it may experience all the generations of

accumulated mutations as ageing. The Mutation Accumulation Theory (10) gave scientists a new way to look at ageing and what caused it to arise. Shortly after the publication of Medawar's theory, George C. Williams proposed an alternative theory, Antagonistic Pleiotropy (11). He proposed that as genes have different effects on an organism's fitness at different life stages, there exists a subset of genes (pleiotropic genes) with a beneficial affect early in life that were selected for by natural selection that became harmful as to an organism as it became older (antagonistic pleiotropy). By the time the genes become harmful, they would already be passed on to the next generation. Furthermore because of the time dependent nature of the genes natural selection would act more strongly on the early beneficial effects that play a part in reproductive fitness than it would on the later detrimental effects on the health of the organism (11). These two genetic theories continue to attract empirical tests but conclusive evidence remains to be found (8), largely due to the complexity and multifaceted nature of the systems that genes function in making it extremely hard to identify an outcome that is totally beneficial to a cell. To date the best example of a gene whose action may be consistent with antagonistic pleiotropy is the one which codes for the tumour suppressor p53. This gene has the ability to protect tissue from cancer at young age but promote tissue aging through induction of senescence in later life. The complexity of senescence within the ageing process and its potential beneficial roles throughout the lifespan of a tissue make it status as a clear cut example questionable.

In 1977 Tom Kirkwood proposed a much broader theory. The disposable soma theory (12) suggests that an organism allocates limited resources between maintenance and repair of cellular components and reproduction. So, if an organism repairs and maintains itself using most of its resources (energy, amino acids etc.) it has less resources to put into increasing its reproductive output, this would result in it being less capable of successfully passing on its DNA to the next generation. On the other hand an organism can use up more resources in increasing its reproductive capability to enhance its chances of successfully reproducing and passing on its genes to the next generation, but this would mean fewer resources could be allocated to the repair and maintenance of the cell and its components (the soma), which would collect damage from external stresses and the products and by-products of its metabolic processes.

Recently the Disposable Soma theory has been challenged: one proposal is that heat dissipation is more important than resource allocation and argues that the lower dissipation by larger animals is the reason why fecundity declines as species size increases (13); another takes a TOR centric view and suggests the existence of a quasi-program whereby ageing is the simply the result of natural selection favouring growth in early life and that a high level of growth becomes detrimental late in life (14). Each of these proposals raises more problems than they solve, the former can only be used for explaining observations in endothermic animals, whilst the latter focuses on a single pathway of an extremely complex and interconnected signalling system that is unlikely to be controlled by just one part. More over the existence of systems that limit growth in favour of reproductive capacity suggest that there is more than growth involved in the causes of ageing.

The current theories of why we age make predictions about the mechanisms of ageing that can be tested with the complementary question of how we age. Do single genes govern ageing or is it multi-causal as predicted by the disposable soma theory?

1.5 How do we Age?

Ageing is the accumulation of unrepaired damage to molecules, cells and tissues. The Free Radical Theory of Ageing (15), which was later modified to the Oxidative Stress Theory of Ageing (16), proposed that reactive oxygen species (ROS) generated as a by-product of normal cellular metabolism are the major source of this damage. Since the theory's proposal over half a century ago much time has been spent investigating the role of oxidative damage within a cell. There are three different ROS frequently studied whilst investigating the Oxidative Stress Theory of Ageing, the hydroxyl radical ($^{\cdot}OH$), the superoxide radical (O_2^-) and hydrogen peroxide (H_2O_2). It is suggested that these compounds interact with different parts of a cell's biological system and cause ageing (17) although it has become apparent over time that reactive oxygen species are not the only cause of cellular ageing and instead just make up part of the mechanisms that power the ageing process (18). Beyond being a cause of damage ROS play an important role in the proper functioning of a cell by also being utilised within cellular signalling pathways (19) and in the regulation of many important systems through redox sensitivity of its proteins (20).

Within a cell the three main targets of ROS are lipids, proteins and DNA (21). Biological membranes are largely composed of lipids; eukaryotic cells membranes consist of a phospholipid bilayer. Within the bilayer are lipids with a high number of carbon-carbon double bonds (described as polyunsaturated lipids) and these double bonds can react with hydrogen peroxides to produce hydroperoxides and endoperoxides which are then turned into aldehydes which are toxic to cells (17). The higher the number of double bonds a polyunsaturated lipid has the greater its sensitivity to ROS (22) and so the more prone it is to oxidative damage. Interestingly, longer lived species tend to have more saturated and therefore more ROS resistant cellular membranes (23).

Proteins are also prime targets for investigation when studying ageing as they are involved in a wide variety of cellular functions, usually as enzymes to catalyse the molecular reactions that take place. Previous work has shown that almost all the amino acids that make up peptide chains of proteins can be targeted by ROS (24). ROS can change the physical shape of proteins, which can affect their ability to perform particular tasks and even completely inactivate them. For example glutamine synthetase can be inactivated by an oxidative reaction changing a histidine residue into a carbonyl group (25). Since Levine's study was published in 1983 it has been observed that the number of oxidised proteins (those with carbonyl groups) increases as organisms get older (21).

Nuclear, telomeric and mitochondrial DNA can also be oxidised by ROS and like proteins the amount of oxidised DNA has also been seen to increase as an organism gets older (21). The detection of oxidative damage to DNA is usually made by looking at the levels of 8-oxo-7,8-dihydro-2'-deoxyguanosine (8oxodG) in a cell as it is a by-product of the oxidation reactions and can be measured very accurately. Oxidative damage to DNA is particularly interesting as it has been observed that cells have limited potential to divide into new cells, and after a point they undergo a process called cellular senescence (26). A number of factors have been implicated in causing senescence, and the shortening of telomeres inside of a cell's nucleus is clearly important. Telomeres are terminal ends of chromosomes made up of repetitive sequences of bases (telomeric DNA) and a group of proteins (27) whose functions are to cap the telomere end to stop the binding of a variety of cellular components. As a cell gets older its telomeres shorten during cell replication and once they pass a critical length the DNA damage check point of a cell is triggered, which leads to cell cycle arrest and senescence

(28). It has been seen that other factors such as oxidative stress can also cause telomeres to shorten (29), this of course means that a cell will pass the point where it triggers the damage response sooner if it is under stress than if it was under normal conditions.

During senescence a cell goes into permanent cell cycle arrest and no longer copies its DNA and divides to stop the proliferation of damaged cells, its nucleus has a different gene expression from a non-senescing cell and the cell may become resistant to apoptosis (the controlled destruction of a cell's components and eventual engulfment by other cells) (30). The contribution of senescent cells to the physiological decline that is ageing is becoming increasingly apparent with growing evidence of senescent cells producing a variety of damaging molecules which induce damage and the onset of senescence in neighbouring cells (31,32).

Ageing in multi-cellular organisms is a major risk factor in the development of cancer. In contrast to other ageing related changes which result in a decline and loss of function, cancer is a gain of function where cells undergo hyperplasia (a state of inappropriate cell replication), have increased size and capacity to move and become resilient to environmental stresses (33). Interestingly some of the products secreted by senescent cells have been seen to promote tumour growth in surrounding cells (34) which is somewhat paradoxical given that senescence prevents individual cells from becoming cancerous.

Ultimately the senescent state is a double edged sword, it has advantages in that it can cause inflammation, disrupts normal tissue function and promotes cancer in neighbouring cells whilst also helping stimulate immune clearance and promoting the maintenance of growth arrest to stop cancer development in the senescent cell.

1.6 Systems Biology and Ageing

Systems Biology builds on the field of molecular biology by firmly embedding a systems way of thinking (35). The systems approach to biology is not new, having been employed in biological research since the 1950's (36) when the idea that a great number of biological systems were open and could not be categorised and analysed in the same way chemical systems were became widespread. However systems biology as a discipline has been greatly

enabled by the availability of powerful experimental tools and genomic data at the start of the 21st century. The aim of systems biology is to look at all parts of a biological system: to analyse and try to understand how they work together as a part of the system, instead of looking at what they do individually. Systems Biology makes use of an iterative cycle of experiment, analysis and modelling (37) in which we use current data and knowledge to generate hypotheses, then use computational methods to model our ideas (this is frequently called dry lab work) and generate predictions, which we then test experimentally (wet lab). Once we have new data from the experiments we go back to our original model and incorporate the new data to modify and improve the dry lab work. Ageing is an ideal candidate for the Systems Biology approach because not only does it have many components that interact with one another but it also involves a wide range of systems that function on many levels (from the genetic level through cellular metabolic systems and all the way up to the psychological level in the case of human ageing) (38). Using the systems biology approach we can theoretically model what goes on inside a cell as it ages and create a virtual ageing cell. This is no small task as even in a single cell a huge number of processes take place. For tractability, the whole system can be broken down into its sub-systems and modelled one at a time and then combined to create an integrated virtual ageing cell (39). The reason to model is very simple: by modelling a system we can integrate knowledge from a wide range of data sources, test whether current thinking is feasible, generate testable predictions and most importantly address specific questions that are difficult to target using experimental work alone. A model in its simplest form is a collection of mathematical rules that describe a systems dynamics and how they change over time. We can use these models to carefully study the dynamics of the components and interactions that they contain, for example we can look at how feed-forward and feed-back loops affect a system and how a system produces an oscillating dynamic with its components. Good examples of where modelling has been utilised successfully to investigate cellular signalling dynamics include the characterisation of the oscillatory behaviour of p53 (40) and NF-κB (41) and the subsequent impact this behaviour has on the systems downstream of them. System modelling has also been successfully used in discovery for example in network topology. Dassow and colleagues (42) constructed a gene expression network of segment polarity development in *Drosphila* based on current knowledge of the signalling network structure. The network was shown to lack the stability required generate the known banding patterns

and so the authors went on to introduce random connections within the network and discovered new links that did produce robust behaviour and that have subsequently been experimentally validated. A more recent example of using systems modelling for discovery is from our own labs where a comprehensive model of mTOR signalling network was used to explore different modes of activation of the second and less well understood complex containing mTOR, mTORC2 (43). 3 putative connections were tested with simulation of network perturbation followed by experimental validation using drug and genetic inhibition and led to the suggestion that mTORC2 is regulated by a PI3K isoform different to that involved in regulating mTORC1. As technology has developed so has our capacity to model greater levels of complexity, however one limitation that has often held back modelling has been the difficulty in modelling system that span many temporal scales, where some components have functions that are dependent on events happening over a matter of seconds and minutes whilst others are tied to more long term activity over the course of hours and days.

Traditionally biochemical systems were described using continuous deterministic models (44), which represent a smooth and gradual change in the components that make up the model and contains no element of randomness and unpredictability. With the advent of systems biology, the advancement of computer processing power and the acknowledgement that biochemical kinetics are intrinsically stochastic, i.e. there is a degree of randomness when their components interact, most models are being created to include the element of unpredictability. These stochastic models when tested will yield different results with each test within a range pre-determined by the mathematics of the model. Using these stochastic models means that results obtained from testing are more related to real life systems than those obtained from deterministic modelling. The differential equations of reaction in a model all boil down to two major components: the amount of each substrate taking part in the reaction and the rate at which the components interact expressed as a constant. Within a model there are parameters that the model outputs are sensitive to and those that it is not; we have therefore to determine through testing which parameters are sensitive and so which parameters are important to the model's dynamics. Without these parameters being accurate a model means very little. This means that the major limitation in model construction is that it is very data demanding and in an ideal

situation you would have quantitative data from multiple single cell time courses for each molecule in your system. Particularly useful data is collected from fluorescent probes and quantitative western time courses. Until recently this kind of data was rarely available, however with large scale proteomic studies being carried out such as multiple reaction monitoring (45) and the creation of databases such as BRENDA (46,47) which contain collected kinetic data on a wide range of enzymes the data required to parameterise large models is now accessible.

Beyond the hypothesis-driven approach there is also a hypothesis free-side to Systems Biology which is based on the analysis of large amounts of data. Instead of starting with any hypothesis you start with a high throughput experiment that produces a lot of data (e.g. microarray experiments) and analyse it to find patterns and connections within and between data sets, and once you find connections you use them to generate hypotheses. A good example of this kind of methodology in an ageing context can be found in Passos *et al.* 2010 (48) where hypothesis-free investigation of high throughput data was used to identify the possible paths that caused the production of ROS during senescence.

1.7 Tools and Standards for Systems Biology

Within the field of Systems biology there is a wide range of tools available to assist with a researcher's investigations. A significant part of this project has been devoted to learning about these tools and how they can be applied to my work. Originally dynamic modelling of biological systems was carried out using a series of differential equations encoded and simulated within a programming environment. This meant that each individual researcher would code their work differently to others which made it difficult for other groups to utilise. Recently, a specialised extensible mark-up language (XML), called the Systems Biology Mark-up Language (SBML), was developed (49). This allowed biological models to be represented in a relatively simple, unified language which could then be shared between multiple groups. It also enabled the development of individual tools and resources where models could be developed, stored and simulated.

Although SBML is relatively simple to understand it is a mark-up language which is long and unwieldy to the human eye and there are many tools available to assist with model

development. CellDesigner (50) is a process diagram editor that allows you to construct a model graphically and add rules to each individual equation as you progress which the program will save as a specially modified SBML and export as a full SBML for simulation. There is facility to deterministically simulate your model within the program which is quite useful during parameter calculation. CellDesigner provides an easy to use environment for the construction and basic simulation of SBML, but is limited by restrictions in the editing of SBML. To have a greater amount of editing control you can use the Python based SBML converter to change the SBML model into SBML-shorthand (51). To assist with the construction of SBML models with in CellDesigner a plug-in called SBML Squeezer has been created which contains in it the mathematical equations for most types of chemical reactions that take place within a cell and helps overcome the highly error-prone and time consuming process of assigning kinetic equations to reaction within models (52).

In addition to model creation there is a wide variety of tools available for simulation and testing of SBML models. BASIS is a web based service designed for the stochastic simulation of SBML model using the Gillespie2 simulator (39) which uses the Gillespie algorithm (53) to generate statistically correct trajectories of the models reactions . Unlike deterministic simulation which gives out a set value from the interaction of the reactants in a reaction stochastic testing produces a variable result by adding in a level of variability to the reactions taking place. The variability produced in stochastic testing is a lot more representative of biological and chemical reactions than the set results that are produced by deterministic simulation; however the stochastic testing of SBML models can be very demanding on most computers' processors and so take up a lot of time. BASIS allows us to upload a model onto a dedicated server and allows quick reliable stochastic testing without using up a PC's entire resources.

Once the tools are in place the process of constructing a SBML model is relatively straight forward. The first step is to create a network of the components of the system (called species) from knowledge of how these molecules interact/react within the system. For each of the reactions or state change that occur within the network you assign an equation which is used to work out the rates at which amounts of species change over a period of time. All equations consist of the amount of substrates present in the reaction and a rate constant that defines the rate at which the reaction takes place. When an SBML simulator reads the

equation for each time point in a simulation it multiplies the amount of reactants in the equation by the rate constant to calculate the rate at which the reaction takes palace. The amounts of reactants and products are adjusted as appropriate following each reaction . These modified substrate levels for each species are then used to calculate the change in species levels at the next time step. The amount of each species within SBML models is measured in either number of particles of the species or concentration, the rate constant of a rate equation varies depending on the order of the equation. First order reactions in which one substrate undergoes a change to become the products has a rate constant of per model time unit, so if the model was measured in seconds a first order rate equation would have a rate constant measured in per second (s^{-1}). For a second order rate equation, the rate constant has two substrates that react to make the products and is measured in per number of molecules (or per concentration) per model time unit so in a model that has is species modelled in concentration (mol) and is measured in seconds a second order reaction would have a rate constant of $mol^{-1}s^{-1}$. For a simple model in which two species, A and B, combined to become C at a rate of k1 and species C would then combine with a species D to become E at a rate of k2 our model would consist of two rate equations:

$$A + B \overset{k1}{\rightarrow} C$$

$$C + D \overset{k2}{\rightarrow} E$$

Once the model's rate equations are defined all that would remain is to give the give the model's species their starting amounts and the rate constants their values, both of which are calculated from experimental data.

The advantages that modelling presents to the field of biology is two-fold. First it is a way of integrating knowledge and data from large scale multi-level complex biological systems which is not possible with wet lab experimentation alone. Additionally, computational modelling is relatively inexpensive compared to an equivalent program of laboratory experimentation and because of its modular nature it can be used in an explorative manner to find targets of interest within a system.

Modelling also has a number of limitations Firstly it is reliant on the existence and quality of experimental data used to calculate and parameterise the reactions within the model.

Secondly a model can only produce behaviours within its scope; if a species is not included it cannot affect the model. The inability to be able to account for unknown factors can often lead to the reliability of models being brought into question.

Modelling needs to be backed up closely with wet lab experimental work so that it can be refined which then allows for more targeted experimentation to lead to further improvement.

1.8 Towards a Virtual Ageing Cell

With the continuing development of the tools and standards, the ability to investigate the network of mechanisms that make up the ageing cell (54) is becoming much more viable. The ambition of modelling and linking together the various systems that make up ageing into a working ageing cell model was spelt out almost a decade ago (39) but the experimental data required to undertake such a task was not fully realised and it has only been in recent years that we have started to see the maturation of experimental technique and collection of data to really undertake this which has in turn led to the development of models of key ageing related systems such as protein homeostasis (55) and insulin/TOR signalling (56,57). However one area of the idealised virtual ageing cell that is still missing is the direct effects of ROS and other stresses on components of the cell and the early response to them.

1.9 DNA Damage and Ageing

DNA is one of the targets of ROS and the damage to it can take many forms. There is single stranded DNA damage, single base DNA damage, mis-paired nucleotides and double strands DNA damage just to name a few, and these can be caused by a variety of sources ultraviolet light, oxidising agents, hydroxylating agents, X-rays and ionising radiation etc. (58).

To fix damaged single strand damage a cell has a number of repair options depending on the type of damage caused to DNA. Nucleotide-excision repair (NER) which is used to fix damaged bases and disrupted base pairings caused by UV light and oxidative damage. Base-excision repair (BER) is used to repair single stranded DNA damage, which is caused by

products of metabolic reactions (e.g. ROS) and X-rays and is the most common type of damage that can occur to DNA. Both BER and NER share common repair proteins, PARP-1, XRCC1 and DNA ligase III (59,60). Mismatch repair (MMR) is used to fix mis-paired nucleotides which are a result of DNA polymerase slipping during replication of repetitive DNA sequences or recombination.

1.10 DNA Doubled Stranded Breaks and Their Repair

Ionising radiation such as X-rays and gamma rays have been found to cause a large number of double stranded breaks in cells (61). They do this by knocking electrons out of oxygen species and turning them into free radicals (62), which can then damage DNA. DNA double strand breaks are the most dangerous type of damage that DNA can suffer and the handling of the damage is of vast importance to the survival of the cell given that the mechanisms of DNA repair sits at the top of a long signalling system which is used to determine whether a cell undergoes apoptosis, goes into cell cycle arrest then senescence or escapes the arrest before senescence is triggered (63). DSBs have been seen to show varying levels of complexity and can be categorised into either Simple or Complex DSBs (64,65). Simple DSBs are breaks in which the DNA chain is simply split in two whereas complex DSBs on the other hand are breaks that are closely flanked by various single strand damages such as base deletions and other DSBs in a cluster of damage.

When a cell is stressed and sent into a senescent state via treatment with gamma irradiation or forms of chemical induction a number of changes take place within the cell including a change in the levels of Reactive Oxygen Species (ROS) which has been observed to have a 2.5 fold increase (48). This rise in ROS leads to more DNA damage within the cell and therefore more damage foci. These foci show a shift in dynamics both in the short term and in the long term, in which the number of short lived foci lasting less than 2 hours decreases and long lived and potentially permanent foci form. The increased ROS level is not exclusive to the senescent state and is instead something that occurs when a cell is stressed which impacts on the various pathways that trigger and modulate cell cycle arrest, apoptosis and antioxidant activity in a variety of cell types (66,67) making ROS a major player in what response the cell makes to stress events rather than a bi-product of the senescent state.

Ultimately, understanding of the mechanisms of the DNA Damage Response (DDR) and how they interact is paramount to our understanding of what determines a cell's fate after damage. This is especially important given that the role of DNA damage and repair is essential to our progress in cancer research and the development of treatments. Simply put, we need to know how a cell's damage response reacts to the insults involved in treatments such as Radiotherapy, which involves high doses of irradiation and by extension large rapid production of ROS and how it differs from the response from the handling of breaks produced under normal situations. Beyond irradiation of cells, there are a number of therapies being investigated that target components of the DDR pathways (68). Proper development of these also requires us knowing what effects they have on the pathways and that can only be understood properly if we know what is going on within the pathway.

Double stranded DNA damage is repaired by two different pathways, Homologous recombination (HR) and Non-homologous End Joining (NHEJ). HR is used to fix double stranded breaks by replacing the lost DNA sequence with an exact copy made from the intact sister chromatid. For this process to work there has to be a sister chromatid present, unfortunately this is not always the case and there are times in the cell cycle (the G1 phase) when there is no replicated strands of DNA to make the copies from that can be used to plug the gap in the damaged DNA strand. NHEJ is the damage response used to fix DNA during the G1 phase of the cell cycle; although it is also utilized during the other cell cycle phases (69). In the yeast *Saccharomyces cerevisiae* double stranded breaks are repaired mostly by HR (70) whereas in multicellular eukaryotes NHEJ seems to dominate (61), this is because a yeast cell is constantly going through the cell cycle and spends a significant amount of its time with copies of its DNA present, this makes repair by HR a much more viable option for yeast, on the other hand, cells of multicellular organisms are less frequently in a state with copies of its DNA present to be utilised in HR so instead uses HNEJ. The process of HR is quite accurate because it makes a copy from existing DNA; NHEJ on the other hand is not. It is described as an 'error-prone' process as nucleotides at the site of the DNA damage can be lost or added. One possible reason why organisms such as humans use this repair mechanism more often even though it is faulty is that most of their genome does not code for proteins and so they can tolerate imperfect repair.

1.11 Initial Aims

It is becoming increasingly clear that cell senescence plays an important role in ageing of the whole organism (71). Although we have an ever expanding knowledge on what happens during senescence the precise mechanics of how a small number of cells have such an impact is not yet fully known (32). It is clear however that a fuller understanding of the processes leading to cellular senescence, an enhanced characterisation of the senescent phenotype and a flexible framework for integrating and representing current knowledge would be very valuable.

Computational modelling offers a means for making progress with these aims and presents a useful complement to an experimental approach. Much is already known of the molecular mechanisms involved in cellular senescence. Oxidative stress accelerates telomere shortening leading to telomere uncapping and the triggering of a DNA damage response (DDR) that is the major cause of cellular senescence (28). The DDR is similar to the response triggered by double strand breaks (DSB) where damage foci constructed around the site of DNA damage during the repair process of Non-homologous End Joining play a key role in the initiation and maintenance of signalling to downstream systems. These systems produce either a pro-apoptotic or pro-survival response which appears to be governed by characteristics of the damage foci. One important characteristic is the longevity of individual foci which has been observed to range from minutes to hours. An explanation for these differences is lacking but may be due to specific interactions within the NHEJ pathway or a by-product of simple stochastic processes. A systems approach to enable a link between damage foci formation and cellular outcome would help clarify this issue. The process of NHEJ is complex; however the network of molecular interactions is reasonably well understood and can be separated into two quite distinct modules: one whose role it is to repair the damage and the other which is concerned with signalling the presence of damage to the cell. Knowledge however is lacking on the dynamics of DSB repair and there are no comprehensive mathematical models that describe the repair of the DSB and the construction of the signalling mechanism, the Damage Foci (72). The overall aim of this work was to develop a stochastic model of NHEJ and the signalling systems downstream of it to

help better expand our understanding of what we observe in live cells and to provide a tool for the development of hypothesis in the investigation of DSBs.

Chapter 2: An SBML Model of Non Homologous End Joining

2.1 Introduction

Non Homologous End Joining (NHEJ) comprises of two distinct sub-systems that work simultaneously. The first is the repair system whose role is to repair the double stranded break and the second the Signalling or Flagging system that signals to the cell that there is DNA damage present by forming a damage focus around out of various proteins along the DNA chain flanking the site of the break.

The role of the DNA repair system is to recruit proteins into the site of the DNA damage and carry out the repair of the double stranded breaks. When a DSB occurs the heterodimer Ku70/80 binds to the broken ends of the DNA, this is followed by recruitment of the DNA-dependent protein kinase catalytic subunit (DNA-PKcs), which together form the complex called the DNA-dependent protein kinase DNA-PK (73). The Ku70/80 heterodimer is made up from a 70kDa subunit, Ku70, and a 83 kDa subunit, Ku80, the DNA-PKcs is a large 469 kDa kinase from the family of kinases known as the phosphoinsitide 3 kinase-related protein kinase (PIKK) family (61). Ku70/80 has a structure shaped like a doughnut, in which the hole in its centre is large enough for the DNA double stand to fit through (74). It is thought that Ku70/80 is attached to the end of the double stranded break to provide a platform that enhances the binding of DNA-PKcs to the damaged DNA (75), however it has been shown that Ku70/80 is not required for the actual binding of DNA-PKcs to occur (76). Following binding of Ku70/80 to DNA, DNA-PKcs, makes a synaptic complex between the two broken ends of DNA to prepare the DNA for re-joining (77) along with Artemis which assists in the tidying of the broken ends (78). The break itself is fixed by ligation of the two broken ends, this ligation is carried out by a complex made up of DNA ligase IV and the protein XRCC4 (79). Figure 1 displays a summary of the repair of a DNA double stand break by NHEJ.

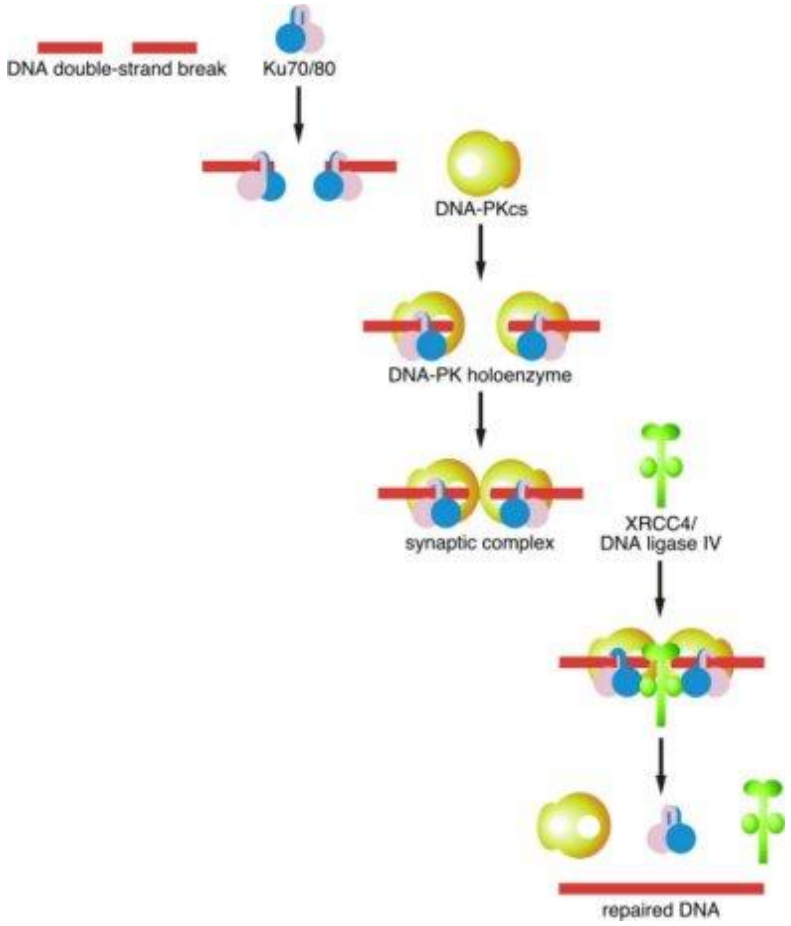

Figure 1. The first step in Non-homologous End Joining is the recruitment of Ku70/80. Then DNA-PKcs is recruited and binds with Ku70/80 and DNA to form DNA-PK. A synaptic complex is then made between the broken ends of DNA. Once the synapse is formed, a complex of DNA ligase IV and XRCC4 ligates the two ends together. Image from Reactome

As repair proteins are being recruited to repair the double stranded break the Signalling/Flagging system is activated to signal the presence of the damage to a variety of cellular pathways, which induce cell cycle check points to arrest the cell (80) to reduce the possibility of further damage and to promote cell survival whilst at the same time being at the top of the signalling pathways that ultimately decides whether a cell senesces, apoptoses or recovers into the cell cycle (81,82). This signalling involves formation of a Damage Focus made up of a number of proteins (83). It is thought that MRN, a complex of three proteins, Mre11, Rad50 and Nbs1 localises to the site of DNA damage first followed by ATM (ataxia-telangiectasia mutated) (84), however it is unclear as to which actually localises at the damage site first. Recent work has implicated the apoptotic regulator protein Aven as a crucial factor in the activation of ATM at the site of DNA damage (85) which then

autophosphorylates (86) and causes H2AX histones around the DNA damage site to phosphorylate (87) (the phosphorylated form H2AX is denoted as γ-H2AX). The γH2AX becomes the centre of a foci to which proteins such as p53 binding protein 1 (53BP1) and mediator of mammalian DNA damage checkpoint 1 (MDC1) are recruited, the presence of these around the focus have been detected after 1 minute, ATM and MRN are also incorporated into the foci but not until about 30 minutes after a cell is damaged, however they are still present at the site of the damage (88). DNA-PKcs also causes the phosphorylation of H2AX in a similar manner to that of its family member ATM (89). Together the NHEJ damage repair system and the damage flagging system form an effective defence against double stranded breaks. More recently a slower, more inaccurate system Backup NHEJ (B-NHEJ) (90,91) mediated by the single strand break repair factor PARP-1 has been proposed that functions alongside the more well documented DNA-PK mediated Non-Homologous End Joining pathway (D-NHEJ).

DNA repair and by extension Non-homologous End Joining are all part of a larger system that maintains the cellular functions of an organism and within the repair and flagging mechanisms there are a number of large proteins at work that function in other cellular systems. Ku70 of the Ku70/80 heterodimer is involved in the inhibition of cellular apoptosis (92,93) by interactions with NAD^+-dependent histone deacetylases which allows Ku70 to sequester the pro-apoptotic protein Bax, which can mediate apoptosis, away from mitochondria within a cell and so stop the pro-apoptotic effect of Bax. Ku70's level and activity within a cell as well as those of its partner Ku80 are regulated by ubiquitination and proteasomal turnover (94,95). Furthermore it has been seen that Ku70/80 levels are much lower in older senescent cells than younger ones (96) and it is suspected that this is because of greater amounts of the ubiquitination in the senescent cells (94). See Table 1 for a summary of the control and turnover of the major repair factors in NHEJ. ATM is important in phosphorylating H2AX, but it also activates Chk1 and Chk2 (80), Chk1 and Chk2 communicate with p53 and p21 (97,98)**,** and are major players in cell cycle arrest and cellular senescence. The phosphoinsitide 3 kinase-related protein kinase (PIKK), DNA-PKcs can also send signals that affect cell survival by interacting with Protein Kinase B (PKB/Akt) at the site of DNA damage when the DNA-PK Complex has formed as PKB/Akt is part of a

signalling cascade that promotes cell survival by affecting the transcription of p21 (99). PKB/Akt major function is in the insulin signalling pathway/PI3K growth pathways (100), which promotes cell growth, where it interacts with another PIKK, mTOR which is involved in the signalling pathway that modifies the forkhead box 0 (FoxO3a) transcription factor (101). ATM, another PIKK, has been observed have many roles related to DNA damage. It activates Chk1 and Chk2 (80,102), Chk1 and Chk2 communicate with p53 and p21 (97,98), and are major players in cell cycle arrest and cellular senescence and also have a function in the insulin signalling pathway, by regulating the activity of PKB/Akt (103). Moreover, ATM also has been found to have a role in the remodelling of chromatin, where together with NBS1 it regulates the modulation of the chromatin structure and the recruitment of repair factors to the sites of damage caused by the endonucleases involved in the remodelling (104,105). What has become apparent in recent experimental research is that the phosphoinsitide 3 kinase-related protein kinases play a large role not only in the repair of DNA damage but also in the much broader pro-survival and growth systems of living organisms. Many components of the NHEJ pathway are multifunctional and highly regulated and are involved in reactions of variable duration. Furthermore a lot of the regulation of the major proteins involved in D-NHEJ is carried out post-transnationally by a variety of modifiers (Table 1), however it has been seen that PP2A the enzyme that is responsible for the dephosphorylation of γ-H2AX undergoes strong transcriptional control (106) which could potentially play a large role in the effectiveness of NHEJ and cell fate. In addition to their level and modifications, the speed in which they are turned over in a reaction (Table 1) determines their input into the system responsiveness.

Repair Factor	Size	Turnover Rate	Regulation	Common Modifications	References
Ku70	70 kDa	Medium (hours)	Posttranslational	Ubiquitination, Acetylation of multiple lysines	(94) (107)
Ku80	80 kDa	Medium (hours)	Posttranslational	Ubiquitination	(95)
ATM	370 kDa	Slow (days)	Posttranslational	Aven, MRN, Autohosphorylation of Serine and Theorine binding sites	(108) (85)
DNA-PKcs	470 kDa	Slow (days)	Posttranslational	DNA Binding, Autohosphorylation of Serine and Theorine binding sites	(109)
Protein Phosphatases **(e.g. PP2A)**	Variable	Fast (minutes)	Posttranslational Transcriptional	Modified by Golgi Apparatus Inhibitors such as Okadaic acid	(110) (106)
DNA Ligase IV	96 kDa	Medium-Fast (minutes to hours)	Posttranslational	XRCC4 stabilises structure and regulates activity through complex formation	(111)

Table 1. Summary of key biochemical parameters of major repair factors involved in D-NHEJ.

It has been known for many years that DSB repair displays both fast and slow repair dynamics (112,113), which result in many breaks being ligated quickly but others being left unrepaired for longer periods of time. Within our labs we have observed that cells treated with γ irradiation undergo a shift from predominantly fast repair to predominantly slow repair and the reason for this is not totally understood. Cellular systems are very stochastic in nature (114,115) and it has been recognised that over the years that a lot of cellular decision making is based upon probability rather than absolutes to the point where genetically identical cells can show massive amount of 'noise' or variation (116). This stochastic nature shows great variation inside cells (44) and is impacted heavily by the interactions and feed backs within networks and even relatively small pathways such as the one between p53 and MDM2 who play a large role in deciding cell fate after damage. As a system can produce this wide range of outcomes it is entirely possible that the dramatic shift in outcomes when an input is altered is achieved simply by the stochastic nature inherent within the system.

Repair of the damaged DNA also has a knock on effect for the cell's function and survival even after the repair has been done. Inaccurately repaired breaks can lead to genome instability which in turn can lead to cell death or the onset of cancer (117) as well as inducing an instability in its progenies if the cell survives the DNA damage it suffers (118) . In general it has been observed that that D-NHEJ is required for accurate repair of DNA double strand breaks and that the B-NHEJ is error prone (64,90,119) so by extension it is assumed that B-NHEJ can lead to genomic instability in a cell. However complete the role that NHEJ plays in the promotion and avoidance of instability is not yet entirely understood and it is possible that factors traditionally linked to accurate repair such as Ku may also be linked to mis-joining of breaks and resulting instability (118).

The initial aim of this project was to create a functioning SBML model of NHEJ to investigate the observed shift in damage foci longevity in MRC5 cells treated with gamma radiation. The cause of this shift in repair dynamics is currently unclear, however since cellular systems are especially prone to stochastic effects (114,115), we hypothesized that the shift in distribution of foci longevity was caused by the stochastic nature inherent in the system when the levels of damage was increased.

2.2 Methods

2.2.1 Tagging of 53BP1 and Live Cell Observation

The usual method of measuring DSB formation and resolution within a cell is by the tagging of one of the proteins that make up the damage focus created around the site of damage. A plasmid encoding the fusion protein AcGFP-53BP1c was built and expressed in human diploid fibroblast cell line, MRC5, as described previously (120). For live cell time-lapse microscopy, MRC5 cells were plated in Iwaki glass bottomed dishes (Iwaki), either without treatment (unstressed cells) or after exposure to 20 Gy of gamma irradiation (stressed cells). Cells were imaged on an inverted Zeiss LSM510 microscope equipped with a Solent incubator (Solent Scientific) at 37^{o}C with humidified 5% CO_2, using a 40 x 1.3 NA oil objective (details in Nelson *et al*. 2002 (121)), with Z stacks obtained every 10 or 12 minutes for each field, as described previously in Passos *et al.* 2010 (48), for 30 hours. Imaging of stressed cells began 48 hours after treatment. The culturing and imaging of these AcGFP-53BP1c cells was carried out by Dr Glyn Nelson. The cells and AcGFP–53BP1c foci were tracked manually using ImageJ (http://rsb.info.nih.gov/ij/); when a focus was formed, the time was recorded and it was tracked through the time course images until it resolved. Some Foci were seen to apparently resolve and then reappear at the same position shortly after they disappeared. This dynamic growth and disappearance is a result of the foci being extended by phosphorylation of adjacent H2AX histones and recruitment of flagging proteins such as 53BP1 and being dismantled by the natural processes of the cell and then reforming because of the continued presence of the DSB. If a focus returned within 2 time frames (24 minutes or less) it was considered a single transient focus rather than two individual foci.

2.2.2 SBML Modelling

To create the model we first constructed a network of the known reactions of D-NHEJ, B-NHEJ and the formation of Damage Foci using CellDesigner (50). SBML Squeezer (52) was then used to generate differential rate equations for each reaction using mass action kinetics. Simplified graphical versions of these networks are shown in Figure 2A and 2B.

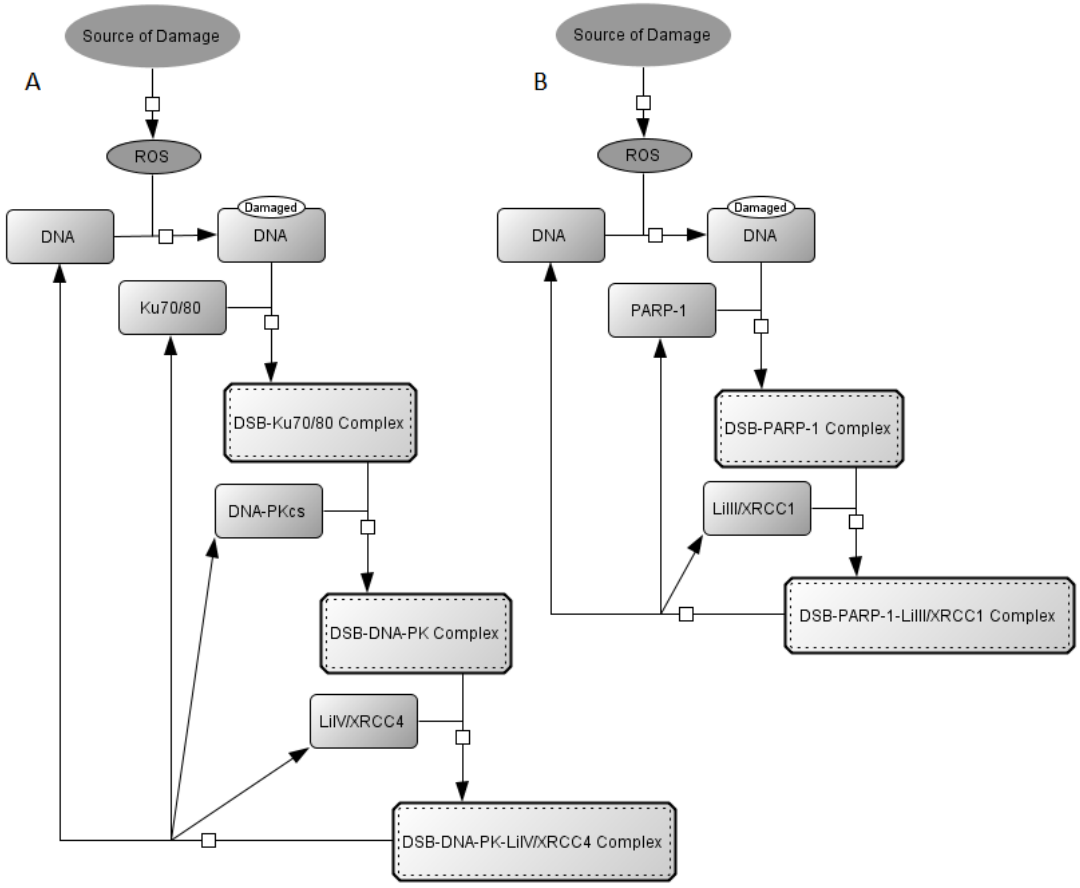

Figure 2. Repair Mechanisms of Non-Homologous End Joining. (A) The primary repair pathway of DSB repair by NHEJ is mediated by a heterodimer DNA-PK which is made up of Ku70, Ku 80 and DNA-PKcs and is commonly named DNA-PK Dependant Non-Homologous End Joining (D-NHEJ). Once the DNA-PK has formed a complex with the site of the DSB the break is readied for repair by ligation from the Enzyme LiIV which is in complex with XRCC4. (B) A second NHEJ pathway called Backup Non-Homologous End Joining (B-NHEJ) mediated by PARP-1 also exists. Once the break is primed by the formation of the DSB-PARP complex, the broken ends are ligated by the LiIII/XRCC1 complex.

As ROS is always present in a cell we needed to create a set of reactions in the model to produce and degrade ROS. To achieve the production of ROS we created a model species called Source of Damage, this species was used in the models first reaction to produce ROS.

$$Source\ of\ Damage \xrightarrow{kass\_rea} Source\ of\ Damage + ROS$$

By being a product of the reaction as well as a reactant the amount of the Source of Damage species would remain constant throughout any simulation of the model and so always be

present at a set level to create ROS. The degradation of ROS was implemented by creating a species called ROS Degradation and having ROS consumed in its production.

$$ROS \xrightarrow{kass\_rec} ROS\ Degradation$$

We could then adjust parameters involved in the level of ROS production and degradation allowing us to produce a steady state level of ROS similar to what is observed in live cells (48). The breaking of a section of DNA was represented by having a ROS and a species that represented the DNA chain, DNA, react together to form either Simple DSB or Complex DSB.

$$ROS + DNA \xrightarrow{kass\_reb} Simple\ DSB$$

$$ROS + DNA \xrightarrow{kass\_rep} Complex\ DSB$$

Once the formation of the break was modelled we moved onto the reactions that made up D-NHEJ. We started with all the proteins that make up the repair DNA-PK complex (Ku70/80 and DNA-PKcs) being recruited to the site of damage by the presence of the simple DSB along with a natural dispersal from the break site.

$$uKu70/80 \xrightarrow{\substack{kass_{red} \\ triggered\ by \\ presence\ of\ a\ DSB}} Ku70/80$$

$$Ku70/80 \xrightarrow{kass_{ree}} uKu70/80$$

$$uDNA\text{-}PKcs \xrightarrow{\substack{kass_{red} \\ triggered\ by \\ presence\ of\ a\ DBS}} DNA\text{-}PKcs$$

$$DNA\text{-}PKcs \xrightarrow{kass_{ree}} uDNA\text{-}PKcs$$

After the recruitment of the DNA-PK components we modelled the binding and dissociation of the DNA-PKcs Complex to the DSB and the auto-phosphorylation of DNA-PKcs (DNA-PK DBS Complex to DNA-PK DBS Complex_2)

$$Simple\ DSB\ + Ku70/80 \xrightarrow{kass\_ref} Ku70/80\ DSB\ Complex$$

$$Ku70/80\ DSB\ Complex \xrightarrow{kass\_reg} Simple\ DSB\ +\ Ku70/80$$

$$Ku70/80\ DSB\ Complex\ +\ DNA\text{-}PKcs \xrightarrow{kass\_rej} DNA\text{-}PK\ DSB\ Complex$$

$$DNA\text{-}PK\ DSB\ Complex \xrightarrow{kass\_rek} DNA\text{-}PK\ DSB\ Complex\_2$$

$$DNA\text{-}PK\ DSB\ Complex \xrightarrow{kdiss\_DNAPK} Simple\ DSB + Ku70/80 + DNA\text{-}PKcs$$

$$DNA\text{-}PK\ DSB\ Complex\_2 \xrightarrow{kdiss\_DNAPK} Simple\ DSB + Ku70/80 + DNA\text{-}PKcs$$

Once we had the DNA-PK complex fully formed we modelled the ligation step by Ligase 4 ('LiIV XRCC4').

$$uLiIV\ XRCC4 \xrightarrow[triggered\ by\ presence\ of\ DNA\text{-}PK\ DSB\ Complex\_2]{kass_{rel}} LiIV\ XRCC4$$

$$LiIV\ XRCC4 \xrightarrow{kass_{rem}} uLiIV\ XRCC4$$

$$DNA\text{-}PK\ DSB\ Complex\_2 + LiIV\ XRCC4 \xrightarrow{kass_{ren}} DNA\text{-}PK\ LiIV\ XRCC4\ DSB\ Complex$$

$$DNA\text{-}PK\ LiIV\ XRCC4\ DSB\ Complex \xrightarrow{kass\_reo} DNA\ + Ku70/80 + DNA\text{-}PKcs + LiIV\ XRCC4$$

The equations for the different stages of the D-NHEJ were then repeated for the repair of a Complex DSB (See Supplementary S1 for full table of reactions).

The same process of recruitment and binding of molecules was then used for modelling of the B-NHEJ pathway.

$$uPARP \xrightarrow[triggered\ by\ presence\ of\ a\ DSB]{kass_{reaq}} PARP$$

$$PARP\text{-}1 \xrightarrow{kass_{rear}} uPARP$$

$$Simple\ DSB\ +\ PARP \xrightarrow{kass\_reas} sDSB\ PARP\ Complex$$

$$sDSB\ PARP\ Complex \xrightarrow{kass\_reat} Simple\ DNA\ +\ PARP$$

$$uLiIII \xrightarrow[triggered\ by\ presence\ of\ sDSB\ PARP\ Complex]{kass_{reau}} LiIII$$

$$LiIII \xrightarrow{kass_{reav}} uLiIII$$

$$sDSB\ PARP\ Complex\ +\ LiIII \xrightarrow{kass\_reaw} sDSB\ PARP\ LiIII\ Complex$$

$$sDSB\ PARP\ LiIII\ Complex \xrightarrow[or\ kass\_reay]{kass\_reax} DNA\ +\ PARP\ +\ LiIII$$

As with the D-NHEJ pathway, the B-NHEJ reactions were repeated to handle the repair of Complex DSBs (See S1). A simplified graphical version of the network is shown in Figure 3.

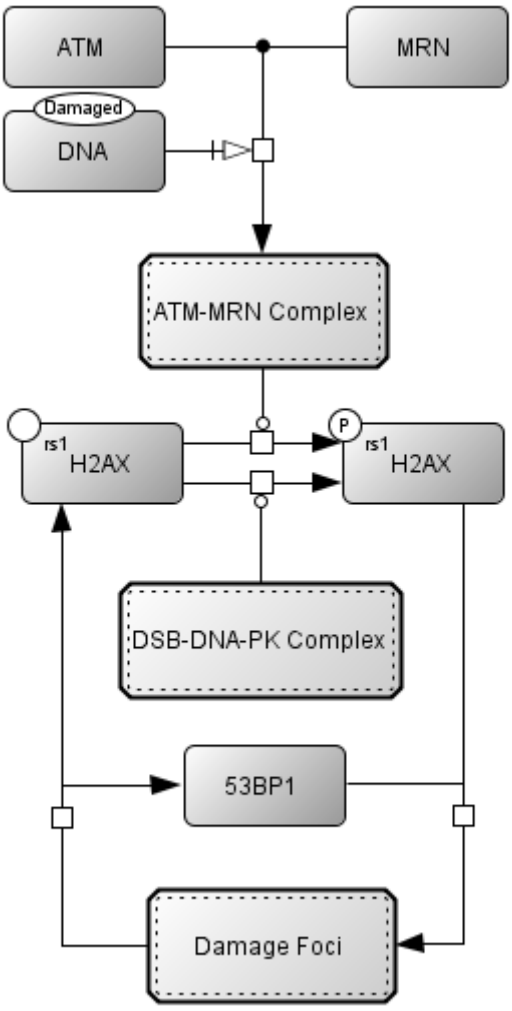

Figure 3. Signalling of DNA double strand breaks is via the phosphorylation of the histone H2AX and the formation of a Damage Focus around the DSB. Phosphorylation of H2AX is caused by autophosphorylation of ATM and DNA-PKcs at the site of damage.

We then modelled the formation of the damage focus at the site of damage beginning with the activation and binding of ATM and MRN.

$$ATM + MRN \xrightarrow[\text{triggered by presence of DSB}]{kMRN} MRN\ ATM\ Complex$$

The ATM MRN Complex along was then used to trigger the phosphorylation of histone H2AX to γH2AX (H2AX_2). The presence of the DNA-PK complex was also modelled to be able to trigger the phosphorylation of the histone.

$$H2AX \xrightarrow[\text{triggered by MRN ATM Complex}]{\text{kass\_rez}} H2AX\_2$$

$$H2AX \xrightarrow[\text{triggered by DNA-PK DSB Complex\_2}]{\text{kass\_reaa}} H2AX\_2$$

After the phosphorylation of H2AX we modelled the formation of the damage focus where proteins such as 53BP1 and BRCA1 form a complex with the γH2AX. As a means to avoid the model from becoming too large for simulation we modelled the formation of the damage focus with a simple first order mass action reaction instead of trying to model multiple reactions of the recruitment and binding of a wide range of highly abundant proteins. The damage focus was then completed by having the MRN ATM Complex bind into the focus and finally resolved back into its original components.

$$H2AX\_2 \xrightarrow{kass\_reac} Damage\ Focus$$

$$Damage\ Focus \xrightarrow{kass\_read} H2AX$$

$$Damage\ Focus + MRN/ATM\ Complex \xrightarrow{kass\_reae} Complete\ Damage\ Focus$$

$$Complete\ Damage\ Focus \xrightarrow{kass\_reaf} H2AX + ATM + MRN$$

After the network was constructed the reactions rates were estimated using data from a variety of sources and our own experimentally determined rates of damage induction for the unstressed/not irradiated cells. See tables S2 and S3 for estimated molecule numbers,

reaction rate constants and a comprehensive list of sources of experimental data. For a large number of individual reactions, kinetic rate constants were not available in the literature so we used available experimental time course data of recruitment and binding to calculate kinetic rate constants. For example, from (122) we know the average amount of Ku found in a eukaryotic cell (400000 molecules). We also know after a DSB is formed Ku shows maximal recruitment at 3 minutes (123). Combined with data of Ku rate of binding and dissociation to DNA (124,125) we could therefore estimate all the kinetic rates of Ku's interaction with a DSB.

2.2.3 Modelling of Multiple Damage Sites

The SBML model initially described how a DNA double strand break at a single DNA site was formed and resolved. However, because the formation and resolution of individual DSBs was important for us to follow, the model had to be modified so that we could simulate each break in it individually. This is step away from traditional modelling with SBML where typically a model is created to represent the interaction between large pools of molecules rather focusing on what happens around a distinct individual molecule. To create a model capable of monitoring separate breaks we converted the initial SBML model into SBML Shorthand (51) and edited it using a Python script to repeat the repair pathways and the flagging pathway multiple times to represent up to twenty sites of damage and the foci that could be formed at it if a break was caused (DNA became DNA_1, DNA_2 up to DNA_20). The number of molecules for each model species of DNA was then set to 1 meaning that there would only ever be one molecule of DNA_1 and it could only be turned into one DSB at any given time. This effectively allowed us to simulate and monitor the creation and repair of multiple individual DSBs and their damage foci simultaneously. We chose to model twenty theoretical break sites because monitoring of damage foci formed in live cells in our labs showed no more than fifteen breaks present at any one time and increasing the number of species in our model much beyond twenty breaks resulted in a model too large to be simulated by the programs available.

2.2.4 Model Simulation

The model was simulated using the stochastic simulator Gillespie2 (51,53) in an unstressed state (not irradiated) and a stressed state (irradiated) 100 times each for 30 hours with 1 minute time points. The stressed state model was represented by increasing the rate of ROS production 2.5 times compared to the unstressed model, in line with observations of the relative amount of ROS in basal and stressed cells (The species 'Source of Damage' in the model which had a fixed constant value and is used in the reaction that produces ROS was increased 2.5 fold) (48). We used an R script to extract the data from the individual simulation files and to calculate the longevity of individual damage foci whilst adjusting the output to account for transient foci by filling in time between a focus resolving and reforming if the duration was 20 minutes or less, in the same way as was done during the analysis of the live cell data. To compare the live cell and *in silico* data sets we constructed histograms and Kaplan-Meier curves and carried out Cox Regression analysis (Type I error rate, alpha=0.05).

2.3 Results and Discussion

When a cell is in an unstressed state, damage foci still form indicating that a cell undergoes some damage when at rest in its typical environment (Figure 4). This is largely because a cell under ambient conditions is still subject to mild stresses from its environment and ROS produced by the electron transport chain during respiration. Unstressed MRC5 cells showed a foci emergence rate of 0.53 foci per hour. Over 60% of the foci were repaired in two hours or less (Figure 5) and only 7% surviving more than 8 hours of which only a few (3 out of 10) are resolved.

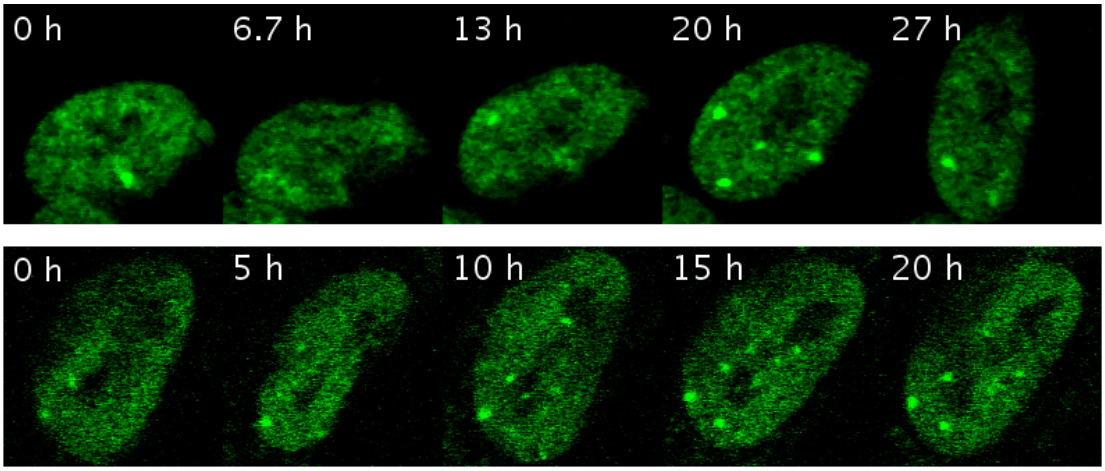

Figure 4. 53BP1 Damage Foci induction in unstressed (top) and stressed (bottom) MRC5 cells tratead with 20Gy γ irradiation measured in vitro using confocal microscopy.

48 hours after treatment with 20Gy of gamma irradiation the foci emergence more than doubled to 1.28 foci per hour and there was a dramatic shift in repair times with 20% of the foci resolved in less than 2 hours and 55% surviving beyond 8 hours (Figure 5) of which only 15% resolved (5 out of 33). Although the amount of foci with a lifetime less than 8 hours was greatly reduced in stressed cells, the mode of the distribution in these short lived foci remains the same, favouring repair within 2 hours of the foci forming.

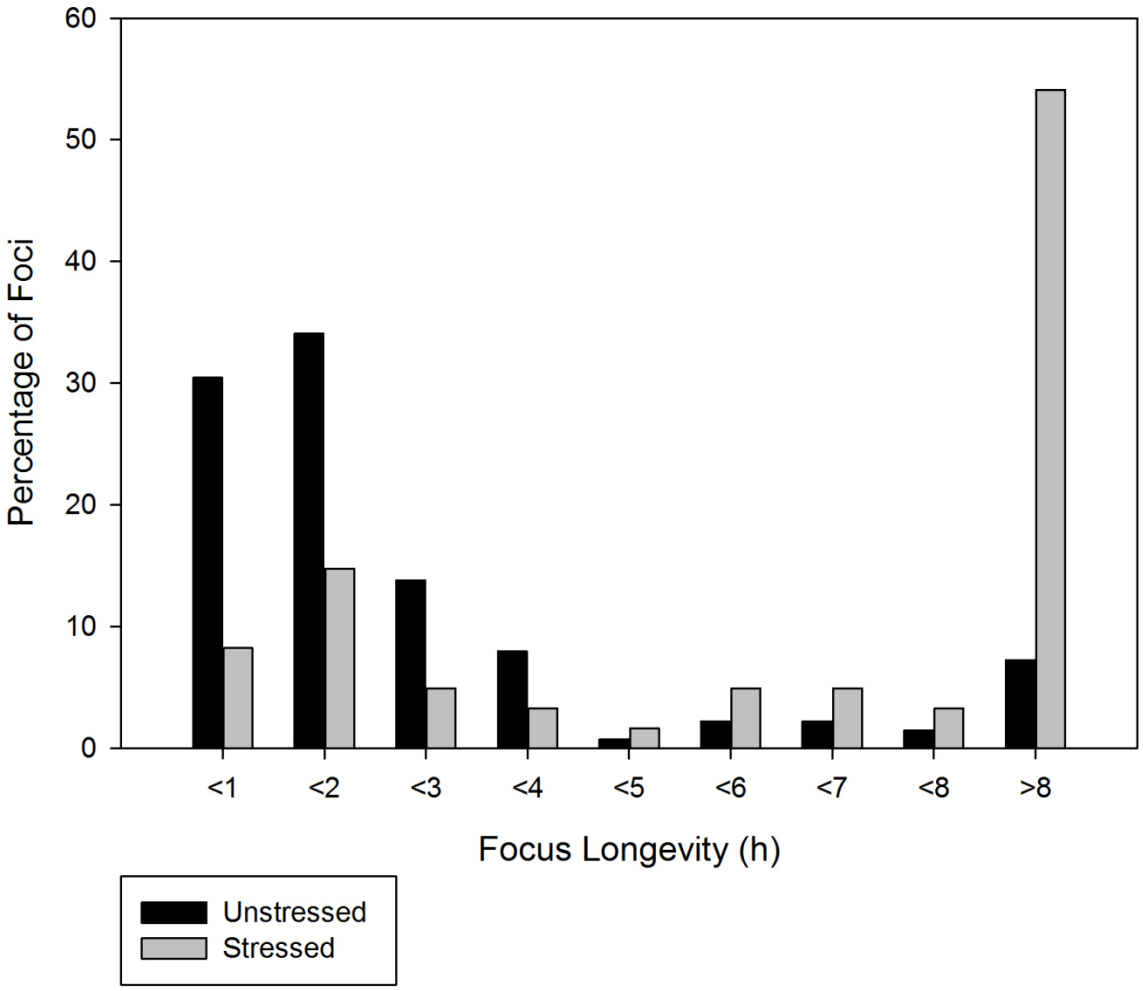

Figure 5. Foci Longevity of live MRC5 cells observed for 30 hours.

Since very few damage foci fully resolve once they have lasted more than 8 hours we viewed them as permanent damage foci. However if our understanding of the NHEJ system as a whole is correct all foci should eventually be resolved, the fact that they are not suggests that either these DSB are irreparable telomeric breaks (126) or there is a downstream effect that feeds back into the NHEJ causing permanence. Transient foci were observed in both resting and stressed live cells although stressed cells had a higher fraction of transient foci on average (Figure 6).

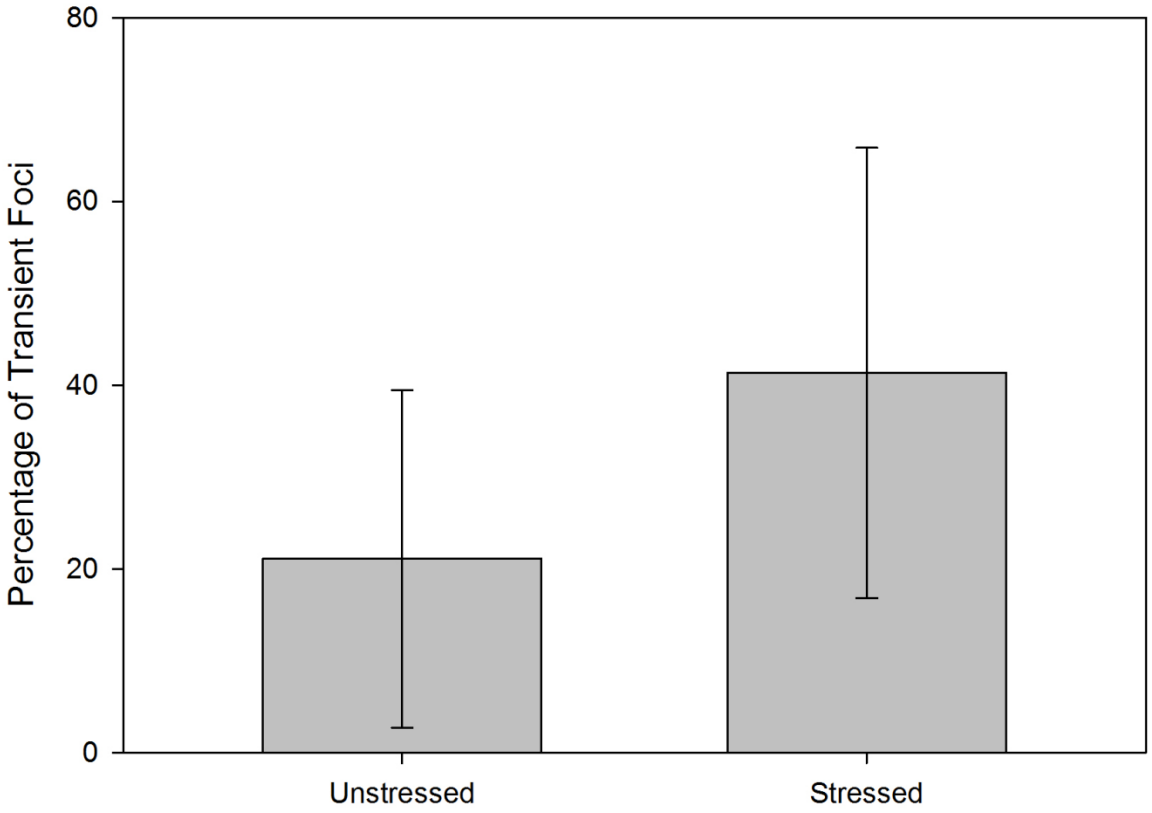

Figure 6. Percentage of transient Foci in MRC5 Fibroblasts. These are foci that disappeared and then reformed. 10 unstressed cells (53 Foci) and 6 stressed cells (135 Foci) were observed in total. Results are presented as mean ± SD.

Using the parameters calculated from work within our labs and the data available in published literature the model of the Ku mediated D-NHEJ pathway and the PARP-1 mediated B-NHEJ pathway was found at rest to produce very similar results to the live MRC5 cells with over half the breaks being resolved in less than 2 hours (Figure 7B and 7C) and a majority of remaining foci being resolved within 8 hours. Our model not only matched the short term foci dynamics, but also the long term dynamics (those of foci lasting longer than 8 hours). Cox regression comparison of simulated and experimental short lived foci survival curves yielded a p-value of 0.65, indicating no significant difference between the model and experiment. Since the foci longevity data was not used in the calculation of the kinetic rates of the model, the matching of the live cell data to the simulation is a positive validation of the unstressed model.

However, increasing ROS production of the unstressed model to represent the stressed state of a live cell 48 hours after being treated with gamma radiation yielded different short term (less than 8 hours) foci longevity distributions than those experimentally observed in

the stressed cells (Figure 7A and C) and instead appeared to have the same dynamics as the unstressed model. From this we concluded that the change in foci dynamics in stressed cells is not brought about by an increase in the amount of damage and natural stochasticity inherent in the system. However it is apparent that our understanding of the NHEJ mechanisms is good enough to explain what determines the repair dynamics in an unstressed cell.

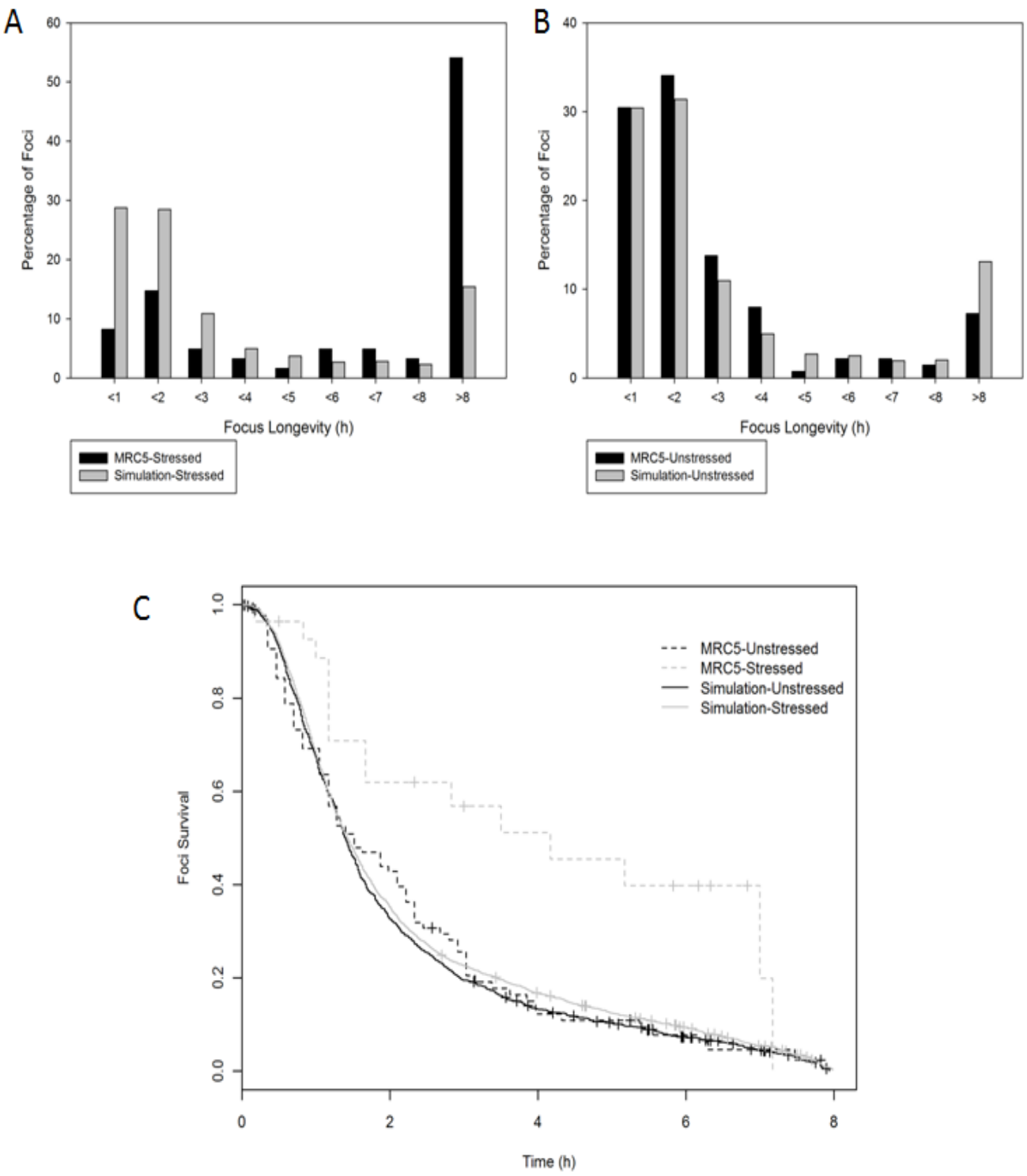

Figure 7. (A) Longevities of damage foci recorded in stressed MRC5 cells irradiated by 20 Gy of γ irradiation and the corresponding stressed D-NHEJ and B-NHEJ model simulations. (B)Longevities of damage foci recorded in unstressed MRC5 cells with unstressed D-NHEJ and B-NHEJ model simulations with ROS production increased 2.5 times. Simulated data shows no change other than an increase in the number of breaks produced. (C) Survival curves of short lived foci (8 hours and less) for resting and stressed MRC5 cells (dotted lines) and resting and stressed simulated data (solid lines).

Chapter 3: The Role of Oxidation in DNA Damage Repair

3.1 Introduction

Given that we were able to replicate unstressed foci dynamics with our SBML model but did not observe a change in damage foci dynamics when we increased the ROS in the model to levels the same as in the irradiated MRC5 cells 48 hours post gamma irradiation treatment we had to conclude something else happens to the cell's NHEJ system after irradiation.

Many proteins involved in cellular signalling pathways are redox regulated (127) therefore a change in the levels of ROS could have large impacts on the functioning of proteins by oxidising them. Important signalling proteins such as PKA and MEKK1 have been identified as being redox regulated by the oxidation of cysteine residues (128) and interestingly the Ku70/80 heterodimer has been shown to have a massive increase in dissociation from DNA when in an oxidised environment (125). Initially it was hypothesised that oxidation of Cys-493 residue on Ku80 was the potential cause of the dramatic shift in the dynamics however it was determined that oxidation of Cys-493 played at best only a minor role in the redox related binding and dissociation dynamics of Ku (129). The other cysteines on Ku80's surface and were not tested and the method by which Ku's binding activity is modified in an oxidised environment is still unclear.

Because the irradiation of cells causes production of large amounts of ROS it is highly plausible that Ku becomes oxidised at the same time that a cell's DNA is damaged during the treatment and that this increase in dissociation slows down repair by D-NHEJ and allows the slower B-NHEJ pathway to carry out more repair.

3.2 Methods

3.2.1 Model Adaptation

To test the hypothesis that Ku dissociation plays a role in the change in foci repair dynamics in irradiated cells we increased the rate of dissociation of Ku70/80 from the DSB in the

stressed model tenfold in line with observations made in (129) and simulated the model using Gillespie2 like we did with the previous versions of the model, running it 100 times simulating a 30 hour period of time with measurements of molecule numbers made every minute.

3.2.2 Ku 80 pK_a Shift Analysis

Cysteine residues that are ionised at physiological pH have an increased susceptibility to oxidation and redox regulation (130). To determine whether any of the cysteine residues within Ku 80 had this characteristic we used continuum electrostatics calculations to carry out pK_a shift calculations. The pK_a is the natural log of the acid dissociation constant (K_a) which is a measure of acids strength whilst in solution, the lower the pK_a the stronger the acid. By applying the knowledge of an amino acid's strength when free in a solution compared to that when it is part of a polypeptide we can calculate if the pK_a. If the amino acids pK_a becomes lower when in a polypeptide then it becomes a stronger acid meaning it is more likely it is to have become ionised (lost a proton) leaving it with a free electron which could then be removed by ROS or other oxidisers via oxidation.

Two PDB files of the Ku70/80 heterodimer, one bound to DNA (PDB ID: IJEY) and the other free (PDB ID: IJEQ) (74) were obtained from the RCSB Protein Data Bank (www.pdb.org) (131). The X-ray crystal structures within the files were protonated and had atomic partial charges assigned using PDB2PQR (132,133). The structures were then used to calculate the free energy change of ionisation of the cysteine residues 157, 235, 249, 296, 346 and 493 in the protein environment and isolated in solution, using the Adaptive Poisson Boltzmann Solver (APBS) (134). The obtained energy changes were then used to calculate each residue's pK_a shift using the method described (135) and detailed on the APBS website www.poissonboltzman.org

3.3 Results and Discussion

The number of breaks repaired in less than two hours dropped significantly and the number of breaks taking more than 8 hours to repair rose similar to stressed live cell (Figure 8A). Cox regression analysis produce a p-value of 0.88 indicating that there is no significant difference in the resolution times of short-lived foci (Figure 8B). This indicates Ku's increased dissociation from a DSB altering repair dynamics due to its redox sensitivity is enough to explain the observed shift in short term foci dynamics when cells are stressed with gamma radiation.

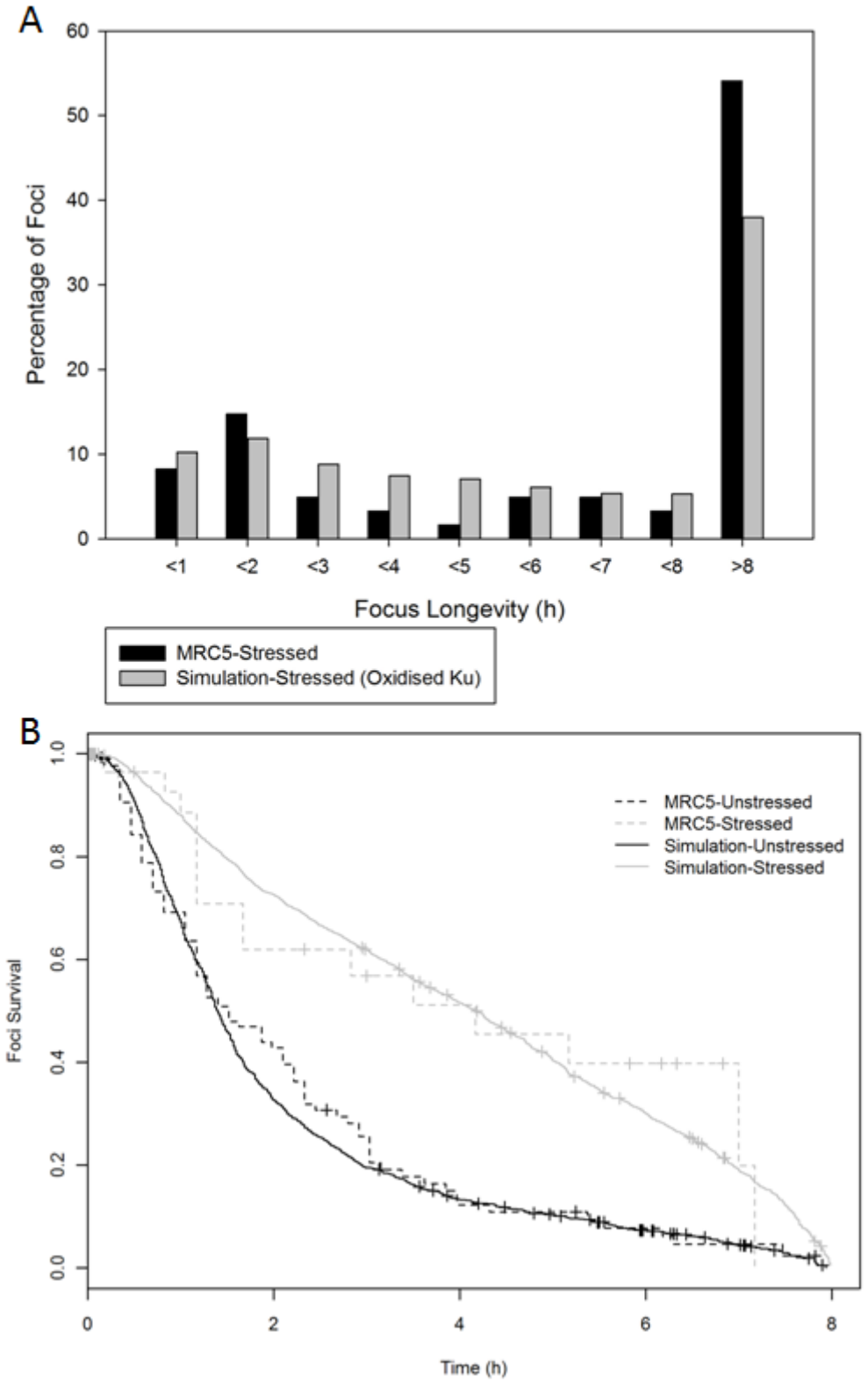

Figure 8. (A) Increasing the dissociation rate of Ku70/80's and DNA-PK from DNA in line with observations from the literature (15) results in a decrease in short lived foci similar to that of stressed live cell. (B)Survival curves of short lived Foci (8 hours and less) for resting and stressed MRC5 cells (dotted lines) and resting and stressed simulated data (solid lines). Stressed data was collected from the model with increased Ku70/80 dissociation from DNA DSBs.

Cysteine amino acids have a pK_a of 8.7 when isolated in solution (136) and shifts in the logarithmic pK_a to a value less that 7 when part of a polypeptide chain suggests that a cysteine residue in a protein is ionisable and therefore a viable target for oxidation via oxidisers such H_2O_2 (130). The calculated pK_a shifts for Cys-493 in Ku 80 when bound to DNA and unbound show a pK_a shift from 8.7 to 9.06 and 7.97 respectively (Table 2) . As neither is below 7 our calculations support the findings of (129) in that Cys-493 does not play a significant part in oxidation of the Ku heterodimer. The only surface cysteine to show a large enough drop in pK_a to be ionisable is Cys-249 (Figure 9) for which the calculated pK_a values are 5.59 and 4.39 when unbound and bound to DNA respectively. Moreover, it is close to the DNA binding site. This, together with the lowered pK_a values suggest that the residue could be oxidised with a concomitant effect on DNA binding and is therefore the potential cause of Ku's observed increase in dissociation from DNA when placed in a oxidising environment (125).

CYS	$\Delta xferG_A$	$\Delta xferG_{HA}$	pka shift
157	-1.49	-5.92	10.63
235	5.54	-0.57	11.36
249	-12.88	-5.73	5.59
296	3.71	-5.28	12.61
346	-0.41	-4.25	10.37
493	-4.89	-5.71	9.06

Table 2. Pka shift calculation results for the Cysteine residues on the surface of the DNA-PK component Ku 80. Cys 157,235, 249 296, 346 and 493 pKa shifts were calculated using the Ku 80 protein binding domain model 1JEQ from the RCSB Protein Data Bank.

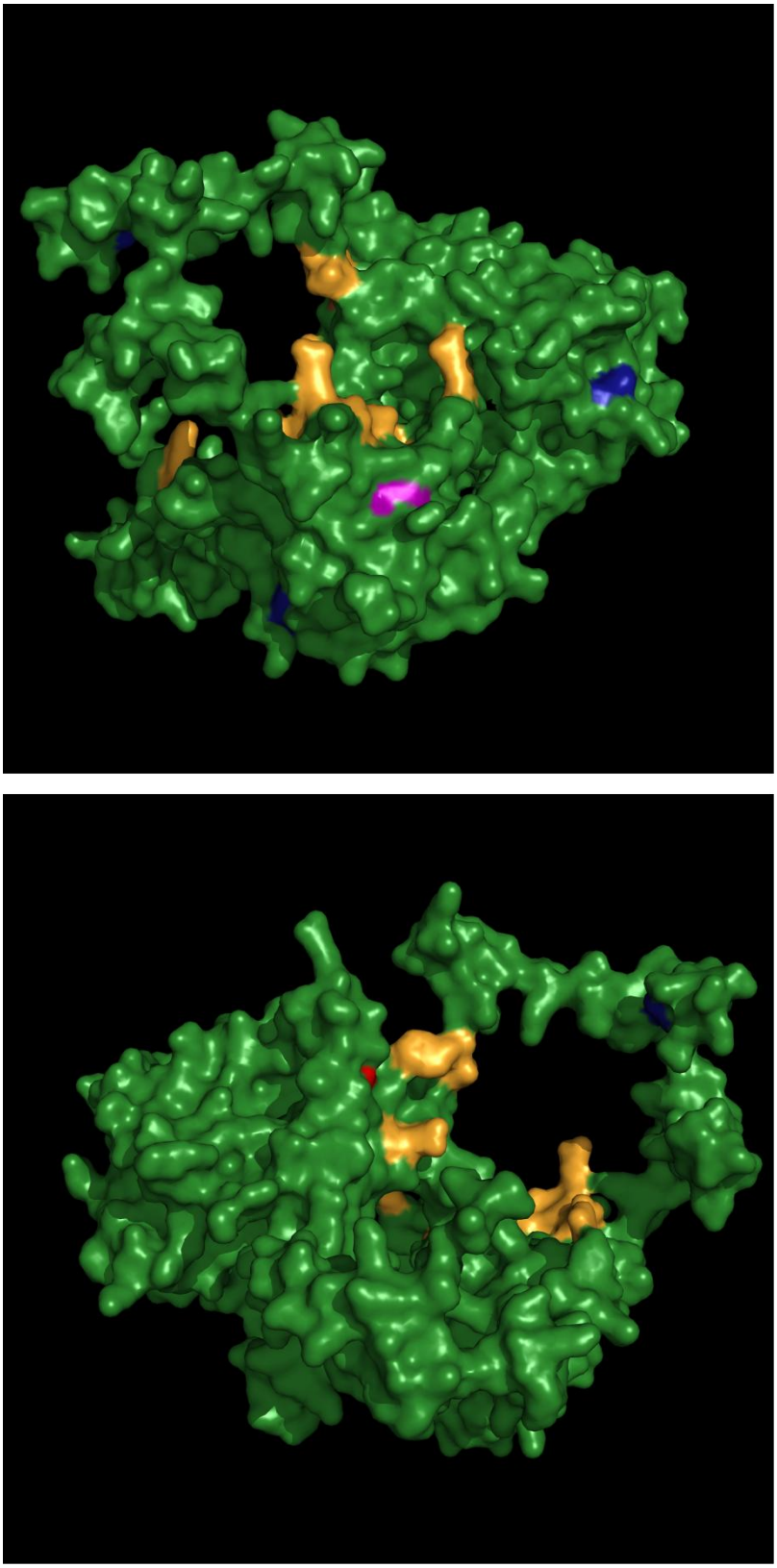

Figure 9. Crystal structures of Ku 80 front (top) and back (bottom), displaying the DNA binding domain (yellow), surface cysteines (blue) Cys-493 (red) and Cys-249 (pink).

Overall our results suggest that the cause of the shift in short term focus dynamics seen in stressed cells is not due to natural stochastic behaviour within a biological system but rather

due to an increased rate of dissociation of the heterodimer Ku70/80 from a DSB caused by the oxidising environment within the stressed cell. This increased dissociation alters the competition between Ku and PARP-1 for binding to the DNA, causing the latter to take place more often than it does in an unstressed cell.

Although the apparent competition between D-NHEJ and B-NHEJ can explain the short term NHEJ dynamics it does not explain those of the foci that last longer than 8 hours. We can speculate that the cause of the maintained long lived foci is the result of downstream pro-survival and pro-apoptotic pathways triggered by the presence of the DSB through signalling pathways, such as the p53/p21 signalling that feeds back into the damage repair mechanism further altering how it responds to damage over longer periods of time. When damage is caused, ATM phosphorylates H2AX which then also influences the p53, p21 and Chk1 pathways which go on to stall the cell cycle and/or trigger apoptosis. At the same time, whilst Ku70 is being used to repair double stranded breaks it is no longer suppressing Bax and its apoptotic function (92,93), and is no longer inhibiting the cell cycle arrest governed by FOXO4 (137). In later chapters, we take into account some of these downstream responses and their feedback; however as our model seems to have reached the limits of what SBML can currently handle another modelling approach is necessary to carry out this extension. The options we considered were the proposed arrays and sets package of SBML level 3 (www.sbml.org), or similar features of rule-based modelling or kappa calculus (138). One limitation that we found with the model was that due to its large size parameter sensitivity was not viable. Parameter sensitivity analysis is both computationally and time intensive for stochastic models as each permutation to a reaction's rate constant that is made to analyse its sensitivity has to be tested many hundreds of times to be able to account for the effects of stochasticity in the reaction. The larger the model is the more time is required to test sensitivity and unfortunately for our HNEJ model with its 1200 plus reactions made testing of the models sensitivity impractical. There is therefore a potential risk that a reaction in the model is extremely sensitive to small changes that could affect its dynamics. Fortunately given the nature of stocasticity and the large number of reactions in the model, it is likely very robust and therefore resistant to small changes in its parameters.

Throughout this investigation we have treated D-NHEJ and B-NHEJ as competing systems due to the observed competition between DNA-PK and PARP-1 for binding to a DNA end

(124,139). However Mitchell *et al.* (2009) proposed the hypothesis that PARP-1 and Ku work co-operatively to repair DSBs with 5' overhangs. The obvious way in which this system would function is that PARP-1 is utilised to loosen the chromatin around the damage site to allow the repair proteins greater access to the site of damage to allow repair to take place. However recent work has also produced evidence of DNA-PK and PARP-1 forming a complex (140) that can bind to the site of damage at the same time. Either way, preliminary modelling of the co-operation of Ku and PARP-1 (results not shown) does not significantly alter the observed dynamics of damage repair proposed in our model. We believe this is because ultimately the ligation of the DSB can only be undertaken by a single ligase enzyme, be it LiIII or LiIV. However, given that PARP-1 has roles beyond repair of a DSB and is a potential target in cancer therapy (68), knowing precisely how it functions in the DNA damage response, and how this interaction is regulated, is of great importance for development of better therapies and is vital to our understanding of how the various systems of DNA repair have evolved.

What is apparent from our work is that DNA repair and by extension cell survival is not a straight forward process: rather than a single factor determining the outcome of the damage response, it is more likely the interplay between various mechanisms and processes influencing the cell's response and therefore its survival. This capacity for interplay is clear when the system's major players and their roles are viewed as a whole.

Currently, although our knowledge of individual components of the entire NHEJ DDR and its downstream effects is quite well informed and ever growing, how these systems function as a whole is not. What is obvious is that the classical approach to investigating these systems in isolation is not enough; the systems biology approach and creation of large computational models using experimentally derived data provides us a with the capacity to monitor large scale interactions between known systems that traditional experimentation alone cannot. Our model is the first stochastic model of NHEJ that attempts to model both the D-NHEJ and B-NHEJ pathways as well as the formation of the damage foci that are often visualised in wet lab experimentation as the marker of DSB presence, and is the first step in producing a large scale systems model of a cell's response to DNA damage. It has allowed us to rule out that the observed change in foci dynamics could occur without a relative shift in

the contributions of the two NHEJ pathways, whilst showing that the redox sensitive change in Ku—DNA binding affecting D-NHEJ provides a plausible mechanism for it.

Chapter 4: Rule based modelling of the NHEJ and the p53 mediated DDR

4.1 Introduction

A cell responds to DNA damage by activating the DNA damage response (DDR) which is composed of repair mechanisms such as BER, NHEJ and HR (65) and downstream cellular signalling networks that govern the appropriate cellular response (63). Under favourable conditions the damage will be quickly repaired but if damage is sustained cellular senescence or even cell death may result (102). Even in the case that damage is repaired this repair may not be accurate and can lead to the induction of more damage and genomic instability for the surviving cell as well as its progeny (118). The DDR is a complex system and to gain a full understanding we must consider the repair and signalling process together. In this chapter we will consider an integrated model of NHEJ and p53 signalling.

As we have described, double strand breaks (DSB) are repaired by either Non-Homologous End Joining (NHEJ) or Homologous Recombination (HR) depending on the stage of the cell cycle where damage occurs (141). The presence of the DSB also causes the activation of signalling pathways via phosphorylation of the tumour supressing protein p53 and of MDM2, by either of the phosphatidylinositol 3-kinase-related kinases (PIKKs) ATM and ATR (142). These phosphorylation events cause a decrease in the binding of p53 by MDM2 thereby releasing it from MDM2-dependent degradation which leads to an increase in the levels of p53 in a cell. Once phosphorylated, p53 triggers the transcription of p21 which induces the transcription of GADD45 which induce cell cycle arrest at G1 or G2/M respectively (143).

At the same time as triggering cell cycle arrest, p53 and p21, also trigger the process of senescence. This is initiated by a large change in gene expression that leads to the production of cyclin-dependent kinase inhibitors (CDKIs) which inhibit the activity of various cyclin dependent kinases resulting in the activation of retinoblastoma tumour suppressor gene product (pRb) (144) which causes the cell cycle arrest to become permanently maintained and the cell entering a state of permanent growth arrest in which it no longer proliferates. The altered gene expression also causes a repression of genes that code for

proteins involved in cell cycle progression and over expression of genes coding for secretory proteins which alter the cell's external microenvironment (30).

Interestingly, at the same time as promoting pro-survival responses p53 also initiates a pro-death response by inducing apoptotic pathways (145). In the presence of DNA damage, p53 levels rise and promotes the production of Bax and PUMA which cause the release of Cytochrome C (146), which, along with APAF-1 and procaspase-9, form a complex called the apoptosome which cleaves the procaspase-9 to make caspase-9 (147). Caspase-9 causes the activation of caspase-3, caspase-6 and caspase-7 which in turn begin the organised degradation of the cellular organelles. p53 can also activate the extrinsic apoptotic pathway by inducing the production of Apo-1, a tumour necrosis factor receptor (TNF-R) which induces apoptosis by activation of caspase-9 via caspase-8 activation (148). p21 provides an inhibitory influence on these p53-dependent apoptotic pathways (149).

As a cell's fate is being decided by systems downstream of p53 and p21, their actions feed back into the DNA damage repair mechanism via p38 by enhancing the production of Reactive Oxygen Species (ROS)(48). Increases levels of ROS induce further DSBs leading to further activation of DDR which in turn causes more ROS production via p38. DNA damage thereby primes a cell for both death and survival by the opposing actions of p53 and it is the balance between the various signalling systems and the capacity of the DNA repair mechanisms to resolve the damage - and the additional p38-dependent damage - before the activity of pro-survival pathways are superseded by activity of the pro-death pathways. This competition is an ideal issue to study with systems modelling.

In Chapter 2 and 3 we presented an SBML model of NHEJ that we used to investigate the role of stochasticity and redox state on the altered DNA damage foci dynamics observed in human MRC5 fibroblasts when exposed to gamma irradiation. Whilst our model was able to accurately simulate the foci dynamics in non-irradiated cells and the dynamics of short-lived foci in irradiated cells, it was not able to simulate long-lived foci. In the live cells the majority of the foci that lasted more than eight hours were observed to not resolve permanently indicating that the DSB that had formed had not been repaired whereas in our model all breaks would eventually be repaired and the foci formed eventually disappear permanently. We concluded that the dynamics of the short-lived foci was determined by the interaction

of the two repair mechanisms of NHEJ that compete to repair DSB, but that the dynamics of long lived foci were being influenced by factors external to the repair pathways linked to cell signalling and cellular senescence.

It has been shown that when cells senesce, Ku70/80, the heterodimer that mediates the DNA-PK dependant NHEJ, shows a decreased rate of binding to DNA and its abundance is halved (96) and PARP-1, the mediator of Backup NHEJ, is almost totally depleted (150). It is possible that this change in key repair components due to senescence causes the observed shift in long term foci dynamics rather than treatment of gamma irradiation and associated increase in ROS. However, when we irradiate a cell and observe its damage foci under a microscope we cannot be certain how long it has been senescent or even if it is senescent. Therefore to accurately model the dynamics of the foci of a live cell treated with irradiation to induce senescence we would have to model the DDR events that lead to cellular senescence followed by the transition of the cell into the senescent state.

Unfortunately our model of NHEJ was already at the upper limits of size for stochastic simulation due to the requirement to model the repair of individual breaks making extension to include the downstream DDR infeasible. Recently rule-based modelling languages such as BioNetGen and Kappa have been developed to allow for the creation and simulation of complex large scale networks (151,152). Traditional systems modelling tools using SBML (49) are based on a collection of distinct model species reacting together to produce new species. For example, the phosphorylation of one molecule in a reaction-based model would produce an entirely new species whereas in rule-based model the species is defined with a set of components that represent structural or functional elements of the molecule and the rules of the model change the state of the components to represent various interactions and reactions. This lets you model molecules with details of its various binding domains and chemical modifications such as phosphorylation sites and to then use rules to govern how different molecules interact. The advantage this has over reaction-based modelling from a techniques perspective is that it allows for the creation of interactions of complex molecules more quickly with a single rule rather than having to create a reaction for each possible permutation of reactants and a new model species for products of the particular reaction. As an example, consider a molecule called X, with several residues that could be phosphorylated, then in a reaction based model a new

species would need to be created for every possible combination of phosphorylation. In a rule based model the definition includes all 7 sites with their phosphorylation status simply left as an on or off option. Only those combinations that are relevant to the biology are therefore considered which results in a dramatic computational saving. The lack of a long list of reactions and species in a rule based model also means that the file produced is much smaller and far less complicated than an SBML file which make editing and modification of a rule based model far simpler. Beyond their ease of creation, we have also found that large rule based models also have a much quicker simulation speed when simulated using tools such as NFsim (153) than SBML models using programs such as Copasi (154) and Gillespie2 (51).

The use of rule-based modelling opened up a path of development for our NHEJ model that was previously unavailable and allowed for the extension of the model with mechanisms downstream of DNA damage repair. One of the key goals of systems biology since its conception has been the capacity to integrate models of various interconnected systems to explore how they function as a whole, however very little integrative work has been published. By recoding and combining our SBML model of NHEJ and a model of p53 and p21 signalling previously published by researchers from our group (48) we have developed and tested a large scale model of the DDR response to DSB using the BioNetGen modelling language and the NFsim stochastic simulator.

4.2 Methods

4.2.1 Live cell Foci dynamics

Methods for carrying out the measurement of induction and longevities of damage foci in human MRC5 fibroblasts are reported in Chapter 2.

4.2.2 Model Creation

In the NHEJ SBML model, a Source of ROS produces ROS which can either degrade or damage a site of DNA. If the DNA was damaged repair proteins of both the Ku mediated,

DNA-PK Dependent NHEJ (D-NHEJ) and/or the PARP-1 mediated, Back-up NHEJ (B-NHEJ) are recruited and a repair complex of one of the pathways is formed which eventually ligates the DSB returning it to its original undamaged form. MRN and ATM are activated in the presence of a DSB and cause the phosphorylation of H2AX to γH2AX followed by the formation of the Damage Foci. The NHEJ model contains over 600 species and 1400 reactions to accurately simulate the induction of individual DSB by NHEJ and the formation and resolution of the damage foci at that specific break.

The p53 SBML model also starts with the induction of a DSB by ROS produced by a Source of ROS however unlike the NHEJ model it only has a single mass action reaction to represent the repair of the damage. When a DSB is present ATM becomes activated and phosphorylates p53 and MDM2 which are created from their respective mRNAs (MDM2 mRNA requires p53 to begin its transcription). These phosphorylation events inhibit the binding of p53 and MDM2 which in turn reduces p53 degradation. The phosphorylated p53 causes the production of p21 by its mRNA, p21 then causes the production of GADD45 which in turn phosphorylates p38, which then triggers the production of more ROS in the model.

We began the conversion of the two models to a single BioNetGen rule based model by first identifying the distinct species of the model that could represent every other species in the model by either version modification or a complex. For the NHEJ model we identified the Source of ROS, ROS, DNA, Ku, DNA-PKcs, LiIV, PARP, LiIII, MRN, ATM and H2AX as distinct species/molecules and for the p53 model we identified Source of Damage, ROS, DNA, ATM, p53 mRNA, p53, MDM2 mRNA, MDM2, p21 mRNA, p21, p38 and GADD 45.

Once the basic species/molecules are established in the model we then identified the components such as binding sites and phosphorylation sites that each one would need to be able to undergo the reactions present in the original model (See list below for summary of the molecules and their components in the BioNetGen model).

In the model, the Source of ROS and ROS itself have no components as they are involved in simple reactions and are not modified or do not bind to anything. The DNA species was assigned a numbered ID so that each DSB caused could be monitored individually. The DNA DSB was defined by giving a DNA component called ‘site’ which could be in an undamaged

state (ok), have a simple DSB (sdsb) or a complex DSB (cdsb). Whereas the original SBML model of NHEJ was capped at twenty theoretical break sites due to size limitations on the simulation of SBML models, we were readily able to model fifty sites in the rule based model. As the histone H2AX is part of a DNA chain we made it a component of the DNA species called h2ax that could be in one of three states, unphosphorylated (u), phosphorylated (p) and within a damage foci (foci). The Ku 70/80 heterodimer required a component to represent its binding to the DSB (dna); another to allow for the binding of DNA-PKcs to form the DNA-PK complex (cs); and finally a component to represent whether cysteine 289 (cys) was in a reduced (red) or an oxidised (ox) state. The DNA-PKcs needed components to represent its binding to Ku70/80 (ku), LiIV (liIV) and a third to indicate whether it had undergone auto-phosphorylation (psite~u~p). LiIV was given a single component to represent binding to DNA-PKcs. PARP-1 was assigned a component to facilitate its binding to the DSB (dna) and another to allow the binding of LiIII (liIII) and the LiIII molecule itself was given a single component so that it could be bound to PARP-1 (PARP).

In the NHEJ SBML model, ATM and MRN were modelled as single molecules located at a specific site of damage to facilitate the phosphorylation of H2AX which eventually form part of the damage focus. However in the p53 model, a pool of ATM was modelled separately so that could it could be activated by the presence of DNA damage and in turn cause the phosphorylation of p53 and MDM2. To merge the models we modelled the ATM with an active and inactive state (state~0~1) but gave it a binding H2AX binding domain (h2ax) so that a molecule of it could also become part of the damage foci as it does in the NHEJ model.

The molecule P was created to induce the transcription of p53 mRNA. The P molecule, mRNA molecules and GADD45 were modelled without any components as they do not undergo any alterations or bindings in the SBML. As p53, MDM2 and p38 all had the capacity to undergo phosphorylation each was given a component with an unphosphorylated and phosphorylated state (psite~u~p). As p21 was produced in 2 steps in the p53 SBML model to simulate its translation dynamics we gave it a component called step with 2 states (1, 2 and 3) where state 3 would represent the final product of the p21 synthesis. In summary the definitions for each molecule are:

Source_of_ROS(); ROS(); DNA(id~1~2~3…~50,site~ok~sdsb~cdsb,h2ax~u~p~foci); Ku(dna,cs,cys~red~ox); DNAPKcs(ku,liIV, psite~u~p); LiIV(cs); PARP(dna,liIII); LiIII(PARP); ATM(state~0~1,h2ax); P(); p53_mRNA(); p21_mRNA(); MDM2_mRNA(); GADD45(); p53(psite~u~p); MDM2(psite~u~p); p38(psite~u~p).

In addition to the active molecules of the system some special molecules were added to the model to handle degradation and destruction of other molecules (D and Sink) as well and a number of molecules to allow for timed events such as an irradiation event (T, Time and IR):

Sink(); D(); T(); Time(); IR()

Each of the reactions from the original two SBML models were then re-created in the rule based model using the molecules defined above. Rate constants were derived from the original models although some reactions such as the recruitment and binding of the repair proteins were combined to enable quicker simulation of the model. Using functions and the special molecules we also recreated a timed irradiation event used in the p53 model to simulate the treatment of a cell with gamma irradiation (48).

4.2.3 Modelling the senescent change

In live cells p21 is the major driving factor behind the transition into senescence due to DNA damage. When its level increases due to damage being present the pro-senescence pathway becomes active, but if the levels of p21 drop via its natural degradation and a reduction in the transcription of its mRNA by p53, then senescence can be avoided. To recreate this behaviour in our model we created a molecule called Sen:

Sen (int~1~10~PLUS~MINUS,State~happy~sen)

Sen has a component made up of integers between 1 and 10 which could be increased or decreased depending on the level of p21: high p21 causes the states integer to increment up and low levels cause it to fall. If the int component became 10 then we would consider the cell to have become senescent and a reaction takes place that changes a second component called State from the state happy to sen. The presence of the molecule Sen with

the component state sen would trigger a number of functions in the model that reduce the levels of Ku70/80 and PARP-1 as well as reduce Ku's ability to bind to a DSB.

4.2.4 Calculation of ROS production in MRC5 cells

To better calibrate the levels of ROS production during senescence in the model we measured the rates of the release of hydrogen peroxide (H_2O_2) – the most common ROS in biological systems - from cultured cells using Amplex ®Red reagent (Invitrogen, A12222). Amplex ®Red (10-acetyl-3,7-dihydroxyphenoxazine) reacts with H_2O_2 in a 1:1 stoichiometry to produce the red-fluorescent oxidation product, resorufin, in the presence of horseradish peroxidase. The cells were trypsinised and resuspended in culture media, and the time courses of resorufin appearance were followed fluorometrically at 37ºC at an excitation 544 nm and an emission 590 nm in a black bottom 96 well plate using a FLUOstar Omega (BMG Labtech). Each well consisted of 150,000cells, 50µM Amplex ®Red and 2U/ml horseradish peroxidase. Known amounts of H_2O_2 were added to blank wells to construct the H_2O_2 standard curve in order to convert the fluorescence arbitrary units to moles of H_2O_2. (Figure 10).

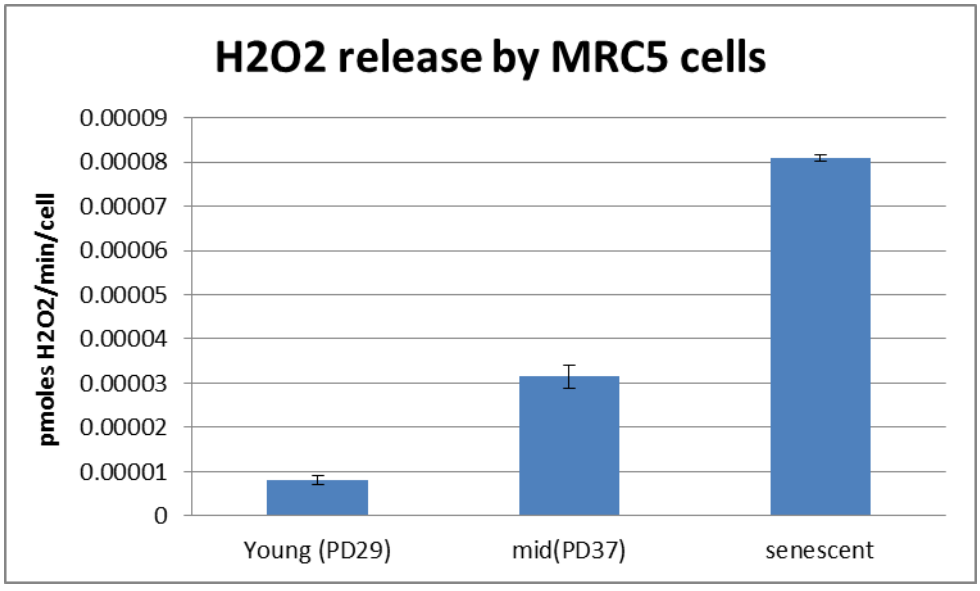

Figure 10. Histogram of ROS produced in pmoles per minute per cell in young, middle aged and replicatively senescent cells (PD refers to the calculated population doubling of a cell). Each group was tested three times. Results are presented as mean±SD.

4.2.5 Model Simulation

Simulation of all versions of the model was carried out using the network free stochastic simulator NFsim (153) running on a desktop PC.

Initially the model was set up to simulate a cell that had not been treated with gamma irradiation (unstressed). 500 simulations were carried out for the unstressed model each of which covered a thirty hour time period, with measurements of the molecules in the model taken every 1 minute.

To simulate the effects of treatment with gamma irradiation of cells we simulated the model for a period of 3 hours to allow for potential formation of DSBs before treatment irradiation, in a manner similar to how they can be induced in live cells before initiating a timed event to induce a large spike of ROS molecules for 5 minutes. The model was then simulated for 78 hours to correspond with the live cell experiments where the cells were left for 48 hours before being observed under the microscope for 30 hours.

Simulations of the model in an untreated state with decreased (20%, 40%, 60%, 80%) or increased (200%, 500%, 1000%) levels of the environmental ROS were then carried out.

We then simulated the treatment of MRC5 cells with greater and lesser amounts of gamma irradiation by increasing and decreasing the rate constant (initially 2000) in the timed event that caused the peak of ROS by a factor of two and five (rate constants of 400, 1000, 4000 and 10000).

Lastly we ran the model in its unstressed format at the various levels of background ROS production as tested above with either the Ku or PARP-1 levels reduced to 0 followed by simulations of stressed model with either Ku or PARP-1 reduced to 0.

4.3 Results and Discussion

More than 60% of DNA damage foci that were observed in the live unstressed MRC5 cells were resolved completely within two hours of being formed (Figure 11) and only 7% of the foci recorded had a longevity greater than 8 hours with only a 30% of these cells actually

being resolved. After treatment with 20Gy of gamma irradiation, a dramatic shift in foci longevity times was observed, with 20% of the foci that were induced in a 30 hour period, 2 days after treatment resolving in less than 2 hours. 55% of the foci lasted more than 8 hours of which only 15% were resolved.

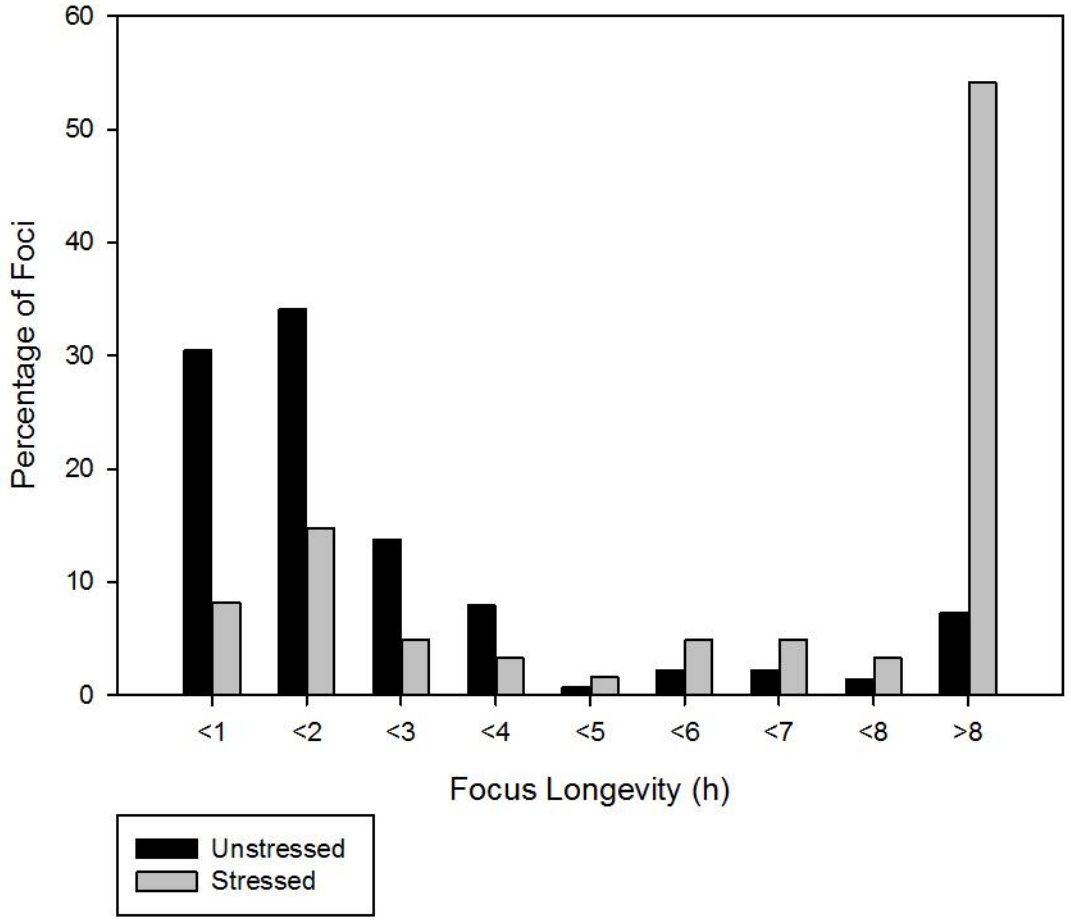

Figure 11. Foci Longevity of live unstressed MRC5 cells and stressed MRC5 cells treated with 20 Gy γ irradiation observed for 30 hours. This histogram is a reprint of Figure 5.

In addition to phosphorylating H2AX to initiate creation of the damage foci, ATM phosphorylates p53 which due to its interaction with MDM2 causes its levels to rise. This rise is countered however by the natural degradation which makes the level fall again, causing the levels of p53 to oscillate with greater amounts of DNA damage resulting in higher peak levels of p53. p53 causes an increase in p21 which in turn causes an increase in ROS production in the cell via p38 activation. This feedback loop is generally weak (Figure11A) in resting cells as the level of DNA damage is generally low. However it is still

possible to observe the feedback loop in some simulations of the unstressed model (Figure 12B and 12C).

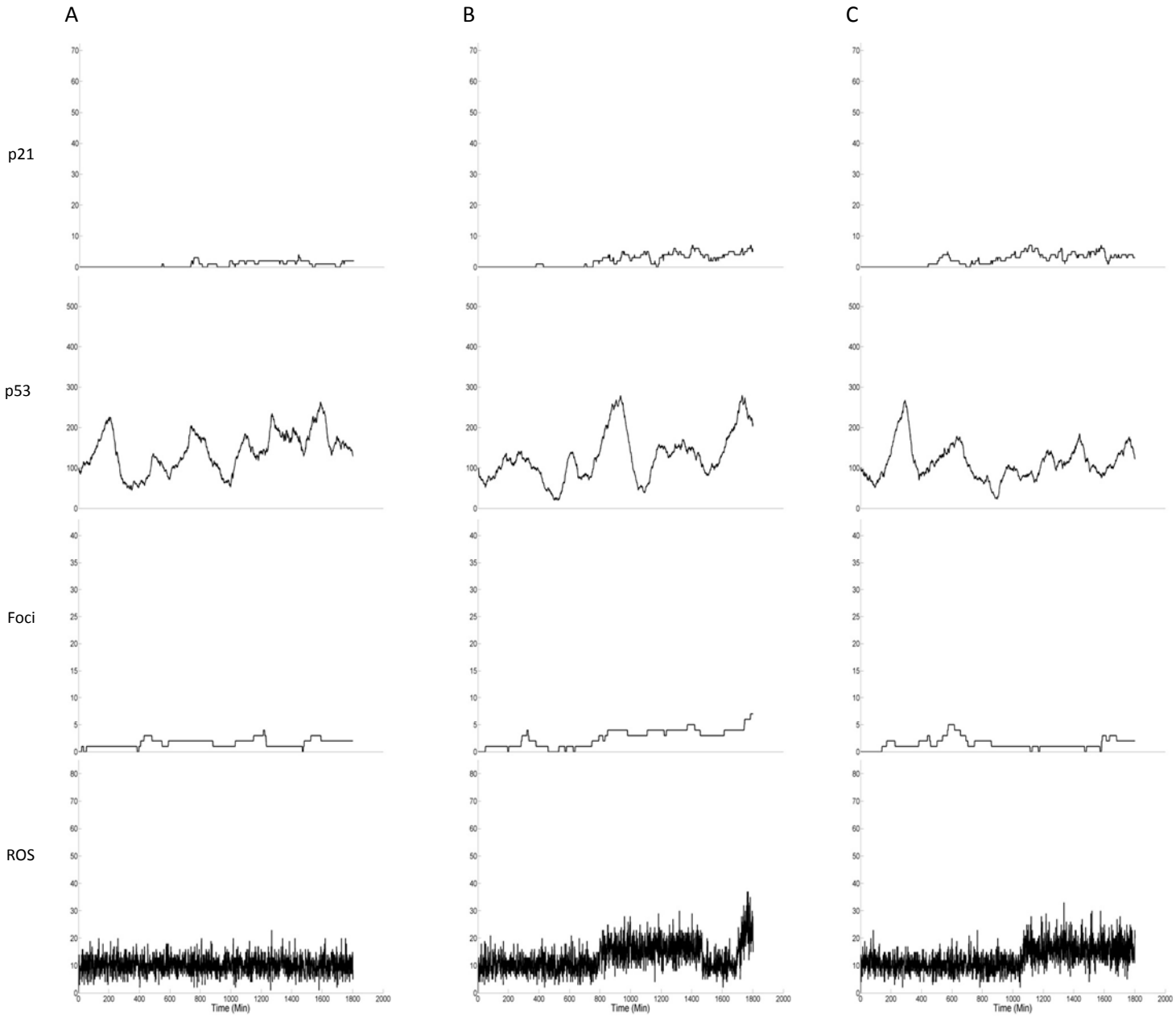

Figure 12. Time courses for 1800 minutes of three simulations under unstressed conditions showing molecule numbers of ROS, DNA damage Foci, p53 and p21.

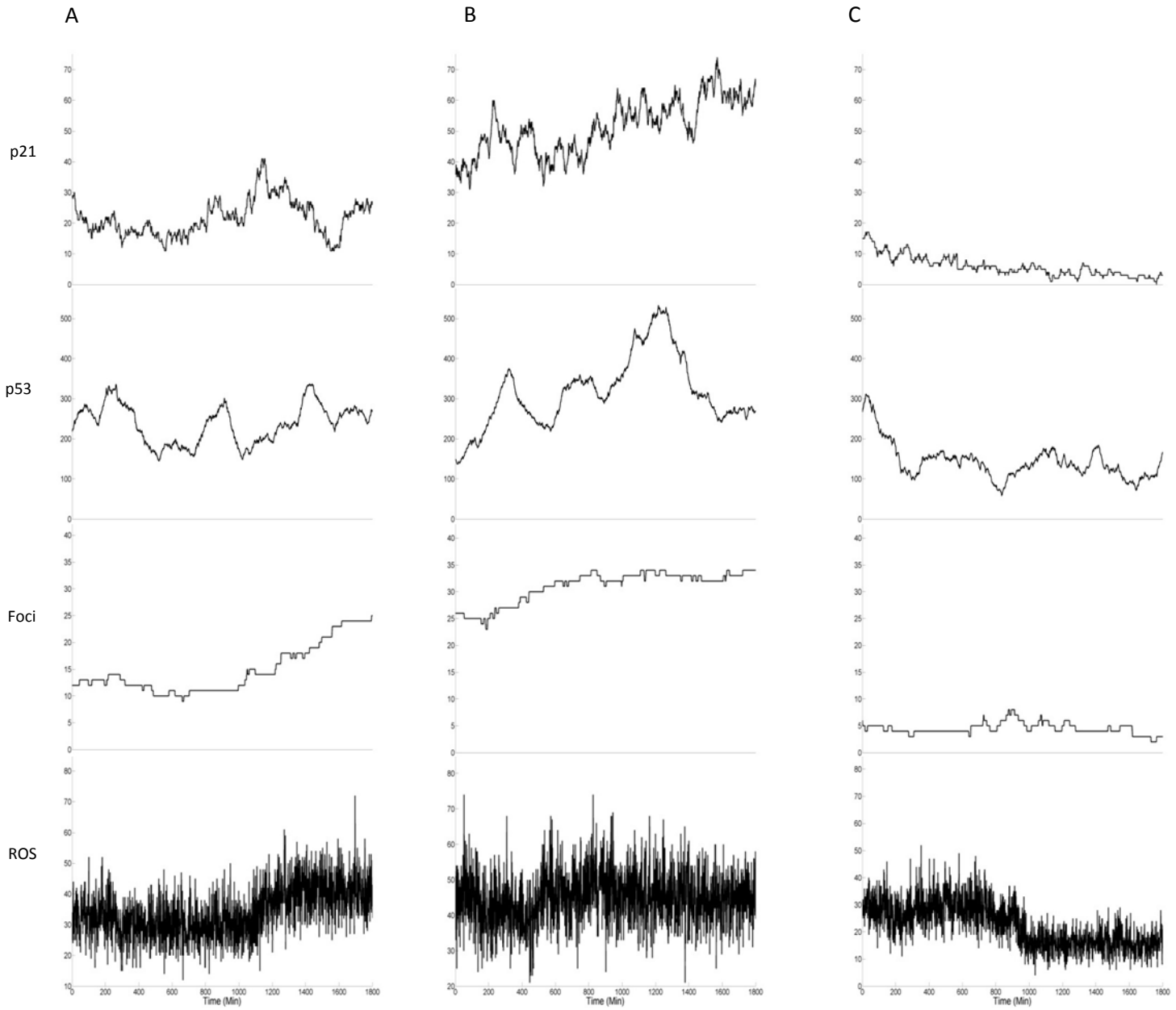

Figure 13. Time courses for 1800 minutes of three simulations under stressed conditions showing molecule numbers of ROS, DNA damage Foci, p53 and p21.

The feedback is much more noticeable in cells that have been treated with gamma irradiation where the repair dynamics, slowed by the reduction in the amount of Ku70/80 and PARP-1 together with the decreased activity of Ku70/80, results in the number of breaks present at any one time increasing. Moreover this is further increased due to the production of ROS via strength of the p53-p21 response (Figure 13A and 13B). However we also observed that some of the simulated cells that are treated with irradiation can recover from the induced damage early enough to avoid senescence and so have a damage profile more similar to basal cells (Figure12C).

Overall the simulation results from the unstressed and stressed model show a similar pattern of foci dynamics in the short lived damage foci (Figure 14A and 14B). Cox Regression Analysis of the entire unstressed simulation compared to the unstressed live cell data and stressed simulation data compared to the stressed live cell data yielded p-values of 0.65 and 0.315 respectively indicating that there is no significant difference between longevities of the foci in the live cells and those of the simulated foci (Figure 15) under stressed and unstressed environments. None of the unstressed simulations were observed to go into senescence, whereas 85% of the cells in the stressed simulations had senesced by the end of the 30 hour observation period. Looking at the complete activity of the stressed model, including the period of time in which it was irradiated, we observe a spike of DNA damage that that coincides with the irradiation event (Figure 16) followed by a period of recovery where damage is repaired relatively quickly which in turn is followed by a slow rise in the number of damage foci as the effects of the feedback cause more breaks to occur.

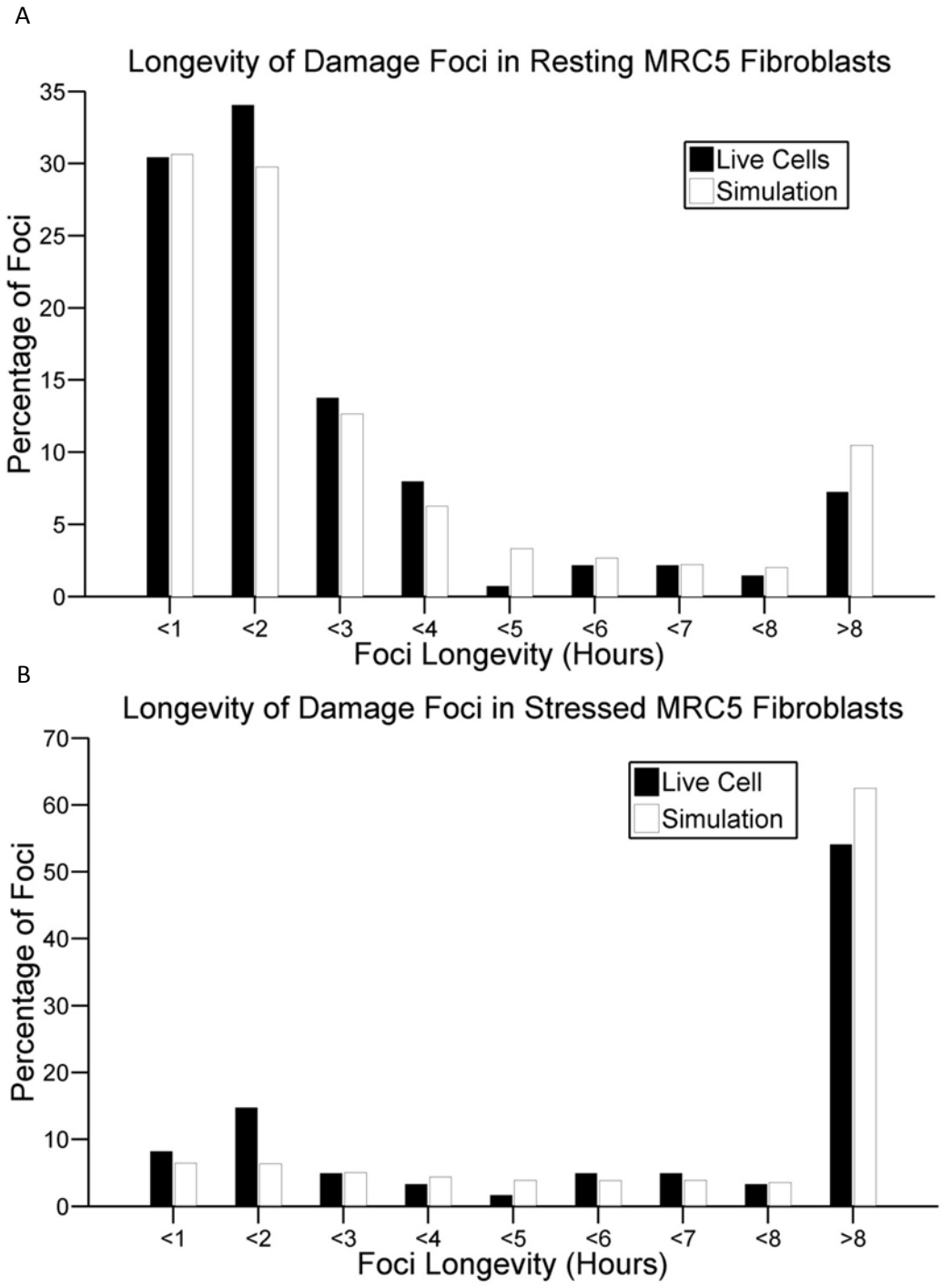

Figure 14. (A) Longevities of damage foci recorded in unstressed MRC5 cells and the unstressed NHEJ DDR model simulations. (B)Longevities of damage foci recorded in unstressed MRC5 cells and the stressed NHEJ DDR model simulations after γ irradiation treatment.

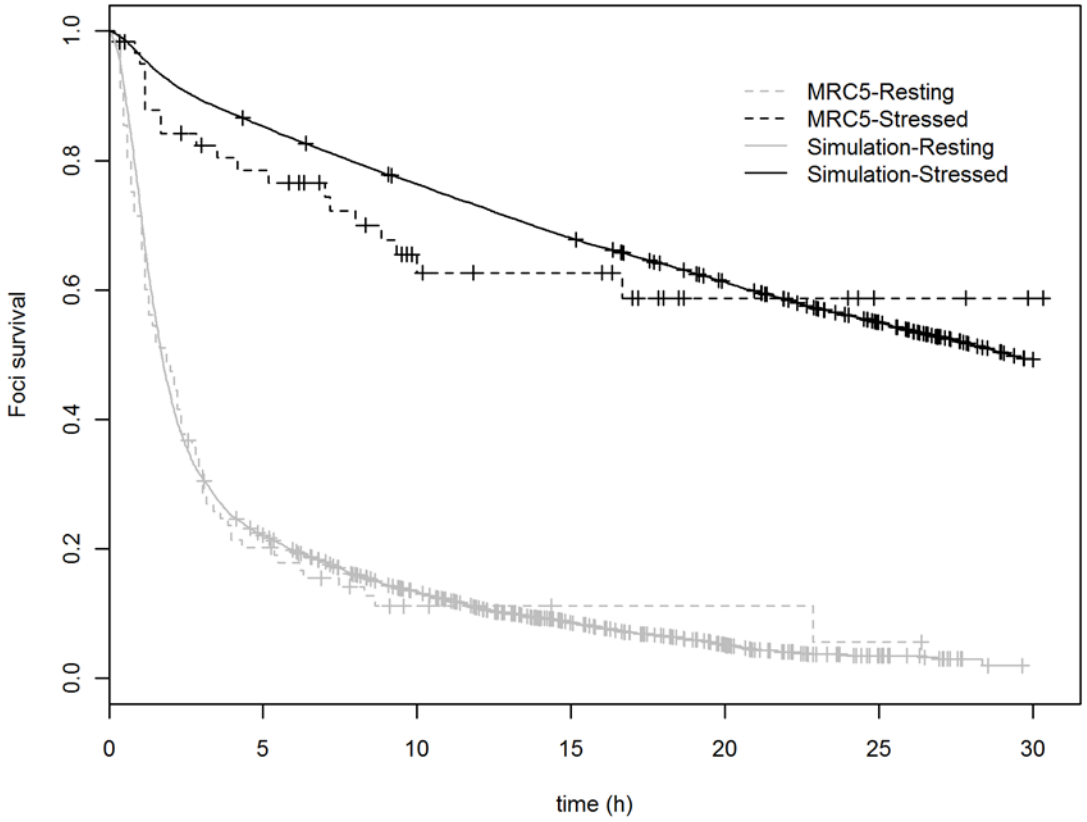

Figure 15. Survival curves of all damage foci for resting and stressed MRC5 cells (dotted lines) and resting and stressed simulation of rule based NHEJ DDR model (solid lines).

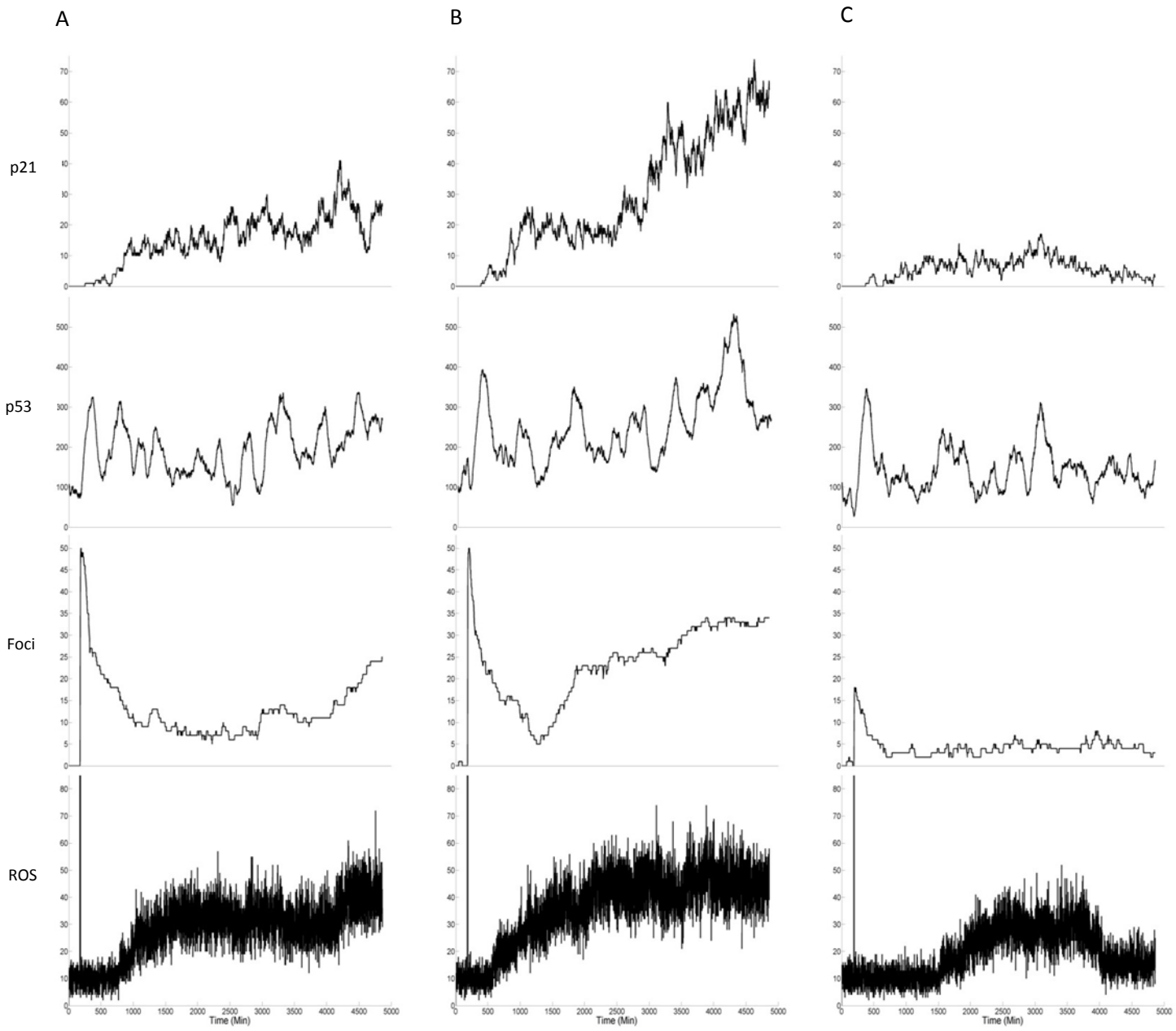

Figure 16. Time courses of ROS, DNA damage Foci, p53 and p21 molecules (bottom tow to top) present in simulations of model with (A) both Ku and PARP-1 intact, (B) model without Ku, and (C) model without PARP-1.

With the model simulation matching well with the observation in the live cells, we went on to investigate the role that various levels of ROS, from both the intracellular environment as well experimentally induced, play on the activity of the major components in the model. By simulating the model with lower and higher levels of basal ROS production to represent less and more stressful environmental conditions in the model we were able to observe how our model functions under various environmental conditions from very low background damage to extremely high levels (Figure 17A). Even without an irradiation event, higher levels of basal ROS production results in a greater number of breaks being induced (Figure 17B) over time. This higher number of breaks causes an increase in the amount of p53 molecules present, although the difference in the amount present at lower levels of ROS production is very similar (Figure 18A). This rise in turn results in increased levels of p21 (Figure 18B) which causes the production of more ROS. The strength of the feedback loop is greater in the model with the higher production of basal ROS as seen in the greater increase in the average levels of ROS towards the end of the 30 hour observation in the models with higher production constants.

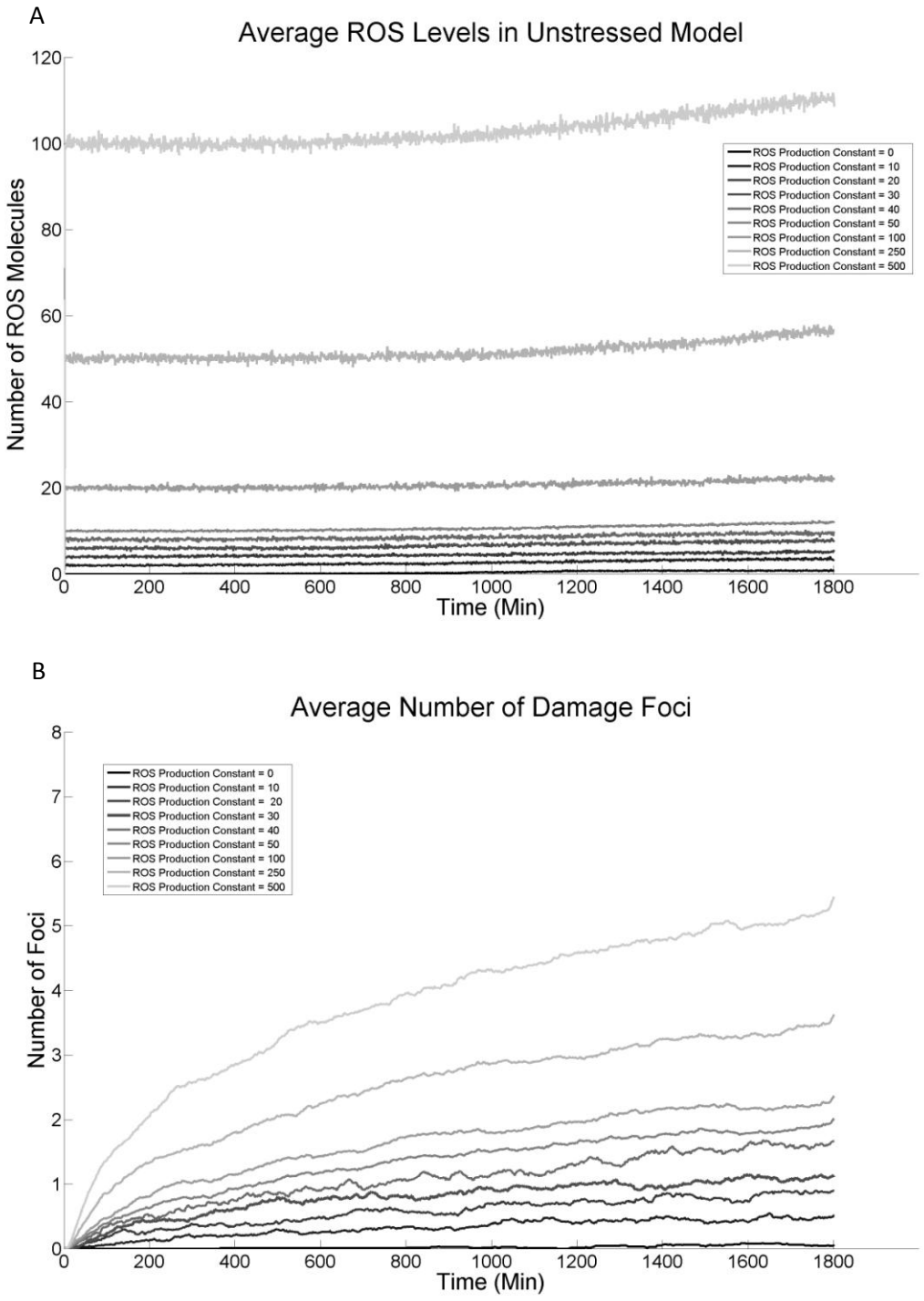

Figure 17. Average ROS levels (A) and average damage foci (B) number over 1800 minutes in unstressed model with differing levels of environmental ROS production ranging from no ROS production (ROS Production Constant = 0) to 10 times the rate detected in live MRC5 cells in standard laboratory conditions (ROS Production Constant = 0)

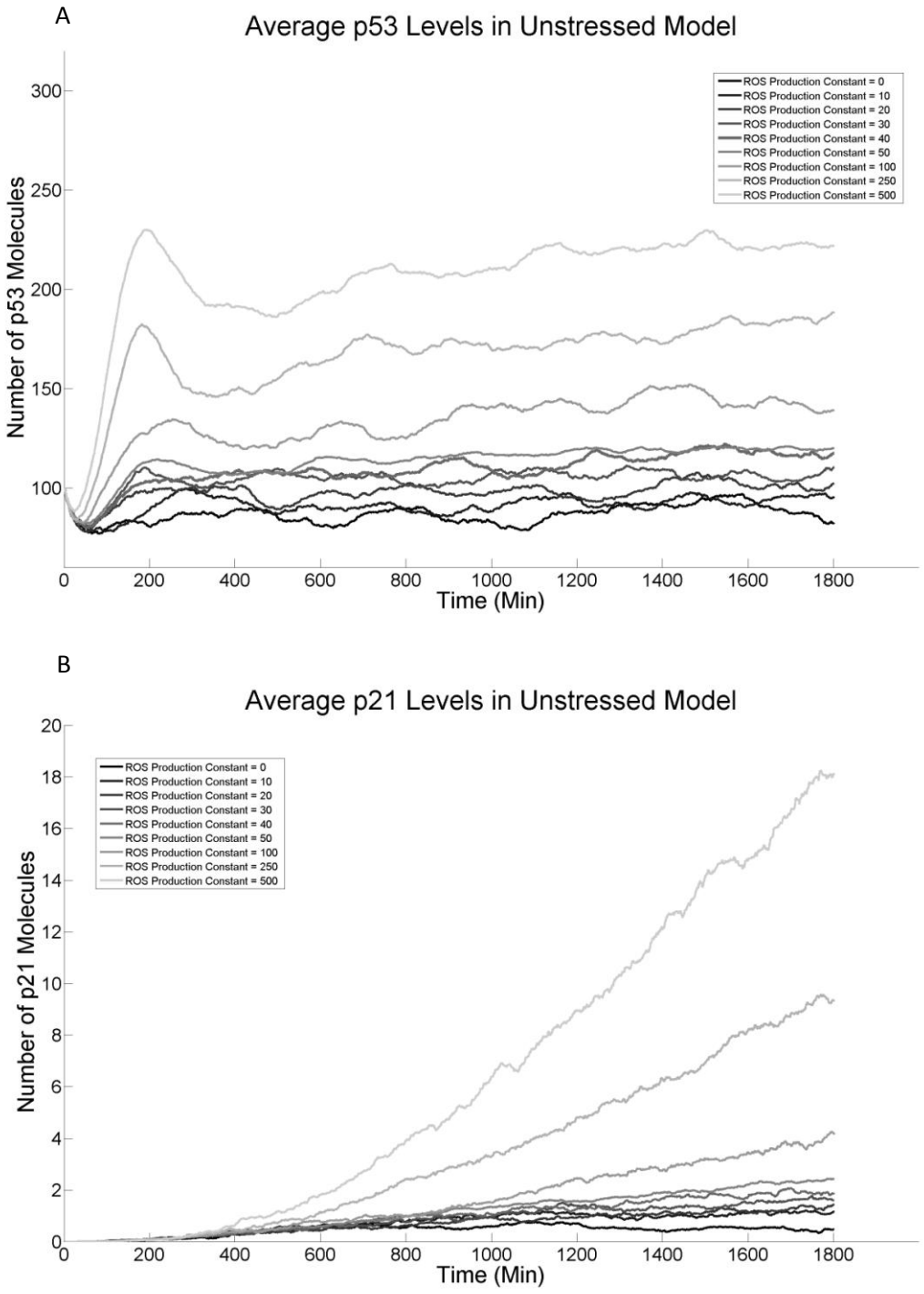

Figure 18. Average levels of p53 (A) and p21 (B) over 1800 minutes in unstressed model with differing levels of environmental ROS production ranging from no ROS production (ROS Production Constant = 0) to 10 times the rate detected in live MRC5 cells in standard laboratory conditions (ROS Production Constant = 0)

In the stressed model, inducing doses of irradiation over the course of 5 minutes by increasing the rate constant that causes the production of the spike of ROS in the timed event results in a stronger feedback than in the unstressed model (Figure 19A, 19B, 20A and

20B) for all levels of damage, with the large spikes of damage inducing higher levels of downstream ROS production and double strand break induction.

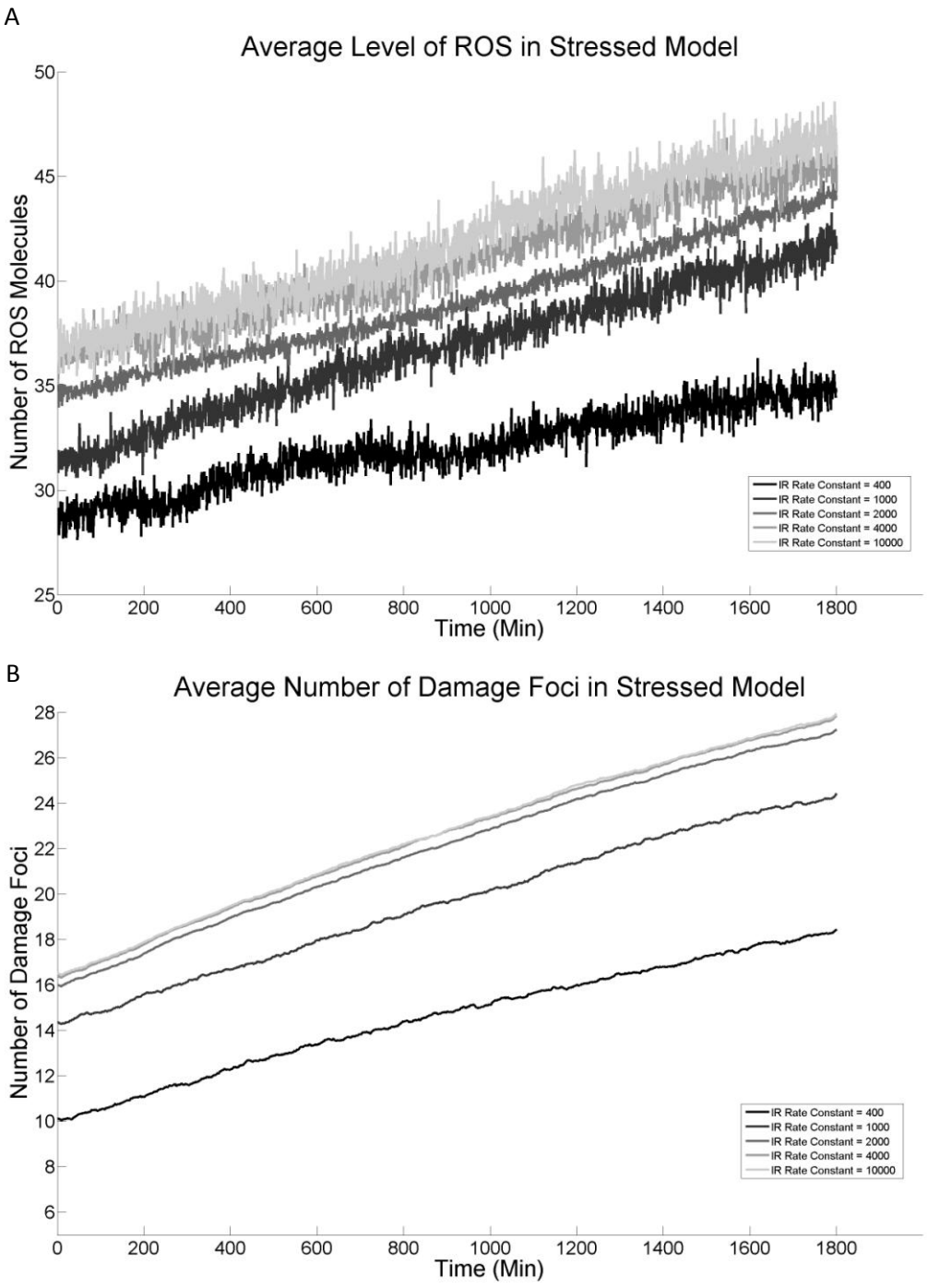

Figure 19. Average ROS levels (A) and average damage foci (B) number over 1800 minutes in stressed model at different strengths of γ irradiation treatment ranging from 4 Gy (IR Rate Constant = 400) to 100 Gy (IR Rate Constant = 1000)

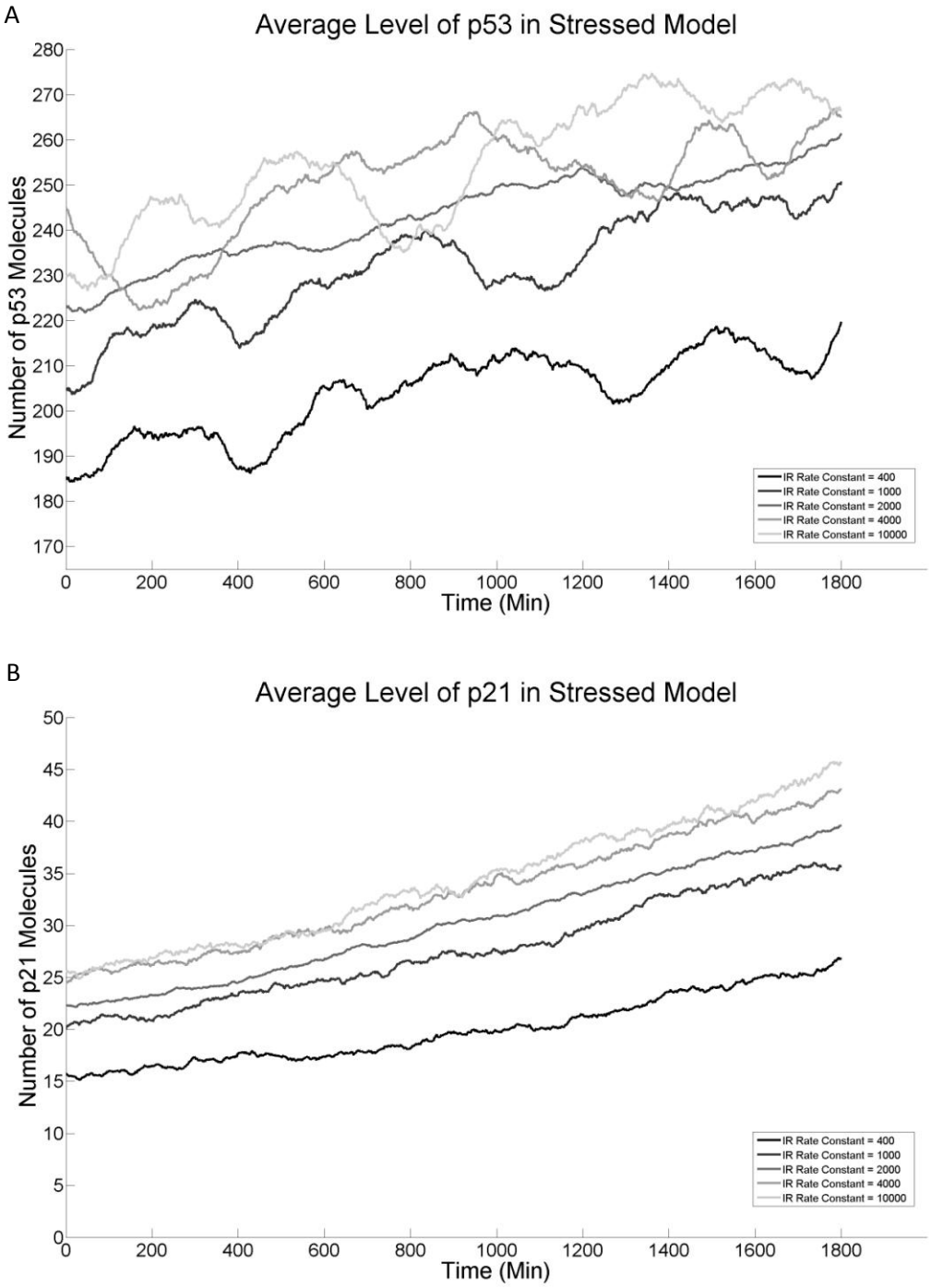

Figure 20. Average levels of p53 (A) and p21 (B) over 1800 minutes in stressed model at different strengths of γ irradiation treatment ranging from 4 Gy (IR Rate Constant = 400) to 100 Gy (IR Rate Constant = 1000)

The NHEJ system consists of two individual mechanisms that compete with one another to repair a double strand break (D-NHEJ and B-NHEJ). As we have a functioning model of the DSB repair and the DDR that matches observations made in live cells we are in a position to investigate the roles that the mediators of each mechanism, Ku and PARP, play within the overall response to DNA damage. Within the unstressed model the removal of PARP-1

results in a lower number of damage foci being present at any given time whilst removal of Ku increases the number (Figure 21A), which in turn results in lower average levels of p53 and p21 in the model with PARP-1 removed and higher average levels of p53 and p21 in the model with Ku removed (Figure 21B and 21C). None of the simulations of cells lacking PARP-1 were observed to senesce, however 8% of the cells lacking Ku did. The removal of either Ku or PARP-1 also has an observable effect on the longevities of the damage foci formed in the model (Figure 22). When PARP-1 is removed, the longevities of the short term foci are reduced compared to the normal model whereas removing Ku increases the longevity of foci producing a profile similar to that of a stressed cell.

A

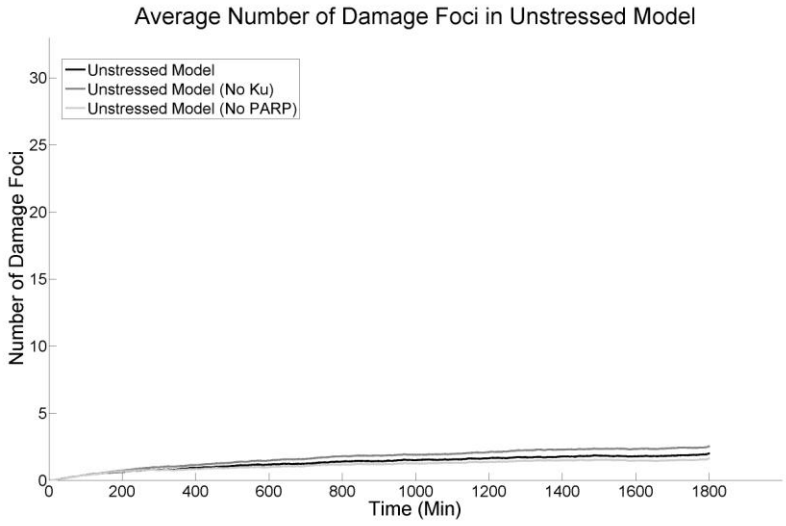

B

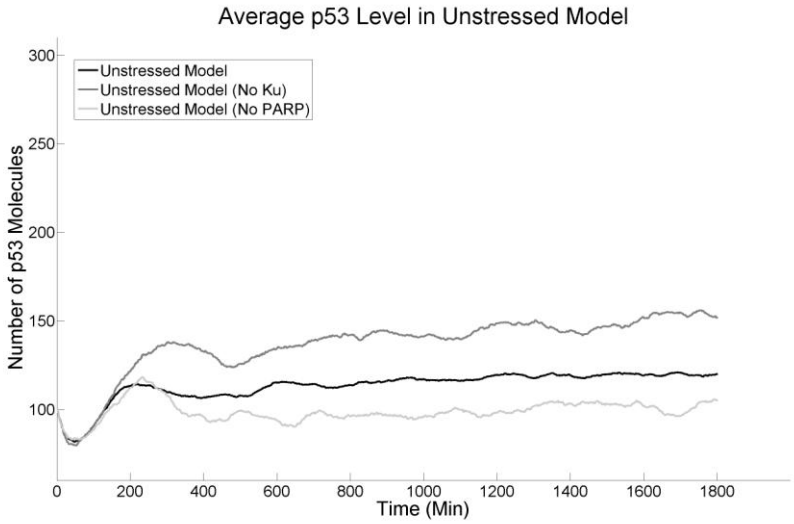

C

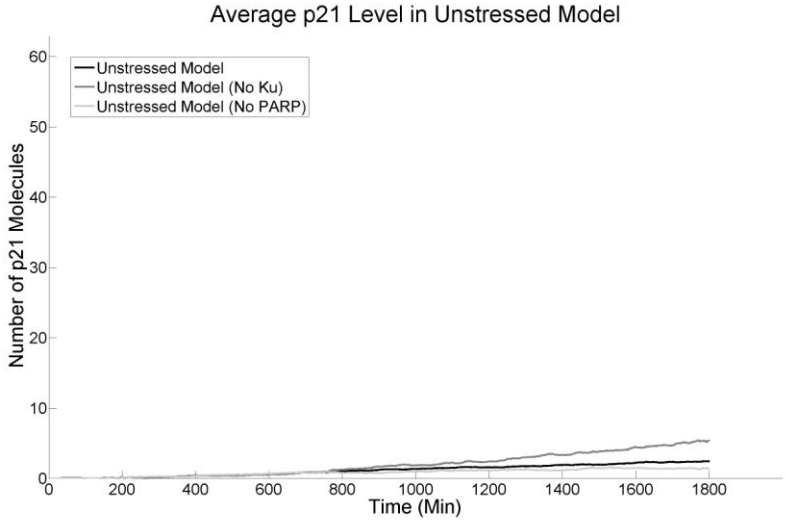

Figure 21. Average number of damage foci (A), p53 molecules (B) and p21 molecules(C) over 1800 minutes in unstressed NHEJ DDR models with Ku and PARP-1 present or either Ku or PARP-1 removed.

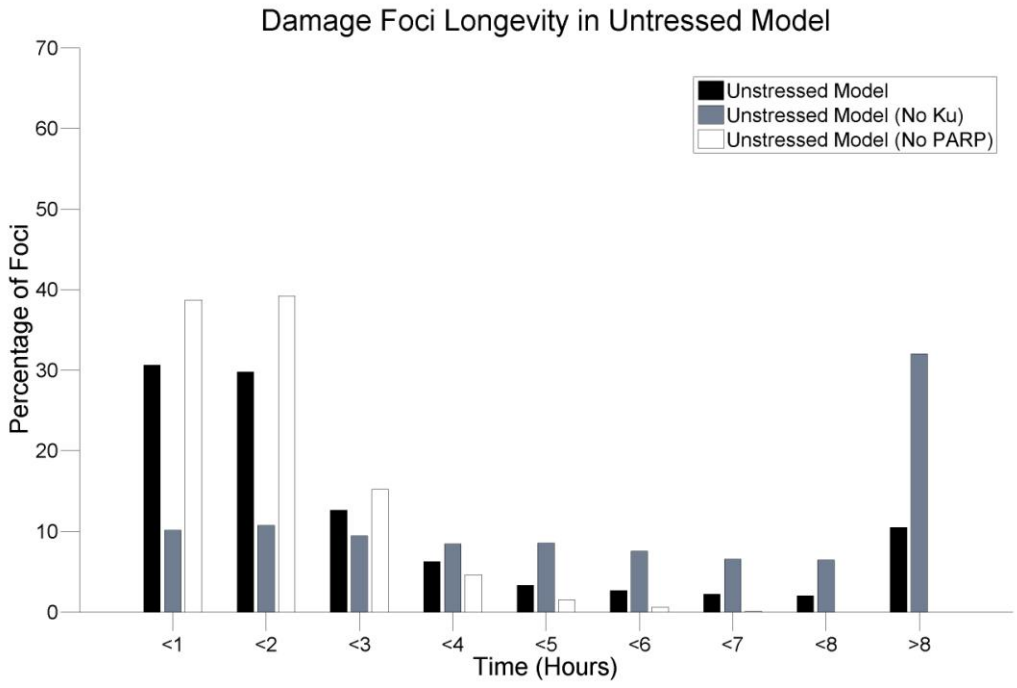

Figure 22. Histogram of damage foci longevities in simulations of unstressed NHEJ DDR models with Ku and PARP-1 present or either Ku or PARP-1 removed.

As in the unstressed model, the removal of Ku from the stressed model caused an increase in the average number of damage foci present in addition to higher levels of p53 and p21 (Figure 23A, 23B, 23C) as compared to the standard stressed model as well as increasing the percentage of cells senesced from 85% to 100%. The removal of PARP-1 results in lower average numbers of Foci, p53 and p21 and decreased the percentage of senescent cells to 5%. In the stressed model lacking Ku we observe damage foci dynamics similar to those of the standard stressed model whilst the model lacking PARP-1 displays dynamics closer to that of the standard unstressed model (Figure 24).

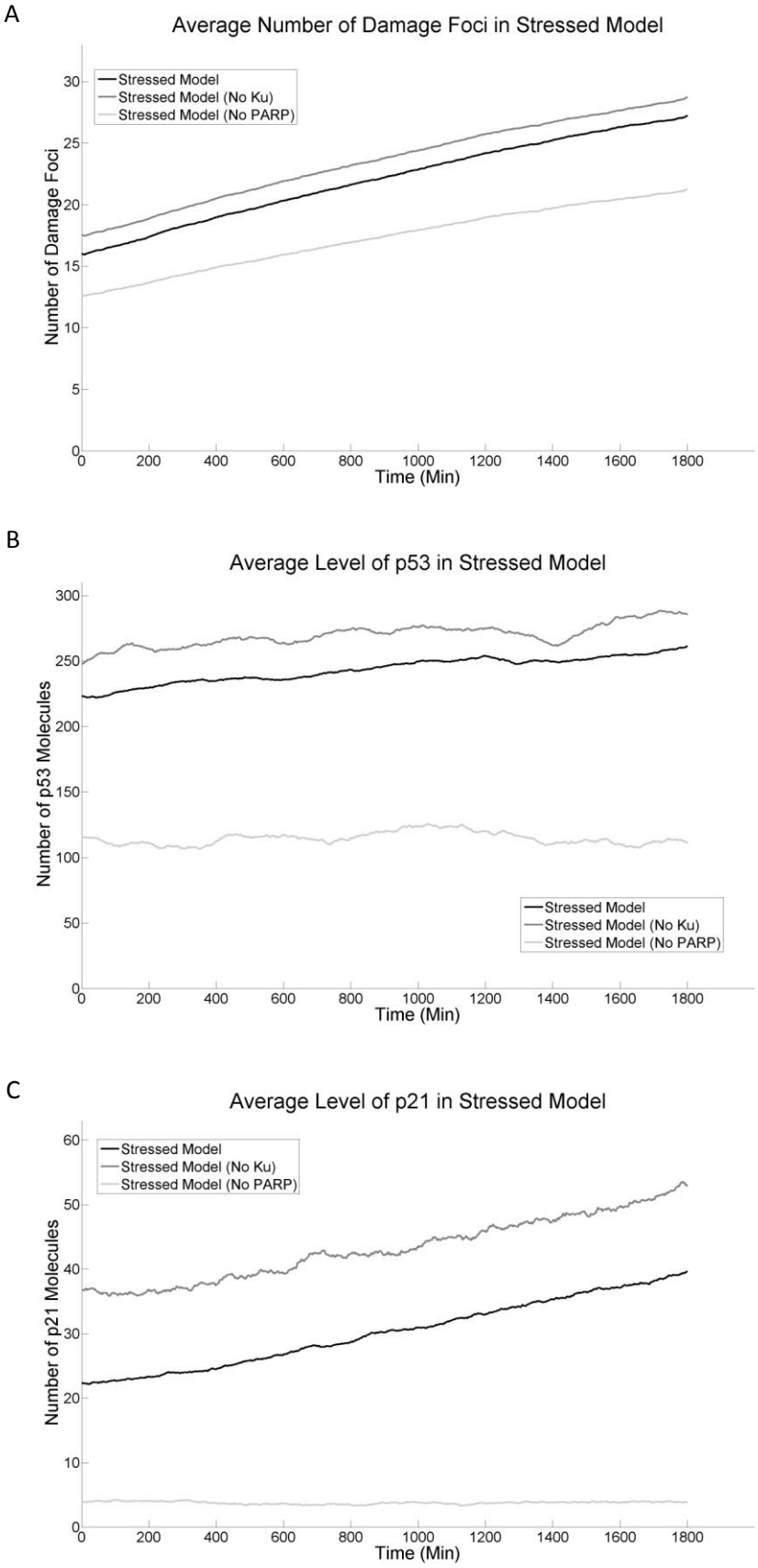

Figure 23. Average number of damage foci (A), p53 molecules (B) and p21 molecules (C) over 1800 minutes in stressed NHEJ DDR models with Ku and PARP-1 present or either Ku or PARP-1 removed.

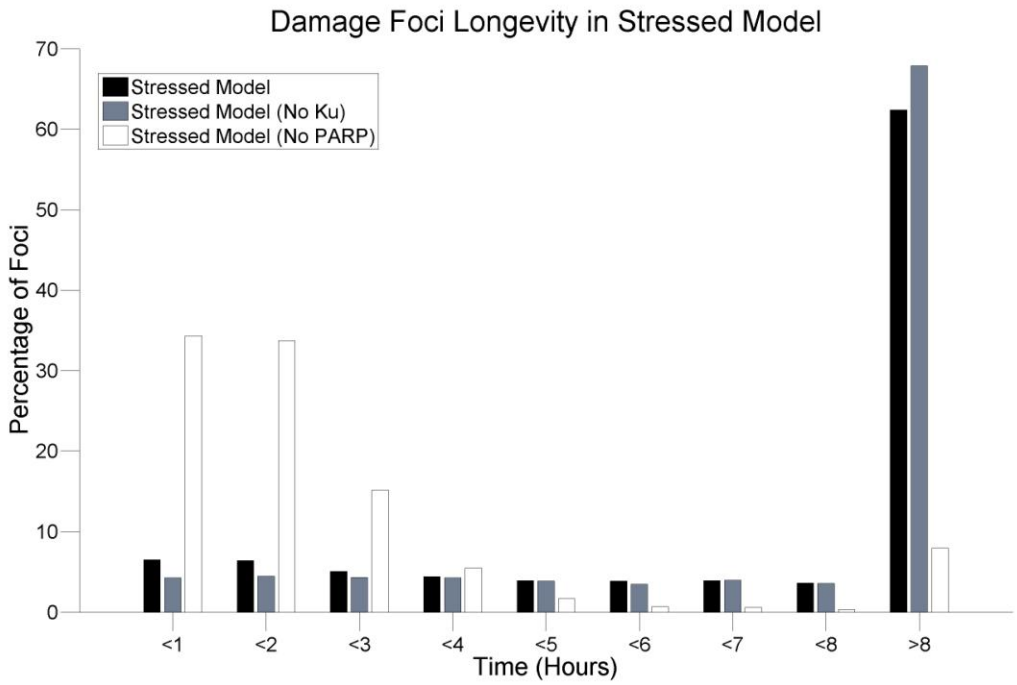

Figure 24. Histogram of damage foci longevities in simulations of stressed NHEJ DDR models with Ku and PARP-1 present or either Ku or PARP-1 removed.

The damage foci dynamics observed in live cells is not only based on a complex interaction of various molecules within the NHEJ system but also the large scale pro-survival changes induced by the cellular DDR when damage is sensed. In cells treated with gamma irradiation damage foci that form around breaks that are repaired are typically resolved within 8 hours and the determinant behind the longevity of these foci is the redox state of Ku70/80. Damage foci that last longer than 8 hours have a much greater chance of not being resolved and the results of our rule based model suggest that this is due to the decreased numbers of major repair factors (Ku and PARP) brought about by the induction of cellular senescence. Moreover we observe that the response to damage and the feedback that it causes is highly dependent on the amount of damage going in - the higher the amount of damage, the greater the feedback. When PARP-1 is removed from the model before the irradiation event is triggered we observed foci dynamics much closer to those of an unstressed cell rather than that of a stressed cell, indicating that the shift in dynamics seen in short term foci in irradiated cells is due to an increase in the amount of repair by B-NHEJ rather than a decrease in the speed of repair by Ku mediated D-NHEJ.

However if B-NHEJ is the cause of decreased DNA repair speed and therefore of triggering greater levels of ROS production and by extension senescence the question that arises is

why did B-NHEJ evolve if ultimately it leads to the inability of a cell to reproduce? One response is that instead of evolving as a back-up pathway, B-NHEJ, is actually an older repair pathway that has been superseded in modern organisms by the function of D-NHEJ and the reason it still remains is due to its components having an essential role maintaining genome integrity separate from B-NHEJ through the single strand break repair mechanism, base excision repair (BER) (155). Another potential reason for its continued presence could be due to the fact that as the majority of environmental conditions a cell would typically be exposed do not induce high levels of DNA damage the activity of the B-NHEJ system does not negatively impact upon the cells survival so is not selected against by the forces of natural selection.

Beyond this, PARP-1 has also been suggested to have a beneficial role in Ku mediated repair (140) via formation of a PARP-1 DNA-PK complex through interaction with Ku. This would mean that that although PARP-1 can have a negative impact on a cells ability to replicate through B-NHEJ following a large damage inducing event where Ku's function is inhibited due to redox dependent alterations to its structure, it may be beneficial to the Ku mediated D-NHEJ repair pathway under the normal unstressed environmental conditions and so be selected for by natural selection.

Using the collected knowledge of the NHEJ repair mechanism and the cells extended DDR to double strand breaks we have created and parameterised a model that can explain the observed shift in damage foci dynamics when a cell is treated with gamma irradiation as well as highlighting the need for a deeper investigation into the evolution of the DDR.

Chapter 5: Signalling Dynamics of p53

5.1 Introduction

Cellular signalling is a means to send information and instructions regarding various internal and external stimuli that affect a cell to downstream systems so that they can respond to them in an appropriate manner. These stimuli are more often than not dynamic and rarely constant and can interact with other stimuli to produce different effects within an organism. As a result our cells functions are driven by highly complex spatiotemporal mechanisms and the response to them can often be difficult to discern, however if we wish to understand how a cell fate in response to stimuli is made we need to further our knowledge of these underlying spatiotemporal temporal networks (156).

This complex input of stimuli has resulted in a complex signalling network evolving to help an organism react and adapt, however it is only recently that we have developed the technology to fully identify components of the cellular signalling system and the connections that exist between them to allow us to understand the depth of the complexity. The goal of research into the signalling systems is now to work out how these systems actually function and how a stimulus results in certain dynamics of the signalling pathway by looking at how the various proteins of that make up the signalling pathways interact and form complexes, change their concentrations, undergo post-translational modification, alter their chemical states and spatial localisation to produce the behaviour we observe when a cell is exposed to a stimulus (157).

As more research into cellular signalling has been carried out it has become more apparent that temporal dynamics of proteins such as oscillation in their levels have the capacity to affect both gene expression and a cell's ability to progress through the cell cycle (41,158), highlighting the need for a greater understanding of the signalling pathway on a systems level to further our understanding on how a cell makes its choices.

Within the DNA damage response pathways of the cell, the tumour suppressor protein p53 has an important role in inducing a multitude of cellular systems in response to stresses that

result in damage to the cell's DNA including cell cycle arrest, apoptosis and senescence (63). Interestingly, live cell microscopy has revealed that the protein has an oscillatory behaviour in response to damage (159). This oscillation arises due to the interaction of p53 and MDM2. Transcription of MDM2 mRNA is induced by p53, and MDM2 when present in a cell binds to and ubiquitinates p53 marking it for degradation by the proteasome. However when DNA damage is caused, p53 and MDM2 undergo phosphorylation which inhibits their binding and subsequent degradation which results in an increase in their levels. Once they are dephosphorylated they are able to bind again and undergo active degradation which then causes their levels to drop again. It has become apparent that the dynamics of p53 differ depending on the type of DNA damage the cell is responding to as the individual DNA repair pathways activate p53 through different proteins - ATM in the case of double strand breaks and ATR in the case of single strand damage (160). Treatment with UV irradiation which induces a high level of single strand damage results in a single sustained pulse of p53 whilst γ radiation which causes a high number of DSBs results in a repeated pulsing dynamic. However due to the fact that double strand breaks and single strand breaks activate different pathways other than p53 DDR pathway which are independent of p53, comparing the dynamics on the cell's response to various types of stress becomes difficult: the ultimate response is going to be modulated by these different independent pathways. An alternate way to investigate the role that p53 behaviour plays on cell fate is by experimentally perturbing p53 using the drug Nutlin-3 and treating the cells with just γ irradiation so that the damage type is the same, meaning the p53 independent pathways activated are the same but the p53 response is different (161). By binding to MDM2, Nutlin-3 inhibits the formation of the MDM2-p53 complex and the subsequent degradation of p53 (162). This inhibition of p53 degradation causes the multiple pulses of p53 to become a single sustained pulse and thereby allowed for investigation into how the dynamics of p53 actually influence the cell fate. The conclusions made from the modelling of p53 pulsing behaviour and experimental perturbation research it guided suggested that the induction of senescence was due to the temporal dynamics of p53 and not the extent of DNA damage.

However our own model of the DNA damage response indicates that higher levels of DNA damage have a greater feedback effect on the system (Chapter 4) than lower levels of damage through the p53 pathway by activating the production of p21 which in turn

increases the production of ROS in the cell and promotes senescence, suggesting that the extent of DNA damage does play an important role in a cell's fate. To investigate how this difference in our conclusions arises we modified our model to take into account the effects of Nutlin-3 on MDM2 and simulated our model under the conditions similar those in the p53 perturbation experiment (161) as well as simulating the conditions in the earlier experimental study of p53 dynamics that led to the perturbation work being carried out (159).

5.2 Methods

5.2.1 Model Adaption and Simulation

For this investigation we initially used both the unstressed and stressed variants of our rule based DDR model. The unstressed model was used to compare output with the data collected on cells that were not treated with γ irradiation (159), whereas we modified the stressed model to accommodate equivalent doses of γ irradiation that the live cells were treated with (10 Gy, 5 Gy, 2.5 Gy and 0.3 Gy) (159). To represent the addition of various amounts of Nutlin-3 to a cell we introduced a timed event in the stressed cell model that reduced the rate of MDM2 and p53 association twofold, tenfold and one hundredfold (0.0693 to 0.035, 0.007 and 0.0007 respectively). As in the experiment, we simulated addition of Nutlin-3 to take place shortly after the irradiation event.

The base unstressed model was simulated for a period of 1800 minutes (500 runs). The stressed model was simulated for a total of 4860 minutes (120 runs) for each of the 10 Gy, 2.5 Gy and 0.3 Gy stress events with 50 runs for the 5 Gy stress event. Finally the stress models with the Nutlin-3 treatment event were simulated for 4860 minutes for the 10 Gy, 5 Gy and 2.5 Gy treatments of γ irradiation, with each model being simulated 50 times.

The model was further modified to have multiple regularly timed irradiation events instead of a single damage event. One model was set up to simulate 2 treatments of 2.5 Gy, one with 5 treatments of 1Gy and another with 10 treatments of 0.5Gy. Fifty simulations of each model were taken for both 3 and 6 hours gaps between γ irradiation treatments.

5.2.2 Data Analysis

For each Simulation we monitored the number of p53 molecules present at each time point of each run. For the unstressed model and the 10 Gy, 2.5 Gy and 0.3 Gy model we initially collected data for 16 hours (960 mins) in line with the live cell experiment reported in Lahav *et al.* 2004 (159). The first time point monitored in the unstressed model was simply the first step of the simulation whereas the first time point in the stressed model corresponded to the first step post-irradiation treatment event. Each individual run was then analysed and the amplitude and duration of distinct pulses in p53 was recorded. A pulse was defined as a spike in number of p53 molecules rising over twice the average level of p53 molecules in the base unstressed model (280 molecules of p53). We also calculated the average level of p53 over a period of 16 hours corresponding to our own live cell monitoring experiments for each level of stress.

We then extracted the number of p53 molecules present over the course of 24 hours starting at the end of the irradiation event for the 10 Gy, 5 Gy and 2.5 Gy simulations for the models treated with Nutlin-3 and for those untreated. Again we used the data to calculate the average level of p53 over the whole time course of the data sets. We also calculated the average p53 level at any time and the fraction of simulations that had gone into senescence as a result of the senescence marker molecule having its state changed via exposure to continually high levels of p21 and the average cumulative p53 level at end of the 4860 minutes (the time that the rule based stressed models were simulated to in Chapter 4) of each treatment. Using the average level of p53 at any given time point for each of the Nutlin-3 treated models and the average cumulative level of p53 at the end of the Nutlin-3 treated models, we calculated the average time that the Nutlin-3 treated models took to reach the same average cumulative level of p53 as the non-Nutlin-3 treated simulations, and additionally the fraction of senescent cells at the time when the same cumulative level of p53 was attained in the Nutlin-3 treated model. The calculation of the senescent fraction was also carried out on the simulations that had multiple damage events. The data for all runs was analysed using Matlab.

5.3 Results and Discussion

It was originally reported by Lahav *et al.* 2004 (159) that following treatment with γ irradiation p53 showed a digital pulsing behaviour (same amplitude and pulse width) regardless of the level of damage with greater levels of damage resulting in more pulses observed over the 16 hour observation period (Figure 25A). Our own model shows similar behaviour regarding the number of pulses seen: simulations of untreated cells did not display any large spikes in p53 whereas for 10 Gy treatments the simulations have the highest amount of multiple pulses (Figure 25B and 25C). In both in the live cell data and in the model a pulse of p53 lasted for about 400 minutes (Figure 25D and 25E). The average time between the first and second pulse in situations when a second pulse occurred was on average observed to be 440 minutes and 460 minutes for the live cells and model data respectively. Importantly, however the pulse amplitude in the simulation data was seen to increase with higher levels of stress whereas in the live cell data it was reported that the pulse heights were roughly the same (Figure 25F and 25G). This difference likely arises in the way pulse amplitude is calculated. We calculate our pulse amplitude by counting the total number of molecules whereas the data captured in the live experiments using live cell fluorescence microscopy is normalised around the median level of florescence. In other words, we are examining pulse dynamics compared to a reference state with no p53 present whereas the live cell experiments report dynamics compared to the average level of p53. By normalising our data to account for the average level of p53 we find that our pulses do show much closer amplitudes at the various levels of damage (Figure 25H). This suggests that the pulse dynamics of damage are the same regardless of the level of damage put into the system, both in width and amplitude from the lowest point in the pulse to the highest, however the average amount of p53 present in a cell in response to a damage event is higher the larger the irradiation treatment and by extension the higher the amount of damage that is induced (Figure 26).

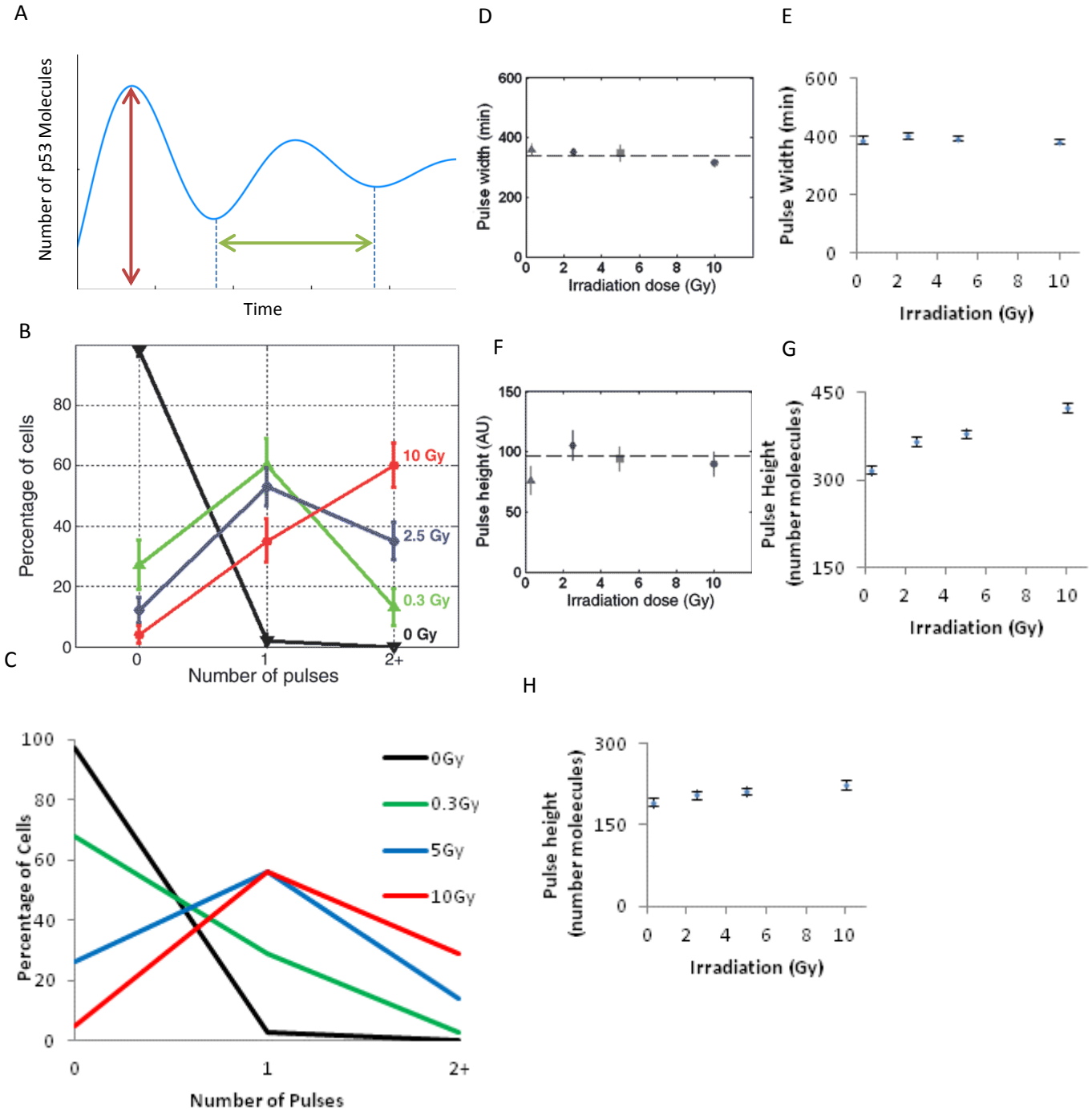

Figure 25. (A) Schematic of p53 pulse showing amplitude and pulse width. (B) Number of pulses observed in live cells after treatment with γ irradiation. (C) Number of pulses observed in NHEJ DDR rule based model after treatment with γ irradiation. (D) Mean pulse width (±S.E.) of first detected pulse in live cells at 0.3 Gy, 2.5 Gy, 5 Gy and 10 Gy. (E) Mean pulse width (±S.E.) of first detected pulse in model simulations at 0 Gy, 0.3 Gy, 2.5 Gy and 10 Gy. (F) Mean pulse height (±S.E.) of first detected pulse in live cells at 0.3 Gy, 2.5 Gy, 5 Gy and 10 Gy normalised to average p53 level. (G) Mean pulse height (±S.E.) of first detected pulse in model simulations at 0 Gy, 0.3 Gy, 2.5 Gy and 10 Gy. (H) Mean pulse height (±S.E.) of first detected pulse in model simulations at 0 Gy, 0.3 Gy, 2.5 Gy and 10 Gy normalised to average p53 level.

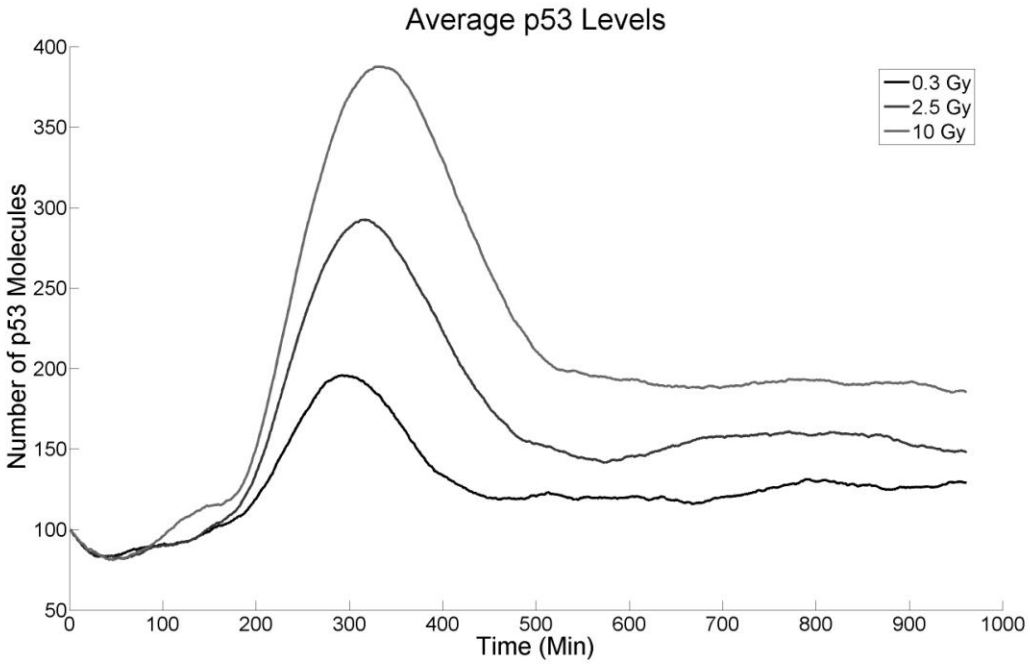

Figure 26. Average p53 levels over 16 Hours (980 minutes) in simulations of model treated with 0.3 Gy, 2.5 Gy and 10 Gy γ irradiation.

Recently it has been hypothesised that the fate of a cell after damage is determined by the dynamics of p53 (161), cells pre-treated with Nutlin-3 have higher factions of senescence even when treated with low doses of γ irradiation compared to cells not treated with Nutlin-3 under higher levels of γ irradiation. By inhibiting the activity of MDM2-p53 binding in our model to represent Nutlin-3 to decrease the pulsing behaviour of p53 (Figure 27) we also see an increase in the fraction of senescent cells, where higher levels of Nutlin-3 treatment result in a greater fraction of senescent cells with lower levels of γ irradiation treatment than the high irradiation non-Nutlin-3 treated cells (Figure 28A, 28B and 28C). Calculation of the fraction of senescent cells at the time point when Nutlin-3 treated cells had accumulated the same amount of p53 as the non-Nutlin-3 treated cells at the end of the simulation showed that models with low and mid-level inhibition of MDM2 by Nutlin-3 resulted in higher fractions of senescent cells than their equivalent non-Nutlin-3 treated models (Figure 29A and 29B). However none of the simulations of the models with the highest level of Nutlin-3 treatment had progressed into senescence at the time point when their cumulative level of p53 was the same as the cumulative p53 level at the end of the non-nutlin-3 treated models (Figure 29C). The reason for this lack of progression into senescence is likely due to the fact that not enough time has passed for the senescence

pathway to activate via p53. These results support the hypothesis that the temporal dynamics of p53 do play an important role in the induction of senescence and the determination of cell fate in response to stress.

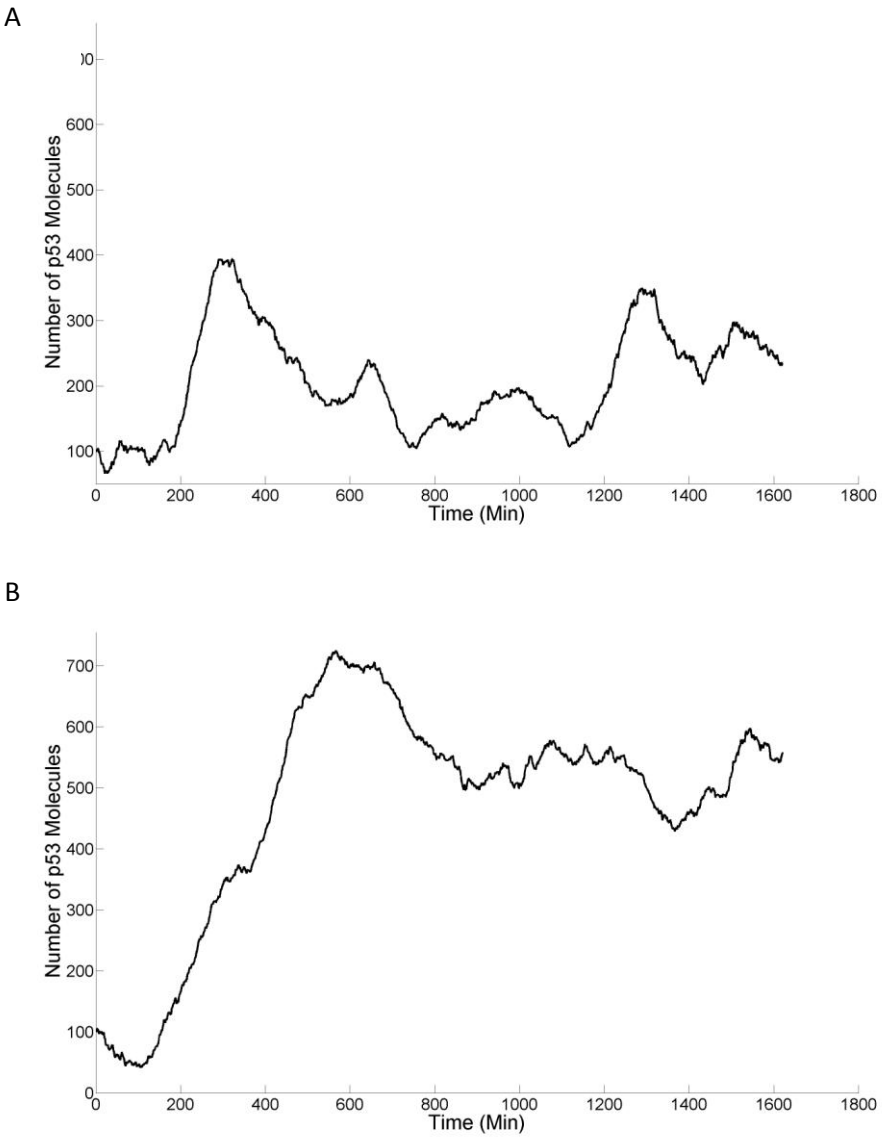

Figure 27. p53 time courses of stressed model (10 Gy γ irradiation treatment) with no Nutlin-3 treatment (A) and mid Nutlin-3 (tenfold decrease in p53 MDM2 binding) treatment (B).

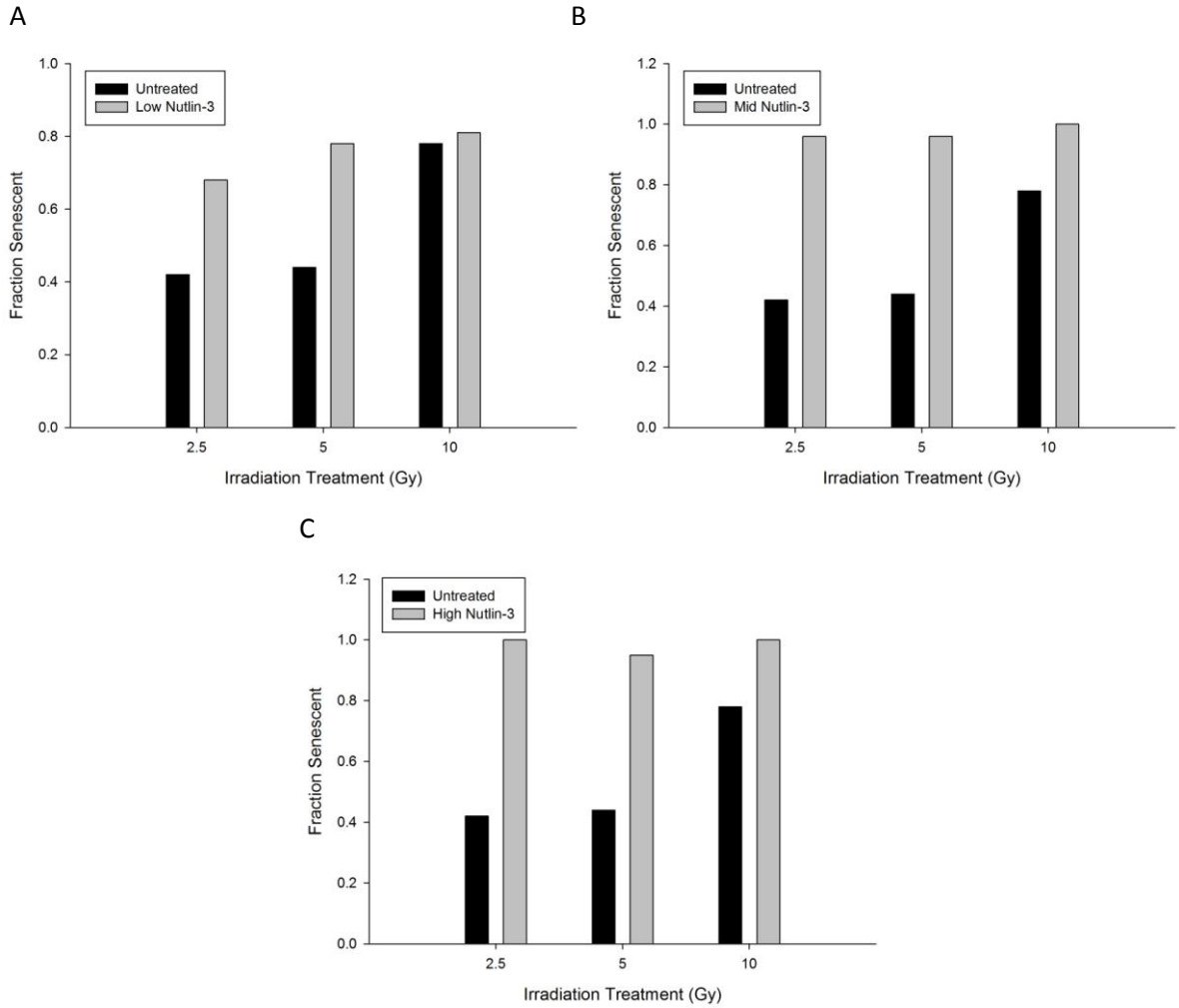

Figure 28. Histograms showing the fraction of senescent cells in rule based model simulations with (A) low, (B) mid and (C) high level Nutlin-3 treatments compared to simulations of no treatment with Nutlin-3 at 4860 minutes following exposure to either 2.5 Gy, 5 Gy or 10 Gy γ irradiation.

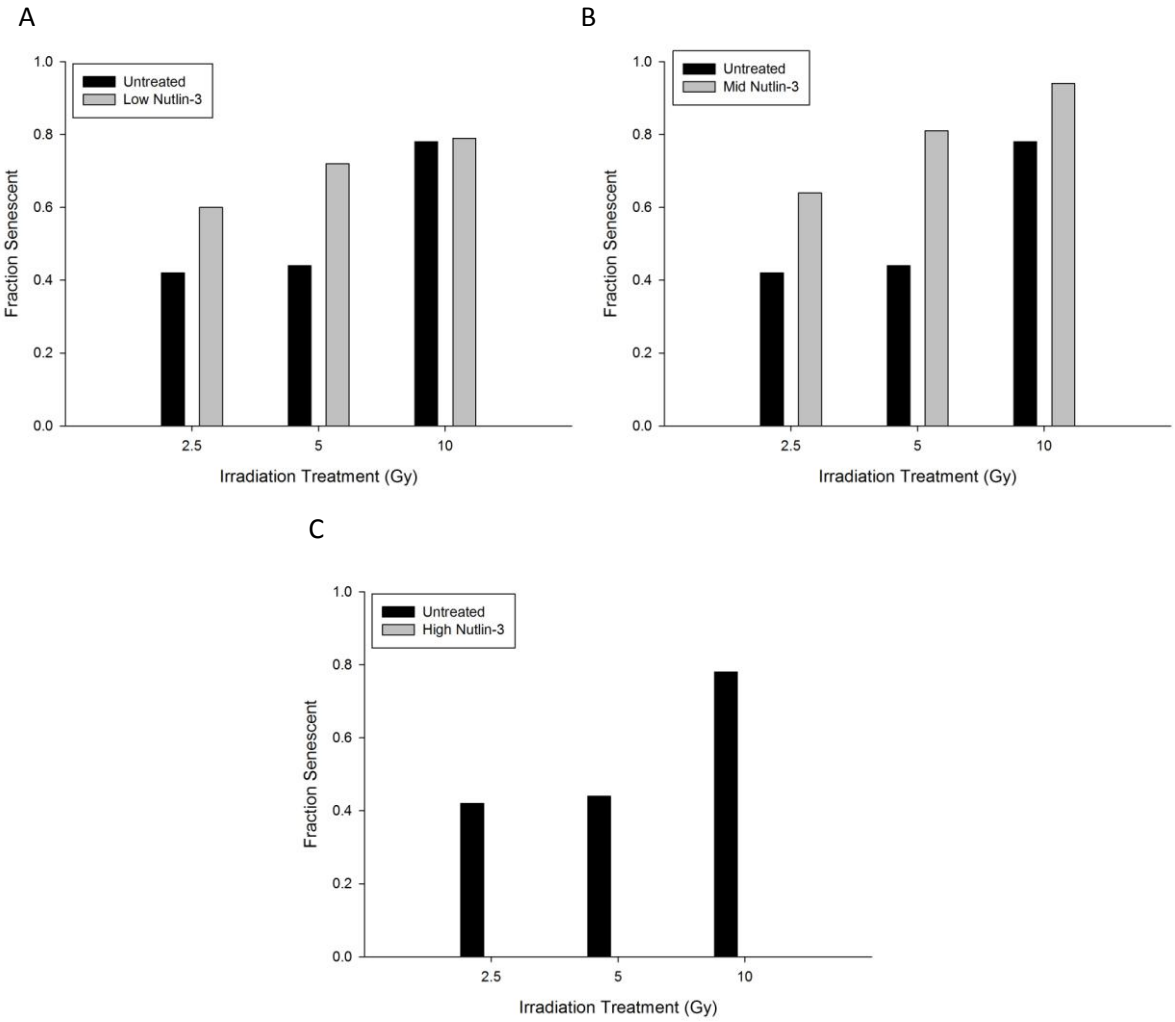

Figure 29. Histograms showing the fraction of senescent cells in rule based model simulations with (A) low, (B) mid and (C) high level treatments of Nutlin-3 compared to simulations that had not been treated with Nutlin-3 after being exposed to 2.5 Gy, 5 Gy or 10 Gy γ irradiation. Senescent fraction of Nutlin-3 treated simulations was calculated at the time point when the average cumulative level of p53 was the same as the average cumulative level of p53 in the non Nutlin-3 treated simulations at the end of the 4860 minute observation period.

When not treated with Nutlin-3 a cell needs a high level of p53 to be maintained for long enough to trigger sufficient p21 production to trigger senescence via the activity of cytokines. By having a pulsing dynamic, p53 slows the activation of the senescent pathways by periodically decreasing the production of p21 providing the cell time to resolve damage and recover and ideally to lower the levels of p53 to a point where the pro senescence pathways are not activated. However any stimulus that can induce and maintain high levels of p53 over long periods of time can play a major role in driving a cell into senescence.

Live cell observations have shown that when treated with γ irradiation a greater proportion of cells enter senescence the higher the level of irradiation (161) and our model suggest that

this could be due to the dynamics of DSB repair resulting in higher levels of p53 being maintained (Figure 26). However because the p53 DNA damage response can activate a feedback loop which causes the production of ROS which in turn causes the induction of more DNA damage it is hard to determine if the initial large spike of DNA damage or the continued presentence DSBs from the feedback is the major influence on the p53 dynamics that help trigger senescence.

By altering the damage events in our model to induce multiple smaller damage events we simulated equivalent total treatments of γ irradiation over extended periods of time to look at the effects of maintained levels of DNA damage. When our model had a single damage event of 5 Gy it caused 44% of the simulated cells to senesce, however when this damage was changed to 2 doses of 2.5 Gy every 3 hours we see an increase in the percentage of senescent cells to 69% and with 10 treatments of 0.5 Gy every 3 hours we see increases the percentage of simulated cells that went into senescence to 78% with similar effects seen with 6 hours between doses (Figure 30). As the fraction of senescent cells increases in the simulations that have maintained lower levels of DNA damage our results suggest that it is the continued presence of DNA damage that influences the dynamics of p53 rather than the amount of damage present at any given time point. This is a novel prediction that requires experimental confirmation.

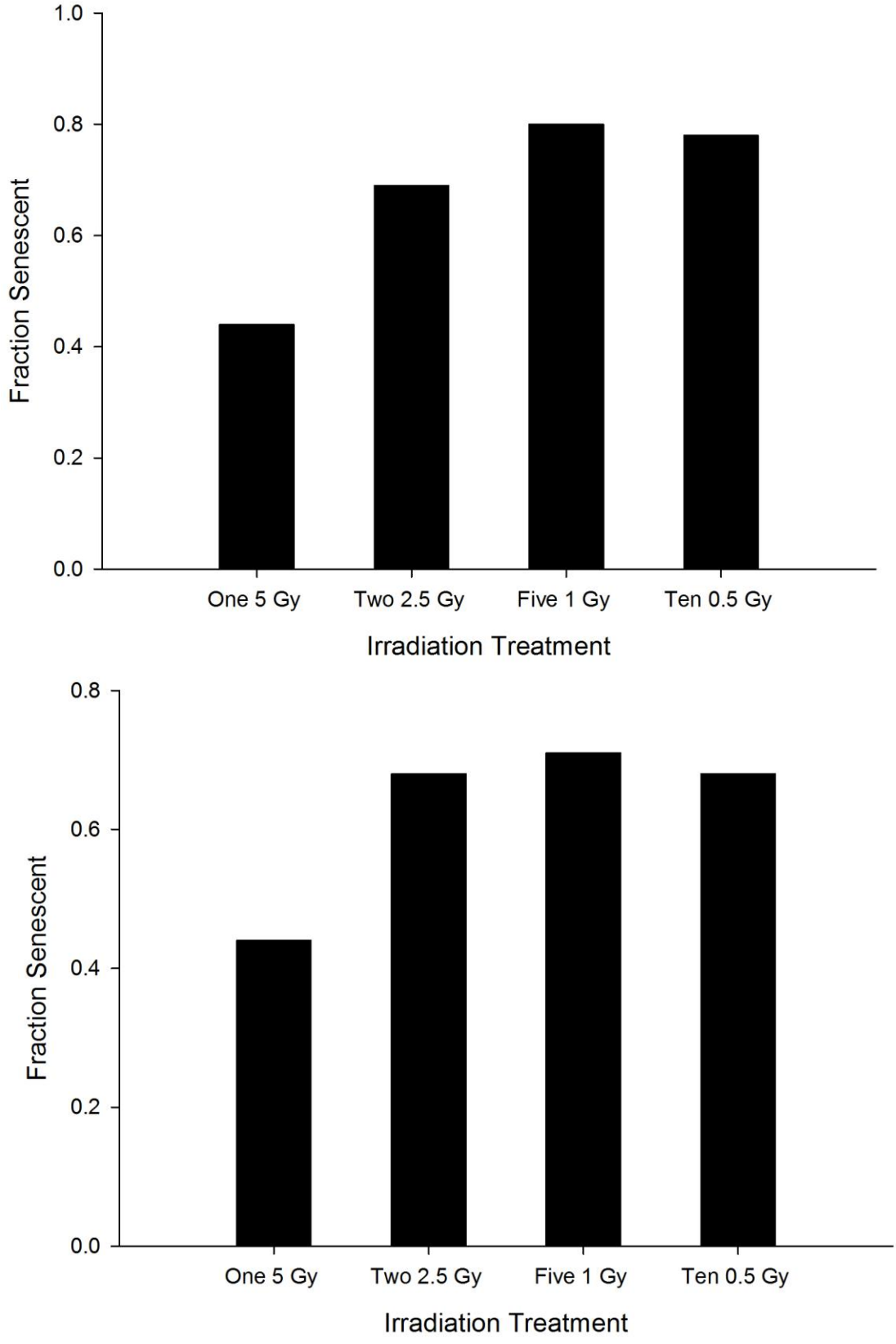

Figure 30. Histograms showing senescent fraction of stressed model simulations after multiple treatments of γ irradiation every 3 hours (top) and 6 hours (bottom). Models were simulated for 4860 minutes.

The DNA damage response is an extremely complex system that ultimately determines a cell's fate in response to damage. For this reason it has to be robust enough to handle a variety of messages and not force cells into fates that can be avoided. Previous work has identified that dynamics of p53 are a major influence on a cell's decision to enter senescence and our own model suggests that the dynamics of p53 are based upon temporal qualities of the DNA damage repair process. From a survival perspective, having the progression into senescence be determined by temporal dynamics of p53 and damage repair makes a lot of sense as damage may be overcome by the repair system so triggering senescence is not required whereas damage that persists is more than likely to be un-repairable and so will directly affect the cells functionality causing further problems meaning senescence is likely the best option for the cell. The dynamics and feedbacks of the components of our DDR model in producing and modulating downstream signals emphasises the need for enhancing our understanding of what is occurring at a systems level in signalling pathways. Knowing how a single component functions and what effect it has is not enough; we need to know how individual processes collectively contribute to dynamics. It is here that the strength of computational modelling is obvious. Models can simulate and monitor the activity of multiple components and see the emergent properties that they produce and how these factors influence the system functions as a whole. This is difficult to achieve through wet lab experimentation alone. Knowledge of this kind of is essential within the field of cellular signalling given that signalling pathways that decide cell fate and methodologies for modifying them are becoming ever more favourable targets for pharmacological interventions for a variety of diseases.

Chapter 6: Discussion of Thesis

6.1 Conclusions

The major aim of this project was to create a model to enhance our understanding of the processes that underlie DNA double strand break repair. The initial question was why do we see a change in the dynamics of short lived damage foci induced when a cell is irradiated? We approached this question with the null hypothesis that the change was simply due to the increased level of ROS species and the stochasticity inherent in the relevant biological systems. To test the theory I created a computational model of Non-Homologous End Joining (NHEJ). My starting point was a to create a network of reactions known to take place during NHEJ and represent each as a mathematical equation with rates derived from previously published data to create a reaction based model which I coded in Systems Biology Mark-up Language (SBML) . We found that when the model was set up to simulate the activity of a resting cell with a constant low level background production of ROS, the repair dynamics of our model behaved like those of a live cell both in the short and long term. However upon testing we found that the only effect of increasing the level of ROS had on our model was to increase the number of breaks caused. Inherent stochasticity in the system wasn't sufficient to account for the altered dynamics observed with higher ROS although the diversity of the rates of repair in both the model and in live cells suggest it does play a large role within the dynamics of repair..

We then began to look at the possible changes that an irradiation event and increased level of intra-cellular ROS production could cause in the system. Upon investigating published work into redox activity we found data that suggested that the Ku heterodimer, which is part of DNA-PK, the integral component of the most commonly employed repair pathway of NHEJ, showed dramatically increased dissociation from a double stranded break when chemically oxidised (125). Given that treatment with irradiation causes a large induction of ROS within a cell we altered our model to test whether the oxidation of Ku could play a role in the observed shift in repair. We found that by increasing Ku's rate of dissociation from a DSB that the model's dynamics was indeed altered such that the distribution of longevities of short term damage foci observed in the model became similar to those of irradiated live

cells. This led us to conclude that Ku oxidation as a result of treatment with γ irradiation resulted in a shift in the competition between the components of Ku mediated D-NHEJ and the PARP-1 mediated B-NHEJ with the latter causing a decrease in repair by D-NHEJ and an increase in B-NHEJ. Furthermore by carrying out pK_a shift calculations using data on the crystal structure of the Ku heterodimer we were able to identify a cysteine (Cys-249) on the surface of Ku80 that could be the oxidised in the presence of ROS and so be the cause of the shift in repair dynamics. The identification of a possible target of ROS on the Ku heterodimer is a significant step towards understanding how redox sensitivity affects HNEJ; however experimentation would need to be carried out to determine if Cys-249 oxidation is the reason for the shift in repair dynamics. One way to approach this could be to construct a Ku80 with its Cys-249 replaced with a serine, which is redox insensitive, introduce it into a cell line and test whether the cell's repair dynamics remain unaffected by redox state when treated with γ irradiation.

Although our model was able to provide an explanation for the shift in short term repair dynamics of a cell it could not explain why foci lasting longer than 8 hours had a tendency to not resolve. We hypothesised that the long term foci dynamics were likely affected by the p53 DNA damage response systems downstream of the NHEJ mechanisms that could feedback into the repair pathways could cause affect its function.

Previous experimental work had established that senescence results in a decrease in the levels of both Ku and PARP-1 in a cell and we believed that this could be a cause of the long term foci observed within live cells. However to model the feedback effects of the p53 DDR pathway and the transition into senescence it could trigger, would require a further increase in the size of the NHEJ model which was already at the size limit for our simulation tools. Expanding the model further was therefore not an option. To counter these limitations imposed by our reaction based SBML model we shifted to a rule based modelling method and converted our model in addition to a previously developed model of the p53 DDR pathway (48) into the BioNetGen language. We then merged the models which enabled us to simulate DNA damage inducing events in the model in the same way damage is induced in live cells by treatment with γ irradiation. Simulation of the rule based model with timed stress events resulted in short term and long term damage foci dynamics similar to those of irradiated live cells. We conclude that whilst the observed short term dynamics of damage

foci are influenced strongly by the apparent competition between Ku and PARP-1 the long term dynamics are a result of the systems that decide cell fate and the alterations to the cellular environment and activity those pathways trigger.

With a model that closely simulated the activity of a live cell in both irradiated and unstressed scenarios we were able to explore the effects that the removal of D-NHEJ and B-NHEJ have on repair of DNA double strand breaks in our model. Interestingly, we found that the removal of the back-up non-homologous end joining pathway from the model with a stress event resulted in repair dynamics similar to those of an unstressed cell. Lastly our model was also used to investigate the dynamic behaviour of p53 in response to damage and its role in a cells transition into senescence. In line with previous experimental work carried out into p53 dynamics we found that senescence is triggered by p53 levels being maintained for sustained periods. From simulations of our model we had observed that larger irradiation events produced higher average levels of p53 which in turn caused more of our simulated cells to senesce and by subjecting our model to more frequent low damage events to cause the maintained presence of DNA damage we found that we could induce greater levels of senescence than a single large event equivalent to the multiple small events. This led us to conclude that it was the continued presence of damaged DNA and by extension the effectiveness of its repair mechanisms that resulted in the raised levels of p53 which influences a cell's transition into senescence. This prediction made using our model is readily testable, and the method of stress used in the simulations can be easily reproduced in living cells to test if our hypothesis is correct.

Prior to this investigation much was already documented and known about HNEJ and the damage response it triggers. The existence of both the D-NHEJ and B-NHEJ pathways are well established, the process by how components of each pathway are recruited and how they interact is reasonably well known (123,163,164). What was lacking was knowledge on how these individual components functioned as a system to produce the change in dynamics of damage repair that had been observed after treatment with gamma irradiation. By modelling the known reactions and paramaterising them using all data available we were able to carry out simulations that suggest that rather than being dependent on any single factor the dynamics of NHEJ repair and the changes those dynamics undergo when a cell is subjected to stress is dependent on a complex interplay of shifts in competition between the

NHEJ pathways as a result of the stress event, feedback effects from the downstream systems and natural stochasticity.

A unique aspect to the models I have created during the course of my work has been the way in which the interactions of the repair pathways have been modelled. Previous models of DNA damage have often followed the standard modelling approach of having different types of damaged DNA pooled together as model species (72). Whilst making the modelling and simulation of these systems much more efficient, pooling of molecules removes a level of resolution that is key to understanding what influences repair by NHEJ and by extension the DDR. My models have each DNA double stranded break modelled as individual species whose repair we can monitor separately from the repair of other breaks within the model. This in turn helped us see the effects that individual have on the system and how the effects each of these unique breaks combines to produce the temporal dynamics that underlie a cells survival mechanisms.

6.2 Discussion

The possibility that the B-NHEJ system was actually an inefficient system that made repair of damage worse led us to ask why the NHEJ system would have developed such a risky pathway that could increase the possibility of a cell senescing and we reasoned that it B-NHEJ could have been an evolutionary ancient repair system that D-NHEJ replaced in such a manner that left B-NHEJ in place. My own view is that the evolution of the signalling systems that function within living cells is extremely important however we as biologists spend a lot of time and effort often asking how a system works and what it does but a lot less attention is focused on why the system exists in the first place. Ultimately if the endeavour of biological research is to understand the processes that make up a living organism then we need to know how these systems arose. To begin looking into the evolutionary aspects of any cellular mechanism let alone HNEJ is no easy task. Building up knowledge from a molecular level that functions on a scale of seconds to days to a process that takes place over lifetimes is fundamentally a hard thing to envisage let alone undertake. One potential starting point could be to use programs like Cystoscape (165) to create a network of the proteins that make up NHEJ in humans then extend out the network to include every other protein that they interact with, then by using an add-on such as the

Ageing Cross Species Interactome Database (ACID) created within our labs we could search for the homologs of each protein in other species of animal such as mice and worms, as well as yeast and even bacteria to create interaction networks for their repair mechanisms. Initially this would allow us to simply look at the differences in DNA repair between model species however this molecular knowledge combined with taxonomical knowledge of the differences between species and how much they have changed from their ancestors as well as their relatedness to the other species for which we have interaction networks we could start mapping out how and potentially even when changes and adaptations of the DNA repair mechanisms happened over the course of time.

The work presented here also has a potential use in cancer research. The goal of cancer therapy is to stop the replication of cancerous cells and promote cell death in a system that is resistant to processes such as apoptosis. To this end much research has been focused on systems that promote cell cycle arrest and cell death including the DNA damage response where both PARP-1 and p53 have been investigated as treatment targets (68,166). The results of this thesis have helped shed light both on how the DDR functions and what modulates its activity, this is or great importance to the development of cancer therapies as accurate knowledge on what components to target and what effects altering the activity of those components will yield. Moreover the model also provides a starting place for the development of a cancer orientated model which could be used to inform wet lab testing of potential new cancer therapies.

Personally, one of the most important outcomes of my work - other than the reported findings - has been the actual models of NHEJ and p53 DDR. On paper although the model can be taken for granted, it is a lot more than it seems, it combines data and observations made over many years by many different researchers and provides us with a powerful tool to investigate the mechanics of the cells response on a systems level. Our model also shows the viability of large scale, multi system stochastic modelling using rule based techniques as a tool for investigation into the mechanics of complex biological pathways.

One of the most attractive aspects of mathematical modelling using standard formats such as SBML is that the models can be extended and refined. With our NHEJ DDR model displaying the repair and damage signalling dynamics of the living cells the it was based upon there is now the potential to extend it out even further to include the systems such as

the double strand break repair mechanism homologous recombination and pathways which active when a DSB is caused at chromosome's telomere producing a permanent repairable break as well as single strand break repair mechanisms. Beyond being able to look at other repair mechanisms the model could also be extended into a more detailed cell fate model in which the pathways that signal cell death and senescence as a result of the activity could be investigated side by side to help further our understanding of what factors truly determine cell fate. In multi-cellular organisms cells don't exist in isolation, they are simply one small interconnected part of something much bigger in which the activity of one cell can have consequences for its neighbours and beyond. Cells that have become senescent are known to produce secretions which can cause DNA damage to their neighbours which may in turn induce senescence in a process known as the bystander effect (32). ROS has been observed to play a large role in the 'transmission' of senescence through a tissue but the role that a single senescent cell has on its neighbours is unknown and is unfortunately not an easy thing to observe experimentally. Our model on the other hand could provide a powerful tool to investigate the role of single cell on neighbouring cells by being expanded out from a single cell model to a tissue level model with rules set up to handle the movement of ROS produced by the activity of one cell across cell membranes into other cells to observe how the neighbours respond. This would allow us to determine how different levels of stress influence the bystander effect and how many senescent cells are needed to actually cause other cells to become senescent.

Over the course of my PhD I have become very mindful of how complexity affects a biological system. As an undergraduate whilst learning about the various cellular systems I understood quite plainly that the systems were complex but never really appreciated what that meant, but know at the end of my PhD I've started to appreciate what complexity means and how trying to research a biological system by looking at individual components as individual entities means missing a lot of details. To learn what can affect the activity of a system we need to know what is going on at all levels. Systems Biology provides us with the tools to do that, to look at proteins and other molecules as part of a whole process and to see what alters its activity and what effects these changes have both downstream of them as well as how these effects can feed back into the process and alter it further.

Supplementary Data

S1

Reaction ID	Reaction Formulae
rea	Background Sources of Damage -> ROS
reb*i*	ROS + DNA*i* -> "Simple DSB*i*"
rec	ROS -> "ROS Degradation"
red*i*	uKu70/80 -> Ku70/80*i*; "Simple DSB*i*"
ree*i*	Ku70/80*i* -> uKu70/80
ref*i*	Simple DSB*i* + Ku70/80*i* -> "Ku70/80 sDSB Complex*i*"
reg*i*	Ku70/80 DSB Complex*i* -> "Simple DNA*i*" + Ku70/80*i*
reh*i*	uDNA-PKcs -> "DNA-PKcs *i*"; "Simple DNA*i*"
rei*i*	DNA-PKcs *i* -> "uDNA-PKcs "
rej*i*	Ku70/80 sDSB Complex*i* + "DNA-PKcs *i*" -> "DNA-PK sDSB Complex*i*"
reDNAPKa*i*	DNA-PK sDSB Complex*i* -> "Simple DNA*i*" + Ku70/80*i* + "DNA-PKcs *i*"
rek*i*	DNA-PK sDSB Complex*i* -> "DNA-PK sDSB Complex*i*_2"
reDNAPKb*i*	DNA-PK sDSB Complex*i*_2 -> "Simple DNA*i*" + Ku70/80*i* + "DNA-PKcs *i*"
rel*i*	uLiIV XRCC4 -> "LiIV XRCC4*i*"; "DNA-PK sDSB Complex*i*_2"
rem*i*	LiIV XRCC4*i* -> "uLiIV XRCC4"
ren*i*	DNA-PK sDSB Complex*i*_2 + "LiIV XRCC4*i*" -> "DNA-PK LiIV XRCC4 sDSB Complex*i*"
reo*i*	DNA-PK LiIV XRCC4 sDSB Complex*i* -> DNA*i* + Ku70/80*i* + "DNA-PKcs *i*" + "LiIV XRCC4*i*" + "sDSB Acurate Repair"
rep*i*	ROS + DNA*i* -> "Complex DSB*i*"
req*i*	uKu70/80 -> Ku70/80*i*; "Complex DSB*i*"
rer*i*	Complex DSB*i* + Ku70/80*i* -> "Ku70/80 cDSB Complex*i*"
res*i*	Ku70/80 cDSB Complex*i* -> "Complex DSB*i*" + Ku70/80*i*
ret*i*	uDNA-PKcs -> "DNA-PKcs *i*"; "Complex DSB*i*"
reu*i*	Ku70/80 cDSB Complex*i* + "DNA-PKcs *i*" -> "DNA-PK cDSB Complex*i*"
reDNAPKc*i*	DNA-PK cDSB Complex*i* -> "Complex DSB*i*" + Ku70/80*i* + "DNA-PKcs *i*"
rev*i*	DNA-PK cDSB Complex*i* -> "DNA-PK cDSB Complex*i*_2"
reDNAPKd*i*	DNA-PK cDSB Complex*i*_2 -> "Complex DSB*i*" + Ku70/80*i* + "DNA-PKcs *i*"
rew*i*	uLiIV XRCC4 -> "LiIV XRCC4*i*"; "DNA-PK cDSB Complex*i*_2"
rex*i*	DNA-PK cDSB Complex*i*_2 + "LiIV XRCC4*i*" -> "DNA-PK LiIV XRCC4 cDSB Complex*i*"
rey*i*	DNA-PK LiIV XRCC4 cDSB Complex*i* -> DNA*i* + Ku70/80*i* + "DNA-PKcs *i*" + "LiIV XRCC4*i*" + "cDSB Acurate Repair"

reMRNa*i* ATM*i* + MRN*i* -> "MRN ATM Complex*i*"; "Simple DNA*i*"

reMRNb*i* ATM*i* + MRN*i* -> "MRN ATM Complex*i*"; "Ku70/80 sDSB Complex*i*"

reMRNc*i* ATM*i* + MRN*i* -> "MRN ATM Complex*i*"; "Complex DSB*i*"

reMRNd*i* ATM*i* + MRN*i* -> "MRN ATM Complex*i*"; "Ku70/80 cDSB Complex*i*"

rez*i* H2AX*i* -> H2AX*i*_2; "MRN ATM Complex*i*"

reaa*i* H2AX*i* -> H2AX*i*_2; "DNA-PK sDSB Complex*i*_2"

reab*i* H2AX*i* -> H2AX*i*_2; "DNA-PK cDSB Complex*i*_2"

reac*i* H2AX*i*_2 -> "Damage Focus*i*"

read*i* Damage Focus*i* -> H2AX*i*

reae*i* Damage Focus*i* + "MRN ATM Complex*i*" -> "Complete Damage Focus*i*"

reaf*i* Complete Damage Focus*i* -> H2AX*i* + ATM*i* + MRN*i*

reaq*i* uPARP -> PARP*i*; "Simple DNA*i*"

rear*i* PARP*i* -> uPARP

reas*i* Simple DNA*i* + PARP*i* -> "sDSB PARP Complex*i*"

reat*i* sDSB PARP Complex*i* -> "Simple DNA*i*" + PARP*i*

reau*i* uLiIII -> LiIII*i*; "sDSB PARP Complex*i*"

reav*i* LiIII*i* -> uLiIII

reaw*i* sDSB PARP Complex*i* + LiIII*i* -> "sDSB PARP-LiIII Complex*i*"

reax*i* sDSB PARP-LiIII Complex*i* -> DNA*i* + PARP*i* + LiIII*i* + "sDSB Acurate Repair (PARP)"

reay*i* sDSB PARP-LiIII Complex*i* -> DNA*i* + PARP*i* + LiIII*i* + "Deleterious sDSB Repair"

reMRNg*i* ATM*i* + MRN*i* -> "MRN ATM Complex*i*"; "sDSB PARP Complex*i*"

reaz*i* uPARP -> PARP*i*; "Complex DSB*i*"

reba*i* Complex DSB*i* + PARP*i* -> "cDSB PARP Complex*i*"

rebb*i* cDSB PARP Complex*i* -> "Complex DSB*i*" + PARP*i*

rebc*i* uLiIII -> LiIII*i*; "cDSB PARP Complex*i*"

rebd*i* cDSB PARP Complex*i* + LiIII*i* -> "cDSB PARP-LiIII Complex*i*"

rebe*i* cDSB PARP-LiIII Complex*i* -> DNA*i* + PARP*i* + LiIII*i* + "cDSB Acurate Repair (PARP)"

rebf*i* cDSB PARP-LiIII Complex*i* -> DNA*i* + PARP*i* + LiIII*i* + "Deleterious cDSB Repair"

reMRNh*i* ATM*i* + MRN*i* -> "MRN ATM Complex*i*"; "cDSB PARP Complex*i*"

reMRNi*i* ATM*i* + MRN*i* -> "MRN ATM Complex*i*"; "DNA-PK DSB Complex*i*"

reMRNj*i* ATM*i* + MRN*i* -> "MRN ATM Complex*i*"; "DNA-PK DSB Complex*i*_2"

reMRNk*i* ATM*i* + MRN*i* -> "MRN ATM Complex*i*"; "DNA-PK LiIV XRCC4 DSB Complex*i*"

reMRNl*i* ATM*i* + MRN*i* -> "MRN ATM Complex*i*"; "DNA-PK cDSB Complex*i*"

reMRNm*i* ATM*i* + MRN*i* -> "MRN ATM Complex*i*"; "DNA-PK cDSB Complex*i*_2"

reMRNn*i*	ATM*i* + MRN*i* -> "MRN ATM Complex*i*"; "DNA-PK LiIV XRCC4 cDSB Complex*i*"
reMRNo*i*	ATM*i* + MRN*i* -> "MRN ATM Complex*i*"; "sDSB PARP-LiIII Complex*i*"
reMRNp*i*	ATM*i* + MRN*i* -> "MRN ATM Complex*i*"; "cDSB PARP-LiIII Complex*i*"

In the table above *i* can be a number between 1 and 20, representing the 20 damage foci in the model; therefore for every Reaction that includes an *i* in its Reaction ID the SBML model contains twenty versions of that reaction and twenty versions of each species involved in the reaction. Species with a _2 after an *i* have the same name in the SBML model but are different species as they represent altered states of the first one listed (e.g. DNA-PK sDSB Complex*i*_2 is the phsosphylated version of DNA-PK sDSB Complex*i*).

S2

Species	Starting Quantity (No. of Molecules)	Reference
Ku70/80	400000	(122)
DNA-PKcs	100000	(167)
LiIV-XRCC4	30000	(168,169)
PARP-1	1200000	(170-172)
LiIII/XRCCC3	30000	(168)

S3

Rate Constant	Value	Reaction	Source
kass_rea	0.001min^{-1}	Production of ROS	Experimental Data
kass_reb	0.15$\#^{-1}min^{-1}$	Induction of a Simple DSB	Experimental Data, (64)
kass_rec	0.03 min^{-1}	Degredation of ROS	Experimental Data
kass_red	0.6$\#^{-1}min^{-1}$	Recruitment of Ku70/80 to sDSB	(123)
kass_ree	0.02 min^{-1}	Ku70/80 leaving site of Damage	Model constant
kass_ref	5e-006$\#^{-1}min^{-1}$	Ku70/80 binding to sDSB	(124)
kass_reg	0.5 min^{-1}	Ku70/80 dissociation from sDSB	(124)
kass_reh	0.6$\#^{-1}min^{-1}$	Recruitment of DNA-PKcs to sDSB	(173)
kass_rei	0.02 min^{-1}	DNA-PKcs leaving site of Damage	Model constant
kass_rej	9e-005$\#^{-1}min^{-1}$	DNA-PKcs binding to Ku70/80-sDSB Complex	(173)
kass_rek	0.3 min^{-1}	DNA-PK Autophosphorylation	(173)
kass_rel	0.001$\#^{-1}min^{-1}$	Recruitment of LiIV/XRCC4 to sDSB	(174)
kass_rem	0.2 min^{-1}	LiIV/XRCC4 leaving site of Damage	Model constant
kass_ren	0.00035$\#^{-1}min^{-1}$	LiIV/XRCC4 binding to DNA-PK-sDSB Complex	(174)
kass_reo	0.075 min^{-1}	Ligation of sDSB and dismantling of Repair Complex	(174)
kass_rep	0.15$\#^{-1}min^{-1}$	Induction of a Complex DSB	Experimental Data, (64)
kass_req	0.6$\#^{-1}min^{-1}$	Recruitment of Ku70/80 to cDSB	(123,175)
kass_rer	4e-006$\#^{-1}min^{-1}$	Ku70/80 binding to cDSB	(124,175)
kass_res	0.4 min^{-1}	Ku70/80 dissociation from cDSB	(124)
kass_ret	0.6$\#^{-1}min^{-1}$	Recruitment of DNA-PKcs to cDSB	((173,175)
kass_reu	7e-005$\#^{-1}min^{-1}$	DNA-PKcs binding to Ku70/80-cDSB Complex	(173,175)

kass_rev	0.3 min^{-1}	DNA-PK Autophosphorylation	(173,175)
kass_rew	0.001$\#^{-1}min^{-1}$	Recruitment of LiIV/XRCC4 to cDSB	(174)
kass_rex	0.0002$\#^{-1}min^{-1}$	LiIV/XRCC4 binding to DNA-PK-cDSB Complex	(174,175)
kass_rey	0.075 min^{-1}	Ligation of cDSB and dismantling of Repair Complex	(174,175)
kMRN	0.75$\#^{-2}min^{-1}$	Activation and Binding of ATM and MRN	(176,177)
kass_rez	0.5$\#^{-1}min^{-1}$	H2AX Phosphorylation	(178)
kass_reaa	0.5$\#^{-1}min^{-1}$	H2AX Phosphorylation	(178)
kass_reab	0.5$\#^{-1}min^{-1}$	H2AX Phosphorylation	(178)
kass_reac	0.5 min^{-1}	Damage Focus Formation	(179)
kass_read	0.1 min^{-1}	Damage Focus Dismantling	(179)
kass_reae	0.5$\#^{-1}min^{-1}$	ATM-MRN Complex binding to Damage Focus	(88)
kass_reaf	0.03 min^{-1}	ATM-MRN-Damage Focus Dismantling	(88)
kass_reaq	0.6$\#^{-1}min^{-1}$	Recruitment of PARP to sDSB	(124)
kass_rear	0.02 min^{-1}	PARP leaving site of Damage	Model constant
kass_reas	5e-007$\#^{-1}min^{-1}$	PARP binding to sDSB	(124)
kass_reat	0.02 min^{-1}	PARP dissociation from sDSB	(124)
kass_reau	0.005$\#^{-1}min^{-1}$	Recruitment of LiIII/XRCC3 to sDSB	(169,180)
kass_reav	0.02 min^{-1}	LiIII/XRCC3 leaving site of Damage	Model constant
kass_reaw	0.00035$\#^{-1}min^{-1}$	LiIII/XRCC3 binding to DNA-PK-sDSB Complex	(169,180)
kass_reax	0.0006 min^{-1}	Accurate ligation of sDSB and dismantling of Repair Complex	(64,90)
kass_reay	0.0009 min^{-1}	Inaccurate ligation of sDSB and dismantling of Repair Complex	(64,90)
kass_reaz	0.6$\#^{-1}min^{-1}$	Recruitment of PARP to cDSB	(124)

kass_reba	4e-007#$^{-1}$min^{-1}	PARP binding to cDSB	(124)
kass_rebb	0.02 min^{-1}	PARP leaving site of Damage	(124)
kass_rebc	0.005#$^{-1}$min^{-1}	Recruitment of LiIII/XRCC3 to cDSB	(169,180)
kass_rebd	0.0002#$^{-1}$min^{-1}	LiIII/XRCC3 binding to DNA-PK-cDSB Complex	(169,180)
kass_rebe	0.0006 min^{-1}	Accurate ligation of cDSB and dismantling of Repair Complex	(64,90)
kass_rebf	0.0009 min^{-1}	Inaccurate ligation of cDSB and dismantling of Repair Complex	(64,90)
kdiss_DNAPK	0.02 min^{-1}	DNA-PK dissociation from DSB	(124,173)

Bibliography

www.reactome.org

http://rsb.info.nih.gov/ij/

1. Finch, C.E. (1994) *Longevity, senescence, and the genome*. University of Chicago Press.
2. Brunet-Rossinni, A.K. and Austad, S.N. (2006) Senescence in wild populations of mammals and birds. *Handbook of the Biology of Aging*, 243–266.
3. Nussey, D.H., Froy, H., Lemaitre, J.-F., Gaillard, J.-M. and Austad, S.N. (2012) Senescence in natural populations of animals: Widespread evidence and its implications for bio-gerontology. *Ageing Research Reviews*.
4. Oeppen, J. and Vaupel, J.W. (2002) DEMOGRAPHY: Enhanced: Broken Limits to Life Expectancy. *Science*, **296**, 1029-1031.
5. Arking, R. (2006) *The biology of aging: observations and principles*. Oxford University Press, USA.
6. Weismann, A. (1891) *Essays upon heredity and kindred biological problems*. Clarendon press.
7. Longo, V.D., Mitteldorf, J. and Skulachev, V.P. (2005) Programmed and altruistic ageing. *Nat Rev Genet*, **6**, 866-872.
8. Kirkwood, T.B.L. (2005) Understanding the Odd Science of Aging. *Cell*, **120**, 437-447.
9. Kirkwood, Thomas B.L. and Melov, S. (2011) On the Programmed/Non-Programmed Nature of Ageing within the Life History. *Current Biology*, **21**, R701-R707.
10. Medawar, P.B. (1952) *An unsolved problem of biology*. Lewis London.
11. Williams, G.C. (1957) Pleiotropy, Natural Selection, and the Evolution of Senescence. *Evolution*, **11**, 398-411.
12. Kirkwood, T.B.L. (1977) Evolution of ageing. *Nature*, **270**, 301-304.
13. Speakman, J.R. and Król, E. (2010) The Heat Dissipation Limit Theory and Evolution of Life Histories in Endotherms—Time to Dispose of the Disposable Soma Theory? *Integrative and Comparative Biology*, **50**, 793-807.
14. Blagosklonny, M.V. (2010) Why the disposable soma theory cannot explain why women live longer and why we age. *Aging (Albany NY)*, **2**, 884.
15. Harman, D. (1956) Aging: a theory based on free radical and radiation chemistry. *Journal of gerontology*, **11**, 298-300.
16. Sohal, R.S. and Allen, R.G. (1990) Oxidative stress as a causal factor in differentiation and aging: a unifying hypothesis. *Experimental gerontology*, **25**, 499.
17. Sanz, A., Pamplona, R. and Barja, G. (2006) Is the Mitochondrial Free Radical Theory of Aging Intact? *Antioxidants & Redox Signaling*, **8**, 582-599.
18. Kirkwood, T.B.L. and Kowald, A. (2012) The free-radical theory of ageing – older, wiser and still alive. *BioEssays*, **34**, 692-700.
19. Mittler, R., Vanderauwera, S., Suzuki, N., Miller, G., Tognetti, V.B., Vandepoele, K., Gollery, M., Shulaev, V. and Van Breusegem, F. (2011) ROS signaling: the new wave? *Trends in Plant Science*, **16**, 300-309.
20. Buchanan, B.B. and Balmer, Y. (2005) REDOX REGULATION: A Broadening Horizon. *Annual Review of Plant Biology*, **56**, 187-220.
21. Bokov, A., Chaudhuri, A. and Richardson, A. (2004) The role of oxidative damage and stress in aging. *Mechanisms of Ageing and Development*, **125**, 811-826.
22. Bielski, B.H., Arudi, R.L. and Sutherland, M.W. (1983) A study of the reactivity of HO2/O2- with unsaturated fatty acids. *J. Biol. Chem.*, **258**, 4759-4761.

23. Hulbert, A.J. (2005) On the importance of fatty acid composition of membranes for aging. *Journal of Theoretical Biology*, **234**, 277-288.
24. Huggins, T.G., Wells-Knecht, M.C., Detorie, N.A., Baynes, J.W. and Thorpe, S.R. (1993) Formation of o-tyrosine and dityrosine in proteins during radiolytic and metal-catalyzed oxidation. *J. Biol. Chem.*, **268**, 12341-12347.
25. Levine, R.L. (1983) Oxidative modification of glutamine synthetase. I. Inactivation is due to loss of one histidine residue. *J. Biol. Chem.*, **258**, 11823-11827.
26. Hayflick, L. (1965) The limited in vitro lifetime of human diploid cell strains. *Experimental Cell Research*, **37**, 614.
27. Griffith, J.D., Comeau, L., Rosenfield, S., Stansel, R.M., Bianchi, A., Moss, H. and de Lange, T. (1999) Mammalian Telomeres End in a Large Duplex Loop. *Cell*, **97**, 503-514.
28. Fagagna, F.d.A.d., Reaper, P.M., Clay-Farrace, L., Fiegler, H., Carr, P., von Zglinicki, T., Saretzki, G., Carter, N.P. and Jackson, S.P. (2003) A DNA damage checkpoint response in telomere-initiated senescence. *Nature*, **426**, 194-198.
29. von Zglinicki, T. (2002) Oxidative stress shortens telomeres. *Trends in Biochemical Sciences*, **27**, 339-344.
30. Campisi, J. and d'Adda di Fagagna, F. (2007) Cellular senescence: when bad things happen to good cells. *Nat Rev Mol Cell Biol*, **8**, 729-740.
31. Campisi, J. (2005) Senescent Cells, Tumor Suppression, and Organismal Aging: Good Citizens, Bad Neighbors. *Cell*, **120**, 513-522.
32. Nelson, G., Wordsworth, J., Wang, C., Jurk, D., Lawless, C., Martin-Ruiz, C. and von Zglinicki, T. (2012) A senescent cell bystander effect: senescence-induced senescence. *Aging Cell*, **11**, 345-349.
33. Campisi, J. (2013) Aging, Cellular Senescence, and Cancer. *Annual Review of Physiology*, **75**, 685-705.
34. Liu, D. and Hornsby, P.J. (2007) Senescent Human Fibroblasts Increase the Early Growth of Xenograft Tumors via Matrix Metalloproteinase Secretion. *Cancer Research*, **67**, 3117-3126.
35. Westerhoff, H.V. and Palsson, B.O. (2004) The evolution of molecular biology into systems biology. *Nat Biotech*, **22**, 1249-1252.
36. von Bertalanffy, L. (1950) The Theory of Open Systems in Physics and Biology. *Science*, **111**, 23-29.
37. Kitano, H. (2002) Systems Biology: A Brief Overview. *Science*, **295**, 1662-1664.
38. Kirkwood, T.B.L. (2008) A systematic look at an old problem. *Nature*, **451**, 644-647.
39. Kirkwood, T.B.L., Boys, R.J., Gillespie, C.S., Proctor, C.J., Shanley, D.P. and Wilkinson, D.J. (2003) Towards an e-biology of ageing: integrating theory and data. *Nat Rev Mol Cell Biol*, **4**, 243-249.
40. Proctor, C. and Gray, D. (2008) Explaining oscillations and variability in the p53-Mdm2 system. *BMC Systems Biology*, **2**, 75.
41. Hoffmann, A., Levchenko, A., Scott, M.L. and Baltimore, D. (2002) The IκB-NF-κB Signaling Module: Temporal Control and Selective Gene Activation. *Science*, **298**, 1241-1245.
42. von Dassow, G., Meir, E., Munro, E.M. and Odell, G.M. (2000) The segment polarity network is a robust developmental module. *Nature*, **406**, 188-192.
43. Dalle Pezze, P., Sonntag, A.G., Thien, A., Prentzell, M.T., Godel, M., Fischer, S., Neumann-Haefelin, E., Huber, T.B., Baumeister, R., Shanley, D.P. *et al.* (2012) A Dynamic Network Model of mTOR Signaling Reveals TSC-Independent mTORC2 Regulation. *Sci. Signal.*, **5**, ra25-.
44. Wilkinson, D.J. (2009) Stochastic modelling for quantitative description of heterogeneous biological systems. *Nat Rev Genet*, **10**, 122-133.
45. Unwin, R.D., Griffiths, J.R., Leverentz, M.K., Grallert, A., Hagan, I.M. and Whetton, A.D. (2005) Multiple Reaction Monitoring to Identify Sites of Protein Phosphorylation with High Sensitivity. *Mol Cell Proteomics*, **4**, 1134-1144.

46. Schomburg, I., Chang, A., Ebeling, C., Gremse, M., Heldt, C., Huhn, G. and Schomburg, D. (2004) BRENDA, the enzyme database: updates and major new developments. *Nucl. Acids Res.*, **32**, D431-433.
47. Schomburg, I., Chang, A. and Schomburg, D. (2002) BRENDA, enzyme data and metabolic information. *Nucl. Acids Res.*, **30**, 47-49.
48. Passos, J.F., Nelson, G., Wang, C., Richter, T., Simillion, C., Proctor, C.J., Miwa, S., Olijslagers, S., Hallinan, J., Wipat, A. *et al.* (2010) Feedback between p21 and reactive oxygen production is necessary for cell senescence. *Mol Syst Biol*, **6**.
49. Hucka, M., Finney, A., Sauro, H.M., Bolouri, H., Doyle, J.C., Kitano, H., and the rest of the, S.F., Arkin, A.P., Bornstein, B.J., Bray, D. *et al.* (2003) The systems biology markup language (SBML): a medium for representation and exchange of biochemical network models. *Bioinformatics*, **19**, 524-531.
50. Funahashi, A., Morohashi, M., Kitano, H. and Tanimura, N. (2003) CellDesigner: a process diagram editor for gene-regulatory and biochemical networks. *BIOSILICO*, **1**, 159-162.
51. Gillespie, C.S., Wilkinson, D.J., Proctor, C.J., Shanley, D.P., Boys, R.J. and Kirkwood, T.B.L. (2006) Tools for the SBML Community. *Bioinformatics*, **22**, 628-629.
52. Drager, A., Hassis, N., Supper, J., Schroder, A. and Zell, A. (2008) SBMLsqueezer: A CellDesigner plug-in to generate kinetic rate equations for biochemical networks. *BMC Systems Biology*, **2**, 39.
53. Gillespie, D.T. (1977) Exact stochastic simulation of coupled chemical reactions. *The Journal of Physical Chemistry*, **81**, 2340-2361.
54. Kirkwood, T.B.L. and Kowald, A. (1997) Network theory of aging. *Experimental Gerontology*, **32**, 395-399.
55. Proctor, C.J. and Lorimer, I.A.J. (2011) Modelling the Role of the Hsp70/Hsp90 System in the Maintenance of Protein Homeostasis. *PLoS ONE*, **6**, e22038.
56. Sonntag, A.G., Dalle Pezze, P., Shanley, D.P. and Thedieck, K. (2012) A modelling–experimental approach reveals insulin receptor substrate (IRS)-dependent regulation of adenosine monosphosphate-dependent kinase (AMPK) by insulin. *FEBS Journal*, **279**, 3314-3328.
57. Smith, G.R. and Shanley, D.P. (2010) Modelling the Response of FOXO Transcription Factors to Multiple Post-Translational Modifications Made by Ageing-Related Signalling Pathways. *PLoS ONE*, **5**, e11092.
58. Sengupta, S. and Harris, C.C. (2005) p53: traffic cop at the crossroads of DNA repair and recombination. *Nat Rev Mol Cell Biol*, **6**, 44-55.
59. Okano, S., Lan, L., Caldecott, K.W., Mori, T. and Yasui, A. (2003) Spatial and Temporal Cellular Responses to Single-Strand Breaks in Human Cells. *Mol. Cell. Biol.*, **23**, 3974-3981.
60. Frouin, I., Maga, G., Denegri, M., Riva, F., Savio, M., Spadari, S., Prosperi, E. and Scovassi, A.I. (2003) Human Proliferating Cell Nuclear Antigen, Poly(ADP-ribose) Polymerase-1, and p21waf1/cip1: A DYNAMIC EXCHANGE OF PARTNERS. *J. Biol. Chem.*, **278**, 39265-39268.
61. Lieber, M.R., Ma, Y., Pannicke, U. and Schwarz, K. (2003) Mechanism and regulation of human non-homologous DNA end-joining. *Nat Rev Mol Cell Biol*, **4**, 712-720.
62. Riley, P.A. (1994) Free Radicals in Biology: Oxidative Stress and the Effects of Ionizing Radiation. *International Journal of Radiation Biology*, **65**, 27-33.
63. Jackson, J.G., Post, S.M. and Lozano, G. (2011) Regulation of tissue- and stimulus-specific cell fate decisions by p53 in vivo. *The Journal of Pathology*, **223**, 127-137.
64. Covo, S., de Villartay, J.-P., Jeggo, P.A. and Livneh, Z. (2009) Translesion DNA synthesis-assisted non-homologous end-joining of complex double-strand breaks prevents loss of DNA sequences in mammalian cells. *Nucl. Acids Res.*, **37**, 6737-6745.
65. Helleday, T., Lo, J., van Gent, D.C. and Engelward, B.P. (2007) DNA double-strand break repair: From mechanistic understanding to cancer treatment. *DNA Repair*, **6**, 923-935.

66. Xiao, D., Herman-Antosiewicz, A., Antosiewicz, J., Xiao, H., Brisson, M., Lazo, J.S. and Singh, S.V. (2005) Diallyl trisulfide-induced G2-M[thinsp]phase cell cycle arrest in human prostate cancer cells is caused by reactive oxygen species-dependent destruction and hyperphosphorylation of Cdc25C. *Oncogene*, **24**, 6256-6268.
67. Wu, X.-J., Kassie, F. and Mersch-Sundermann, V. (2005) The role of reactive oxygen species (ROS) production on diallyl disulfide (DADS) induced apoptosis and cell cycle arrest in human A549 lung carcinoma cells. *Mutation Research/Fundamental and Molecular Mechanisms of Mutagenesis*, **579**, 115-124.
68. Mason, K.A., Raju, U., Buchholz, T.A., Wang, L., Milas, Z.L. and Milas, L. (2012) Poly (ADP-ribose) Polymerase Inhibitors in Cancer Treatment. *American Journal of Clinical Oncology*, **Publish Ahead of Print**, 10.1097/COC.1090b1013e3182467dce.
69. Rothkamm, K., Kruger, I., Thompson, L.H. and Lobrich, M. (2003) Pathways of DNA Double-Strand Break Repair during the Mammalian Cell Cycle. *Mol. Cell. Biol.*, **23**, 5706-5715.
70. Haber, J.E. (1995) <I>In vivo</I> biochemistry: Physical monitoring of recombination induced by site-specific endonucleases. *BioEssays*, **17**, 609-620.
71. Collado, M., Blasco, M.A. and Serrano, M. (2007) Cellular Senescence in Cancer and Aging. *Cell*, **130**, 223-233.
72. Cucinotta, F.A., Pluth, J.M., Anderson, J.A., Harper, J.V. and O'Neill, P. (2008) Biochemical Kinetics Model of DSB Repair and Induction of Î³-H2AX Foci by Non-homologous End Joining. *Radiation Research*, **169**, 214-222.
73. Smith, G.C.M. and Jackson, S.P. (1999) The DNA-dependent protein kinase. *Genes & Development*, **13**, 916-934.
74. Walker, J.R., Corpina, R.A. and Goldberg, J. (2001) Structure of the Ku heterodimer bound to DNA and its implications for double-strand break repair. *Nature*, **412**, 607-614.
75. Downs, J.A. and Jackson, S.P. (2004) A means to a DNA end: the many roles of Ku. *Nat Rev Mol Cell Biol*, **5**, 367-378.
76. Hammarsten, O. and Chu, G. (1998) DNA-dependent protein kinase: DNA binding and activation in the absence of Ku. *Proceedings of the National Academy of Sciences of the United States of America*, **95**, 525-530.
77. DeFazio, L.G., Stansel, R.M., Griffith, J.D. and Chu, G. (2002) Synapsis of DNA ends by DNA-dependent protein kinase. *The EMBO journal*, **21**, 3192.
78. Ma, Y., Pannicke, U., Schwarz, K. and Lieber, M.R. (2002) Hairpin Opening and Overhang Processing by an Artemis/DNA-Dependent Protein Kinase Complex in Nonhomologous End Joining and V(D)J Recombination. *Cell*, **108**, 781-794.
79. Grawunder, U., Wilm, M., Wu, X., Kulesza, P., Wilson, T.E., Mann, M. and Lieber, M.R. (1997) Activity of DNA ligase IV stimulated by complex formation with XRCC4 protein in mammalian cells. *Nature*, **388**, 492-495.
80. Kobayashi, J., Iwabuchi, K., Miyagawa, K., Sonoda, E., Suzuki, K., Takata, M. and Tauchi, H. (2008) Current Topics in DNA Double-Strand Break Repair. *Journal of Radiation Research*, **49**, 93-103.
81. Lu, C., Shi, Y., Wang, Z., Song, Z., Zhu, M., Cai, Q. and Chen, T. (2008) Serum starvation induces H2AX phosphorylation to regulate apoptosis via p38 MAPK pathway. *FEBS Letters*, **582**, 2703-2708.
82. Endt, H., Sprung, C.N., Keller, U., Gaipl, U., Fietkau, R. and Distel, L.V. (2011) Detailed Analysis of DNA Repair and Senescence Marker Kinetics Over the Life Span of a Human Fibroblast Cell Line. *The Journals of Gerontology Series A: Biological Sciences and Medical Sciences*, **66A**, 367-375.
83. Shiloh, Y. (2003) ATM and related protein kinases: safeguarding genome integrity. *Nat Rev Cancer*, **3**, 155-168.
84. van den Bosch, M., Bree, R.T. and Lowndes, N.F. (2003) The MRN complex: coordinating and mediating the response to broken chromosomes. *EMBO reports*, **4**, 844.

85. Gross, A. (2008) A new Aven-ue to DNA-damage checkpoints. *Trends in Biochemical Sciences*, **33**, 514-516.
86. Falck, J., Coates, J. and Jackson, S.P. (2005) Conserved modes of recruitment of ATM, ATR and DNA-PKcs to sites of DNA damage. *Nature*, **434**, 605-611.
87. Burma, S., Chen, B.P., Murphy, M., Kurimasa, A. and Chen, D.J. (2001) ATM Phosphorylates Histone H2AX in Response to DNA Double-strand Breaks. *J. Biol. Chem.*, **276**, 42462-42467.
88. Cann, K.L. and Hicks, G.G. (2007) Regulation of the cellular DNA double-strand break response. *Biochemistry and Cell Biology*, **85**, 663-674.
89. Stiff, T., O'Driscoll, M., Rief, N., Iwabuchi, K., Lobrich, M. and Jeggo, P.A. (2004) ATM and DNA-PK Function Redundantly to Phosphorylate H2AX after Exposure to Ionizing Radiation. *Cancer Res*, **64**, 2390-2396.
90. Ahmed, E.A., de Boer, P., Philippens, M.E.P., Kal, H.B. and de Rooij, D.G. (2009) Parp1-XRCC1 and the repair of DNA double strand breaks in mouse round spermatids. *Mutation Research/Fundamental and Molecular Mechanisms of Mutagenesis*, **683**, 84-90.
91. Singh, S.K., Wu, W., Zhang, L., Klammer, H., Wang, M. and Iliakis, G. (2011) Widespread Dependence of Backup NHEJ on Growth State: Ramifications for the Use of DNA-PK Inhibitors. *International Journal of Radiation Oncology*Biology*Physics*, **79**, 540-548.
92. Amsel, A.D., Rathaus, M., Kronman, N. and Cohen, H.Y. (2008) Regulation of the proapoptotic factor Bax by Ku70-dependent deubiquitylation. *Proceedings of the National Academy of Sciences*, **105**, 5117-5122.
93. Tapia, P.C. (2006) Histone-deacetylase inhibitors may accelerate the aging process in stem cell-dependent mammals: Stem cells, Ku70, and Drosophila at the crossroads. *Medical hypotheses*, **66**, 332-336.
94. Gama, V., Yoshida, T., Gomez, J.A., Basile, D.P., Mayo, L.D., Haas, A.L. and Matsuyama, S. (2006) Involvement of the ubiquitin pathway in decreasing Ku70 levels in response to drug-induced apoptosis. *Experimental Cell Research*, **312**, 488-499.
95. Postow, L., Ghenoiu, C., Woo, E.M., Krutchinsky, A.N., Chait, B.T. and Funabiki, H. (2008) Ku80 removal from DNA through double strand break-induced ubiquitylation. *J. Cell Biol.*, **182**, 467-479.
96. Seluanov, A., Danek, J., Hause, N. and Gorbunova, V. (2007) Changes in the level and distribution of Ku proteins during cellular senescence. *DNA Repair*, **6**, 1740-1748.
97. Gartel, A.L. and Radhakrishnan, S.K. (2005) Lost in Transcription: p21 Repression, Mechanisms, and Consequences. *Cancer Res*, **65**, 3980-3985.
98. Rodriguez, R. and Meuth, M. (2006) Chk1 and p21 Cooperate to Prevent Apoptosis during DNA Replication Fork Stress. *Mol. Biol. Cell*, **17**, 402-412.
99. Bozulic, L., Surucu, B., Hynx, D. and Hemmings, B.A. (2008) PKB[alpha]/Akt1 Acts Downstream of DNA-PK in the DNA Double-Strand Break Response and Promotes Survival. *Molecular Cell*, **30**, 203-213.
100. Copp, J., Manning, G. and Hunter, T. (2009) TORC-Specific Phosphorylation of Mammalian Target of Rapamycin (mTOR): Phospho-Ser2481 Is a Marker for Intact mTOR Signaling Complex 2. *Cancer Research*, **69**, 1821-1827.
101. Manning, B.D. and Cantley, L.C. (2007) AKT/PKB Signaling: Navigating Downstream. *Cell*, **129**, 1261-1274.
102. Bunz, F., DeWeese, T.L. and Laiho, M. (2011). Springer New York, pp. 35-52.
103. Halaby, M.-J., Hibma, J.C., He, J. and Yang, D.-Q. (2008) ATM protein kinase mediates full activation of Akt and regulates glucose transporter 4 translocation by insulin in muscle cells. *Cellular Signalling*, **20**, 1555-1563.
104. Iijima, K., Ohara, M., Seki, R. and Tauchi, H. (2008) Dancing on Damaged Chromatin: Functions of ATM and the RAD50/MRE11/NBS1 Complex in Cellular Responses to DNA Damage. *Journal of Radiation Research*, **49**, 451-464.

105. Lans, H., Marteijn, J.A. and Vermeulen, W. (2012) ATP-dependent chromatin remodeling in the DNA-damage response. *Epigenetics & Chromatin*, **5**, 4.
106. Legewie, S., Herzel, H., Westerhoff, H.V. and Bluthgen, N. (2008) Recurrent design patterns in the feedback regulation of the mammalian signalling network. *Mol Syst Biol*, **4**.
107. Cohen, H.Y., Lavu, S., Bitterman, K.J., Hekking, B., Imahiyerobo, T.A., Miller, C., Frye, R., Ploegh, H., Kessler, B.M. and Sinclair, D.A. (2004) Acetylation of the C Terminus of Ku70 by CBP and PCAF Controls Bax-Mediated Apoptosis. *Molecular Cell*, **13**, 627-638.
108. Bakkenist, C.J. and Kastan, M.B. (2003) DNA damage activates ATM through intermolecular autophosphorylation and dimer dissociation. *Nature*, **421**, 499-506.
109. Rivera-Calzada, A., Maman, J.P., Spagnolo, L., Pearl, L.H. and Llorca, O. (2005) Three-Dimensional Structure and Regulation of the DNA-Dependent Protein Kinase Catalytic Subunit (DNA-PKcs). *Structure*, **13**, 243-255.
110. Sontag, E. (2001) Protein phosphatase 2A: the Trojan Horse of cellular signaling. *Cellular Signalling*, **13**, 7-16.
111. Bryans, M., Valenzano, M.C. and Stamato, T.D. (1999) Absence of DNA ligase IV protein in XR-1 cells: evidence for stabilization by XRCC4. *Mutation Research/DNA Repair*, **433**, 53-58.
112. Metzger, L. and Iliakis, G. (1991) Kinetics of DNA Double-strand Break Repair Throughout the Cell Cycle as Assayed by Pulsed Field Gel Electrophoresis in CHO Cells. *International Journal of Radiation Biology*, **59**, 1325-1339.
113. Fox, J.C. and McNally, N.J. (1988) Cell Survival and DNA Double-strand Break Repair Following X-ray or Neutron Irradiation of V79 Cells. *International Journal of Radiation Biology*, **54**, 1021-1030.
114. Shahrezaei, V. and Swain, P.S. (2008) The stochastic nature of biochemical networks. *Current Opinion in Biotechnology*, **19**, 369-374.
115. Perkins, T.J. and Swain, P.S. (2009) Strategies for cellular decision-making. *Mol Syst Biol*, **5**.
116. Taniguchi, Y., Choi, P.J., Li, G.-W., Chen, H., Babu, M., Hearn, J., Emili, A. and Xie, X.S. (2010) Quantifying E. coli Proteome and Transcriptome with Single-Molecule Sensitivity in Single Cells. *Science*, **329**, 533-538.
117. Misteli, T. and Soutoglou, E. (2009) The emerging role of nuclear architecture in DNA repair and genome maintenance. *Nat Rev Mol Cell Biol*, **10**, 243-254.
118. Suzuki, K., Kodama, S. and Watanabe, M. (2009) Role of Ku80-dependent end-joining in delayed genomic instability in mammalian cells surviving ionizing radiation. *Mutation Research/Fundamental and Molecular Mechanisms of Mutagenesis*, **683**, 29-34.
119. Guirouilh-Barbat, J.e., Huck, S., Bertrand, P., Pirzio, L., Desmaze, C., Sabatier, L. and Lopez, B.S. (2004) Impact of the KU80 Pathway on NHEJ-Induced Genome Rearrangements in Mammalian Cells. *Molecular Cell*, **14**, 611-623.
120. Nelson, G., Buhmann, M. and von Zglinicki, T. (2009) DNA damage foci in mitosis are devoid of 53BP1. *Cell cycle (Georgetown, Tex.)*, **8**, 3379-3383.
121. Nelson, G., Paraoan, L., Spiller, D.G., Wilde, G.J.C., Browne, M.A., Djali, P.K., Unitt, J.F., Sullivan, E., Floettmann, E. and White, M.R.H. (2002) Multi-parameter analysis of the kinetics of NF-κB signalling and transcription in single living cells. *Journal of Cell Science*, **115**, 1137-1148.
122. Anderson, C.W. and Carter, T.H. (1996) The DNA-activated protein kinase -- DNA-PK. *Curr Top Microbiol Immunol*, **217**, 91-111.
123. Mari, P.-O., Florea, B.I., Persengiev, S.P., Verkaik, N.S., Brüggenwirth, H.T., Modesti, M., Giglia-Mari, G., Bezstarosti, K., Demmers, J.A.A., Luider, T.M. *et al.* (2006) Dynamic assembly of end-joining complexes requires interaction between Ku70/80 and XRCC4. *Proceedings of the National Academy of Sciences*, **103**, 18597-18602.
124. Wang, M., Wu, W., Wu, W., Rosidi, B., Zhang, L., Wang, H. and Iliakis, G. (2006) PARP-1 and Ku compete for repair of DNA double strand breaks by distinct NHEJ pathways. *Nucl. Acids Res.*, **34**, 6170-6182.

125. Andrews, B.J., Lehman, J.A. and Turchi, J.J. (2006) Kinetic Analysis of the Ku-DNA Binding Activity Reveals a Redox-dependent Alteration in Protein Structure That Stimulates Dissociation of the Ku-DNA Complex. *Journal of Biological Chemistry*, **281**, 13596-13603.
126. Fumagalli, M., Rossiello, F., Clerici, M., Barozzi, S., Cittaro, D., Kaplunov, J.M., Bucci, G., Dobreva, M., Matti, V., Beausejour, C.M. *et al.* (2012) Telomeric DNA damage is irreparable and causes persistent DNA-damage-response activation. *Nat Cell Biol*, **14**, 355-365.
127. Kamata, H. and Hirata, H. (1999) Redox Regulation of Cellular Signalling. *Cellular Signalling*, **11**, 1-14.
128. Cross, J.V. and Templeton, D.J. (2006) Regulation of Signal Transduction Through Protein Cysteine Oxidation. *Antioxidants & Redox Signaling*, **8**, 1819-1827.
129. Bennett, S., Neher, T., Shatilla, A. and Turchi, J. (2009) Molecular analysis of Ku redox regulation. *BMC Molecular Biology*, **10**, 86.
130. Kim, J.R., Yoon, H.W., Kwon, K.S., Lee, S.R. and Rhee, S.G. (2000) Identification of proteins containing cysteine residues that are sensitive to oxidation by hydrogen peroxide at neutral pH. *Anal Biochem*, **283**, 214-221.
131. Berman, H.M., Westbrook, J., Feng, Z., Gilliland, G., Bhat, T.N., Weissig, H., Shindyalov, I.N. and Bourne, P.E. (2000) The Protein Data Bank. *Nucleic Acids Research*, **28**, 235-242.
132. Dolinsky, T.J., Czodrowski, P., Li, H., Nielsen, J.E., Jensen, J.H., Klebe, G. and Baker, N.A. (2007) PDB2PQR: expanding and upgrading automated preparation of biomolecular structures for molecular simulations. *Nucleic Acids Research*, **35**, W522-W525.
133. Dolinsky, T.J., Nielsen, J.E., McCammon, J.A. and Baker, N.A. (2004) PDB2PQR: an automated pipeline for the setup of Poissonâ€“Boltzmann electrostatics calculations. *Nucleic Acids Research*, **32**, W665-W667.
134. Baker, N.A., Sept, D., Joseph, S., Holst, M.J. and McCammon, J.A. (2001) Electrostatics of nanosystems: Application to microtubules and the ribosome. *Proceedings of the National Academy of Sciences*, **98**, 10037-10041.
135. Peters, G.H., Frimurer, T.M. and Olsen, O.H. (1998) Electrostatic evaluation of the signature motif (H/V)CX5R(S/T) in protein-tyrosine phosphatases. *Biochemistry*, **37**, 5383-5393.
136. Nielsen, J.E. and Vriend, G. (2001) Optimizing the hydrogen-bond network in Poisson–Boltzmann equation-based pKa calculations. *Proteins: Structure, Function, and Bioinformatics*, **43**, 403-412.
137. Brenkman, A.B., van den Broek, N.J.F., de Keizer, P.L.J., van Gent, D.C. and Burgering, B.M.T. (2010) The DNA damage repair protein Ku70 interacts with FOXO4 to coordinate a conserved cellular stress response. *The FASEB Journal*, **24**, 4271-4280.
138. Bachman, J.A. and Sorger, P. (2011) New approaches to modeling complex biochemistry. *Nat Meth*, **8**, 130-131.
139. Paddock, M.N., Bauman, A.T., Higdon, R., Kolker, E., Takeda, S. and Scharenberg, A.M. (2010) Competition between PARP-1 and Ku70 control the decision between high-fidelity and mutagenic DNA repair. *DNA Repair*, **10**, 338-343.
140. Spagnolo, L., Barbeau, J., Curtin, N.J., Morris, E.P. and Pearl, L.H. (2012) Visualization of a DNA-PK/PARP1 complex. *Nucleic Acids Research*.
141. Branzei, D. and Foiani, M. (2008) Regulation of DNA repair throughout the cell cycle. *Nature Reviews Molecular Cell Biology*, **9**, 297-308.
142. Kulkarni, A. and Das, K.C. (2008) Differential roles of ATR and ATM in p53, Chk1, and histone H2AX phosphorylation in response to hyperoxia: ATR-dependent ATM activation. *Am J Physiol Lung Cell Mol Physiol*, **294**, L998-1006.
143. Wang, X.W., Zhan, Q., Coursen, J.D., Khan, M.A., Kontny, H.U., Yu, L., Hollander, M.C., O'Connor, P.M., Fornace, A.J. and Harris, C.C. (1999) GADD45 induction of a G2/M cell cycle checkpoint. *Proceedings of the National Academy of Sciences*, **96**, 3706-3711.
144. Takahashi, A., Ohtani, N. and Hara, E. (2007) Irreversibility of cellular senescence: dual roles of p16INK4a/Rb-pathway in cell cycle control. *Cell division*, **2**, 10.

145. Haupt, S., Berger, M., Goldberg, Z. and Haupt, Y. (2003) Apoptosis - the p53 network. *Journal of Cell Science*, **116**, 4077-4085.
146. Nakano, K. and Vousden, K.H. (2001) PUMA, a Novel Proapoptotic Gene, Is Induced by p53. *Molecular Cell*, **7**, 683-694.
147. Adams, J.M. and Cory, S. (1998) The Bcl-2 Protein Family: Arbiters of Cell Survival. *Science*, **281**, 1322-1326.
148. Ashkenazi, A. and Dixit, V.M. (1998) Death Receptors: Signaling and Modulation. *Science*, **281**, 1305-1308.
149. Gartel, A.L. and Tyner, A.L. (2002) The Role of the Cyclin-dependent Kinase Inhibitor p21 in Apoptosis 1 Supported in part by NIH Grant R01 DK56283 (to A. L. T.) for the p21 research and Campus Research Board and Illinois Department of Public Health Penny Severns Breast and Cervical Cancer grants (to A. L. G.).1. *Molecular Cancer Therapeutics*, **1**, 639-649.
150. Salminen, A., Helenius, M., Lahtinen, T., Korhonen, P., Tapiola, T., Soininen, H. and Solovyan, V. (1997) Down-Regulation of Ku Autoantigen, DNA-Dependent Protein Kinase, and Poly(ADP-ribose) Polymerase during Cellular Senescence. *Biochemical and Biophysical Research Communications*, **238**, 712-716.
151. Blinov, M.L., Faeder, J.R., Goldstein, B. and Hlavacek, W.S. (2004) BioNetGen: software for rule-based modeling of signal transduction based on the interactions of molecular domains. *Bioinformatics*, **20**, 3289-3291.
152. Danos, V. and Laneve, C. (2004) Formal molecular biology. *Theoretical Computer Science*, **325**, 69-110.
153. Sneddon, M.W., Faeder, J.R. and Emonet, T. (2011) Efficient modeling, simulation and coarse-graining of biological complexity with NFsim. *Nat Meth*, **8**, 177-183.
154. Hoops, S., Sahle, S., Gauges, R., Lee, C., Pahle, J., Simus, N., Singhal, M., Xu, L., Mendes, P. and Kummer, U. (2006) COPASI--a COmplex PAthway SImulator. *Bioinformatics*, **22**, 3067.
155. Woodhouse, B.C. and Dianov, G.L. (2008) Poly ADP-ribose polymerase-1: An international molecule of mystery. *DNA Repair*, **7**, 1077-1086.
156. Kholodenko, B.N., Hancock, J.F. and Kolch, W. (2010) Signalling ballet in space and time. *Nat Rev Mol Cell Biol*, **11**, 414-426.
157. Kholodenko, B., Yaffe, M.B. and Kolch, W. (2012) Computational Approaches for Analyzing Information Flow in Biological Networks. *Sci. Signal.*, **5**, re1-.
158. Süel, G.M., Garcia-Ojalvo, J., Liberman, L.M. and Elowitz, M.B. (2006) An excitable gene regulatory circuit induces transient cellular differentiation. *Nature*, **440**, 545-550.
159. Lahav, G., Rosenfeld, N., Sigal, A., Geva-Zatorsky, N., Levine, A.J., Elowitz, M.B. and Alon, U. (2004) Dynamics of the p53-Mdm2 feedback loop in individual cells. *Nat Genet*, **36**, 147-150.
160. Shiloh, Y. (2001) ATM and ATR: networking cellular responses to DNA damage. *Current Opinion in Genetics & Development*, **11**, 71-77.
161. Purvis, J.E., Karhohs, K.W., Mock, C., Batchelor, E., Loewer, A. and Lahav, G. (2012) p53 Dynamics Control Cell Fate. *Science*, **336**, 1440-1444.
162. Vassilev, L.T., Vu, B.T., Graves, B., Carvajal, D., Podlaski, F., Filipovic, Z., Kong, N., Kammlott, U., Lukacs, C., Klein, C. *et al.* (2004) In Vivo Activation of the p53 Pathway by Small-Molecule Antagonists of MDM2. *Science*, **303**, 844-848.
163. Brissett, N.C. and Doherty, A.J. (2009) Repairing DNA double-strand breaks by the prokaryotic non-homologous end-joining pathway. *Biochemical Society Transactions*, **037**, 539-545.
164. Weterings, E. and van Gent, D.C. (2004) The mechanism of non-homologous end-joining: a synopsis of synapsis. *DNA Repair*, **3**, 1425-1435.
165. Shannon, P., Markiel, A., Ozier, O., Baliga, N.S., Wang, J.T., Ramage, D., Amin, N., Schwikowski, B. and Ideker, T. (2003) Cytoscape: A Software Environment for Integrated Models of Biomolecular Interaction Networks. *Genome Research*, **13**, 2498-2504.

166. Lane, D.P., Cheok, C.F. and Lain, S. (2010) p53-based Cancer Therapy. *Cold Spring Harbor Perspectives in Biology*, **2**.
167. Anderson, C.W. and Lees-Miller, S.P. (1992) The nuclear serine/threonine protein kinase DNA-PK. *Critical reviews in eukaryotic gene expression*, **2**, 283.
168. Leppard, J.B., Dong, Z., Mackey, Z.B. and Tomkinson, A.E. (2003) Physical and Functional Interaction between DNA Ligase III and Poly(ADP-Ribose) Polymerase 1 in DNA Single-Strand Break Repair. *Molecular and Cellular Biology*, **23**, 5919-5927.
169. Windhofer, F., Wu, W. and Iliakis, G. (2007) Low levels of DNA ligases III and IV sufficient for effective NHEJ. *Journal of Cellular Physiology*, **213**, 475-483.
170. D'Amours, D., Desnoyers, S., D'Silva, I. and Poirier, G.G. (1999) Poly(ADP-ribosyl)ation reactions in the regulation of nuclear functions. *Biochem. J.*, **342**, 249-268.
171. Ludwig, A., Behnke, B., Holtlund, J. and Hilz, H. (1988) Immunoquantitation and size determination of intrinsic poly(ADP-ribose) polymerase from acid precipitates. An analysis of the in vivo status in mammalian species and in lower eukaryotes. *Journal of Biological Chemistry*, **263**, 6993-6999.
172. Yamanaka, H., Penning, C.A., Willis, E.H., Wasson, D.B. and Carson, D.A. (1988) Characterization of human poly(ADP-ribose) polymerase with autoantibodies. *Journal of Biological Chemistry*, **263**, 3879-3883.
173. Uematsu, N., Weterings, E., Yano, K.-i., Morotomi-Yano, K., Jakob, B., Taucher-Scholz, G., Mari, P.-O., van Gent, D.C., Chen, B.P.C. and Chen, D.J. (2007) Autophosphorylation of DNA-PKCS regulates its dynamics at DNA double-strand breaks. *J. Cell Biol.*, **177**, 219-229.
174. Yano, K. and Chen, D.J. (2008) Live cell imaging of XLF and XRCC4 reveals a novel view of protein assembly in the non-homologous end-joining pathway. *Cell cycle (Georgetown, Tex.)*, **7**, 1321.
175. Dobbs, T.A., Palmer, P., Maniou, Z., Lomax, M.E. and O'Neill, P. (2008) Interplay of two major repair pathways in the processing of complex double-strand DNA breaks. *DNA Repair*, **7**, 1372-1383.
176. Celeste, A., Fernandez-Capetillo, O., Kruhlak, M.J., Pilch, D.R., Staudt, D.W., Lee, A., Bonner, R.F., Bonner, W.M. and Nussenzweig, A. (2003) Histone H2AX phosphorylation is dispensable for the initial recognition of DNA breaks. *Nat Cell Biol*, **5**, 675-679.
177. Lukas, C., Melander, F., Stucki, M., Falck, J., Bekker-Jensen, S., Goldberg, M., Lerenthal, Y., Jackson, S.P., Bartek, J. and Lukas, J. (2004) Mdc1 couples DNA double-strand break recognition by Nbs1 with its H2AX-dependent chromatin retention. *EMBO J*, **23**, 2674-2683.
178. Leatherbarrow, E.L., Harper, J.V., Cucinotta, F.A. and O'Neill, P. (2006) Induction and quantification of γ-H2AX foci following low and high LET-irradiation. *International Journal of Radiation Biology*, **82**, 111 - 118.
179. Schultz, L.B., Chehab, N.H., Malikzay, A. and Halazonetis, T.D. (2000) P53 Binding Protein 1 (53bp1) Is an Early Participant in the Cellular Response to DNA Double-Strand Breaks. *The Journal of Cell Biology*, **151**, 1381-1390.
180. Wang, H., Rosidi, B., Perrault, R., Wang, M., Zhang, L., Windhofer, F. and Iliakis, G. (2005) DNA Ligase III as a Candidate Component of Backup Pathways of Nonhomologous End Joining. *Cancer Research*, **65**, 4020-4030.